COUPLED DYNAMIC ANALYSIS OF FLOATING OFFSHORE WIND FARMS

A Thesis

by

SANGYUN SHIM

Submitted to the Office of Graduate Studies of
Texas A&M University
in partial fulfillment of the requirements for the degree of

MASTER OF SCIENCE

December 2007

Major Subject: Ocean Engineering

COUPLED DYNAMIC ANALYSIS OF FLOATING OFFSHORE WIND FARMS

A Thesis

by

SANGYUN SHIM

Submitted to the Office of Graduate Studies of
Texas A&M University
in partial fulfillment of the requirements for the degree of

MASTER OF SCIENCE

Approved by:

Chair of Committee,	M.H. Kim
Committee Members,	Robert Randall
	Achim Stoessel
Head of Department,	David V. Rosowsky

December 2007

Major Subject: Ocean Engineering

ABSTRACT

Coupled Dynamic Analysis of Floating Offshore Wind Farms. (December 2007)

Sangyun Shim, B.S., Inha University

Chair of Advisory Committee: Dr. M. H. Kim

During the past decade, the demand for clean renewable energy continues to rise drastically in Europe, the US, and other countries. Wind energy in the ocean can possibly be one of those future renewable clean energy sources as long it is economically feasible and technologically manageable. So far, most of the offshore wind farm research has been limited to fixed platforms in shallow-water areas. In the water depth deeper than 30m, however, floating-type wind farms tend to be more feasible. Then, the overall design and engineering becomes more complicated than fixed platforms including the coupled dynamics of platforms, mooring lines, and blades. In the present study, a numerical time-domain model has been developed for the fully coupled dynamic analysis of an offshore floating wind turbine system including blade-rotor dynamics and platform motions. As a test case, the TLP-type floater system with 3 blades of 70-m diameter designed by the National Renewable Energy Laboratory (NREL) is selected to analyze the dynamic coupling effects among floating system, mooring lines, and wind turbine. The performance of the selected system in a typical wind-wave-current condition has been simulated and analyzed. A similar study for the floater and rotor coupled dynamic analysis was conducted by MIT and NREL. However, in the present

case, the dynamic coupling between platform and mooring lines are also considered in addition to the rotor-floater dynamic coupling. It is seen that the rotor-floater coupling effects increase with wind velocity and blade size. The increased coupling effects tend to increase the dynamic tension of TLP tethers. The developed technology and numerical tool are applicable to the new offshore floating wind farms planned in the future.

DEDICATION

To my wife, Do-Eun Choe

ACKNOWLEDGMENTS

I would like to express my sincere appreciation to my committee chair Dr. M.H. Kim for his encouragement and guidance throughout my research. I would like to thank Dr. Robert Randall and Dr. Stoessel for serving as the committee members and for their guidance throughout the course of this research. I would also like to thank Dr. D. H. Lee, Mr. Seung Jae Lee, and Sung Ho Lim for their support.

Finally, I am indebted to my family for their support and encouragement throughout this work.

TABLE OF CONTENTS

Page

Page

LIST OF FIGURES

Page

Page

Page

Page

Page

Page

Page

LIST OF TABLES

Page

1. INTRODUCTION

1.1 General

As the world population is increased and our society is industrialized, the demand for energy is growing. People are mainly depending on fossil fuel as an energy source. However, fossil fuel is being depleted and it has a negative environmental impact on our world. Therefore there are many investigations about new forms of energy. In researches, wind is found as one of the possible and powerful energy sources.

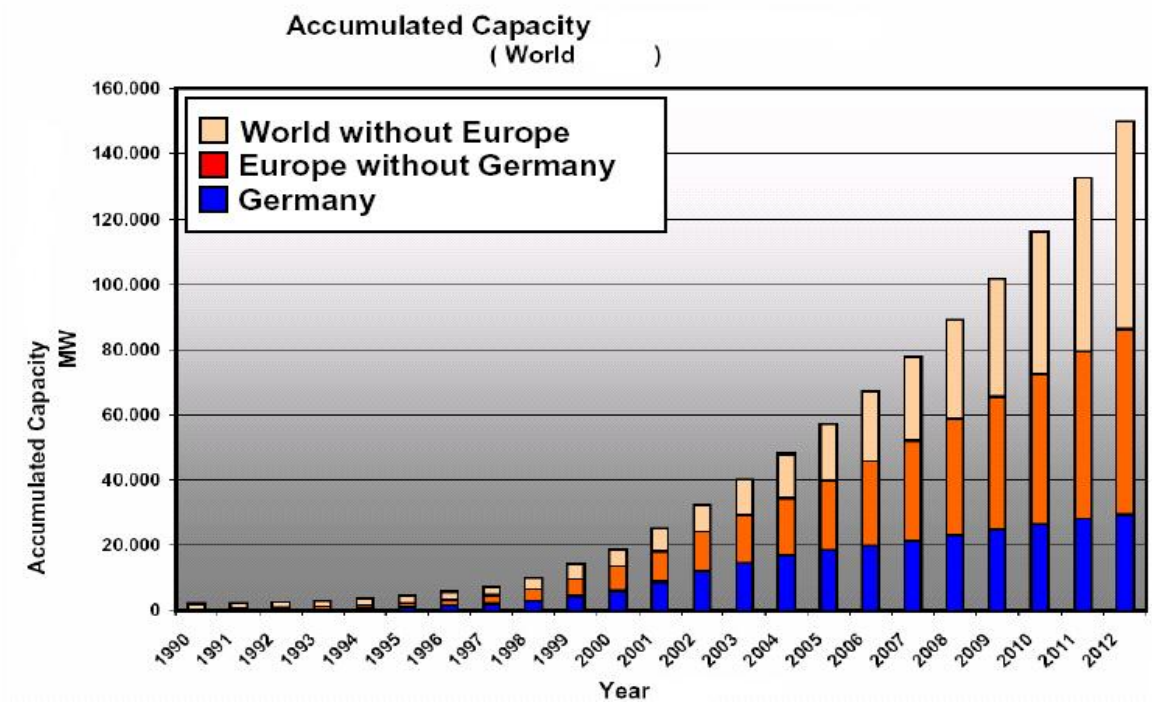

Figure 1-1 Accumulated capacity of wind energy (World Renewable Energy Congress, 2003)

This thesis follows the style of the Ocean Engineering.

Wind energy has become a major resource of renewable and clean energy to our world. Many countries have started to study about wind energy and have already developed several technologies to improve wind power sources. The motivation of the use of wind energy can reduce the dependency on fossil fuel can be reduced by these works. Figure 1-1 shows the past record and projection of the accumulated capacity of wind energy from 1990 to 2012 (World Renewable Energy Congress, 2003).

Wind turbines can produce large capacities of electricity in a competitive and clean way compared to other energy sources. To improve wind energy production systems and to get large scale generation, wind turbine technology needs offshore wind energy resources. So far, most projects of offshore wind farms are located in relatively shallow water (<30 m) using bottom-fixed type wind turbines. However, the use of bottom-fixed wind turbines may not be the best solution for offshore wind farms.

Currently, fixed-bottom wind turbine technology has seen limited deployment to a water depth of 30 m. To extend wind turbine systems to deeper water, practical research of offshore floating wind turbine systems is required. Also, developing offshore floating wind farms is important because it can minimize the scenery disturbance, avoid the noise problems generated by wind-driven blades, provide high wind speed by low surface roughness, and make use of extremely abundant deepwater wind resources. A number of researchers have recently investigated the feasibility of several different types of floating wind farms. The major goal of this research is to develop a fully-coupled dynamic analysis technique that could be used for floating wind turbines. The analysis method integrates wind loading on the wind turbine tower and the rotor blades, and

incorporates wave loading on the floater.

The major objective of this study is to develop a fully-coupled dynamic analysis technique that could be used for floating wind turbines. The analysis method integrates wind loading on the wind turbine tower and the rotor blades, and incorporates wave loading on the floater. Practical models of the floating body and the wind turbine are employed to develop a fully coupled dynamic model of an floating offshore wind turbine system. For the floating system, WAMIT (Wave Analysis at MIT) developed by WAMIT Inc. and Charm3D (Coupled hull/mooring/riser analysis) developed at Texas A&M University are employed (Kim, 1997). For the analysis of wind turbine system, the primary design code of wind turbines, FAST (Fatigue, Aerodynamics, Structures, and Turbulence) promoted by National Renewable Energy Laboratory (NREL), is employed (Jonkman, Jason, and Buhl, 2004).

1.2 Wind turbine

A wind turbine is a machine that converts from wind energy to electrical energy. The most common wind turbine is the horizontal axis wind turbine which is selected in the study. It has seven major subsystems: rotor, nacelle, generator, tower, control system, electrical output system, and floating body.

First, the rotor consists of normally two or three blades attached to a hub. The system performance of the wind turbine is based on the selection of blade number, shape, and length. The rotor can be either upwind or downwind design. Most wind turbines are

three bladed upwind designs. Second, the nacelle is the part that includes the generator and drivetrain. This part protects the wind turbine equipment. Third, the generator converts the mechanical work input of the wind turbine into electrical output. Fourth, the tower supports the wind turbine nacelle and rotor. The height of the supporting tower is over 80 meter in this research. Fifth, the control system changes the blade pitch, nacelle yaw, and generator loading of a wind turbine. The control system can also change the pitch of the blades to alter the amount of torque produced by the rotor. The purpose of the control system is to maximize power output. Sixth, electrical output of the generator must be transferred to the electric gird or electric load. The output passes through other electrical components (cables, transformers, power factor correction capacitors, solid state power converts, and switchgear). Offshore wind turbines typically send power through cables. Last but not least, the floating body has enough buoyancy to supports all wind turbine elements in the ocean. The floating body is tied up by the mooring systems. In this research, a tether system is introduced as the mooring system.

1.2 Literature review

A number of researchers have recently investigated the feasibility of several different types of floating wind farms. Kosugi et al. (2002) performed a feasibility study on a floating wind farm of Japan's coast. They concluded that wind power production cost of the proposed floating type wind turbine is still fairly higher than that of a bottom-fixed type wind turbine. Henderson et al. (2002) conducted a study on potential for floating

offshore wind energy in Japanese waters. They proposed several types of offshore wind turbines. Henderson et al. (2004) performed research on floating wind farms for shallow offshore sites. They suggested many types of wind turbines and compared advantages and disadvantages of types of wind turbines. Musial et al. (2003) conducted a feasibility study of floating platform systems for wind turbines. This study provides a general technical description of several types of floating platforms for wind turbines and evaluates the possibility of offshore floating wind turbines. This study was performed at National Renewable Energy Laboratory (NREL). Wayman et al. (2006) investigated the first step of the development of a floating and moored system for offshore wind turbines. This research set possible design specifications for a floating body for offshore floating wind turbines.

1.3 Objective and scope

Despite many kinds of proposed concepts of floating offshore wind turbines, there are not many practical analyses of offshore wind farms. The main objectives of this study are to develop a numerical model for the fully-coupled dynamic analysis of a floating offshore wind turbine system and to investigate coupling effects between the platform and wind turbine. The coupling effects between floating body and wind turbine can affect the global platform motion and variation of mooring line tension. The newly developed numerical model includes:

- fully-coupled effects on global motion for floating wind turbine

- mooring tension of platform

To couple two individual systems (floating body and wind turbine), the following studies are performed:

- derive coupled equation of motion between floating body and wind turbine
- make one model from two individual stand alone programs

1.4 Organization

In section 2, the developing process of time domain coupling simulation is discussed. In section 3 case studies are performed. In this case study, global motion of floating wind turbines and top tension of mooring lines are investigated. In section 4, summary and conclusion of the research is presented.

2. DEVELOPING PROCEDURE OF TIME DOMAIN COUPLING SIMULATION

In this section, a procedure for developing a floating wind turbine simulation is presented. First, the basic hydrodynamics concept of a floating system is presented. This helps in understanding the background of floating body motions. Secondly, the employed numerical models (CHARM3D and FAST) are introduced. The coupled model of a floating wind turbine is developed based on these models. Lastly, physical and computational background of the coupling model is presented.

2.1 Dynamics of floating structure

2.1.1 Introduction

Wave-structure interaction is an important phenomenon in offshore platforms. In this section, a basic concept of floating structure dynamic analysis is reviewed. First, wave and floating structure interaction in the frequency domain is reviewed. Second, the equation of motion of a floating body in the time domain is reviewed.

2.1.2 Wave and free floating structure interaction in the frequency domain

First of all, to estimate the floating body motions, the potential theory was applied and the velocity potential was calculated. Under the assumption of small motion with regards to amplitude, velocity potential can be written by equation (2.1).

$$\phi(x,y,z,t)=\phi_I+\phi_S+\phi_R=A\Phi_I+A\Phi_S+\sum_{j=1}^{6}\mathrm{X}_j\Phi_j \tag{2.1}$$

Where, $\phi_I = A\Phi_I$: incident wave component which represent potentials without the body obstructing the flow.

$\phi_S = A\Phi_S$: scattered wave component that stands for the disturbance of the incident waves due to the floating body.

$\phi_R = \sum_{j=1}^{6}\mathrm{X}_j\Phi_j$: radiated wave component which corresponds to the wave field generated by floating body motion.

In the frequency domain, the motion of floating body responding to incident regular wave with frequency ω can be written by equation (2.2).

$$\mathrm{X}_j = real\left\{\left|\mathrm{X}_j\right| e^{i\left(\omega t+\zeta_j\right)}\right\} \tag{2.2}$$

where, ζ_j : phase difference

j : numbers 1 to 6 which represent the motion of floating system at each direction (Surge, Sway, Heave, Roll, Pitch, Yaw).

2.1.3 Governing equation of free floating body motion in the time domain

In the time domain analysis, the governing equation of free-floating body motion is from linear and angular momentum conservation.

$$\left[\mathbf{M}+\mathbf{M}^{\mathbf{a}}(\infty)\right]\ddot{\boldsymbol{\xi}}+\mathbf{K}\boldsymbol{\zeta}=\mathbf{F}_{\mathbf{I}}(\mathrm{t})+\mathbf{F}_{\mathrm{R}}(\mathrm{t},\dot{\zeta})+\mathbf{F}_{\mathrm{N}}(\mathrm{t},\dot{\zeta}) \tag{2.3}$$

where, $\mathbf{M}$: 6×6 body mass matrix

$\mathbf{M}^{a}(\infty)$: added mass

$\mathbf{K}$: hydrostatic stiffness matrix

$\mathbf{F}_{I}(t)$: first- and second-order wave exciting force on the floating body.

$\mathbf{F}_{R}(t,\dot{\zeta})$: radiation damping force $(=\int_{-\infty}^{t} R(t-\tau)\dot{\zeta}d\tau)$

where, $R(t)=\frac{2}{\pi}\int_{0}^{\infty} C(\omega)\frac{\sin \omega t}{\omega}d\omega$

($C(\omega)$ is the wave damping coefficient at frequency ω)

$$[M]=\begin{bmatrix} m & 0 & 0 & 0 & mz_{B,g} & -my_{B,g} \\ 0 & m & 0 & -mz_{B,g} & 0 & mx_{B,g} \\ 0 & 0 & m & my_{B,g} & -mx_{B,g} & 0 \\ 0 & -mz_{B,g} & my_{B,g} & \left(I^{B}_{XX}\right) & -I^{B}_{YX} & -I^{B}_{Zx} \\ mz_{B,g} & 0 & -mx_{B,g} & -I^{B}_{XY} & (I^{B}_{YY}) & -I^{B}_{ZY} \\ -my_{B,g} & mx_{B,g} & 0 & -I^{B}_{XZ} & -I^{B}_{YZ} & \left(I^{B}_{ZZ}\right) \end{bmatrix} \quad (2.4)$$

where, m : body mass

$x_{B,g}$, $y_{B,g}$, $z_{B,g}$: coordinates of center of gravity

$$[K]=\begin{bmatrix} 0 & 0 & 0 & 0 & 0 & 0 \\ 0 & 0 & 0 & 0 & 0 & 0 \\ 0 & 0 & \rho g A^{(0)} & \rho g \mathrm{I}_Y^A & -\rho g A_X^A & 0 \\ 0 & 0 & \rho g \mathrm{I}_Y^A & \rho g\left[\mathrm{I}_{YY}^A + V^{(0)} z_{B,b}\right] - mgz_{B,g} & -\rho g \mathrm{I}_{XY}^A & -\rho g V^{(0)} x_{B,b} + mgx_{B,g} \\ 0 & 0 & \rho g \mathrm{I}_X^A & \rho g \mathrm{I}_{YX}^A & \rho g\left[\mathrm{I}_{XX}^A + V^{(0)} z_{B,b}\right] - mgz_{B,g} & -\rho g V^{(0)} y_{B,b} + mgy_{B,g} \\ 0 & 0 & 0 & 0 & 0 & 0 \end{bmatrix} \tag{2.5}$$

where, $A^{(0)}$: waterplane area

$V^{(0)}$: submerged volume

$x_{B,b}$, $y_{B,b}$, $z_{B,b}$: coordinates of center of buoyancy

I_X^A, I_Y^A, I_{XX}^A, I_{YY}^A, $I_{XY}^A = I_{YX}^A$: moments of waterplance area

2.2 Computational models

2.2.1 Introduction

In this section, computational models are introduced. In this research, the fully coupled dynamic analysis model of a floating offshore wind turbine system is developed based on two existing models: CHARM3D and FAST.

2.2.2 CHARM3D

CHARM3D is an efficient 3-D hull/mooring/riser coupled dynamics program based on the finite element method. CHARM3D assumes that the floating body is a rigid body undergoing motion in waves, wind and current. Linear translational/rotational springs and linear translational dampers represent the connections between the floating body and the mooring lines. CHARM3D performs coupled dynamic analyses both in the time

domain and in the frequency domain. In the time domain analysis, various nonlinearities such as the drag force on the mooring lines, the free surface effects, body motion, and the geometric non-linearity of the mooring system are included in a time marching scheme (Cozijn, and Bunnik., 2004). The hydrodynamic forces on the floating body are evaluated by the diffraction theory. The viscous force on the floating body and the hydrodynamic forces on the mooring and riser are calculated in CHARM3D. After calculating the hydrodynamic force on the hull/mooring/riser, the hull/mooring/riser coupled equation of motion is simultaneously solved by CHARM3D. The output of CHARM3D includes the following: the wave elevation, the displacements, velocity, and acceleration of the floating body, the external forces, the nodal point of the legs, the nodal reaction forces of legs, the nodal axial tension of the legs, and the top tension of the legs in the time domain. More information about CHARM3D can be found in the WINTCOL/WINPOST User's Manual (Kim, 1997).

2.2.3 FAST

FAST (Fatigue, Aerodynamics, Structures, and Turbulence) is a comprehensive aeroelastic model for two-and three-bladed horizontal axis wind turbines (Jonkman J.M, and Sclvounos, 2006). This model represents a merger of three different numerical models: FAST2 (code for two-bladed horizontal axis wind turbines), FAST3 (code for three-bladed horizontal axis wind turbines), and AeroDyn (aerodynamics subroutine for horizontal axis wind turbines). In FAST, the hub and the nacelle are assumed to be rigid bodies. A drivetrain's torsional flexibility is represented as linear spring and damper, and

flexibility in the blades, and a tower, is modeled as a linear modal based on the small deflection assumption. These flexibilities are determined by distributed stiffness, mass properties, and mode shapes. In FAST, there are limitations on mode shape. In a blade, two flapwise and one edgewise bending modes are allowed. In a tower, two fore-aft and two side-to-side bending modes are permitted (Withee, 2004). To solve the nonlinear equation of motion, two kinds of time marching schemes are used: Runge-Kutta method is used before the 4th time step and Adams Bashforth Molton method is used from the 5th time step.

FAST can analyze two kinds of wind turbines: a two-bladed horizontal axis wind turbine, and a three-bladed horizontal axis wind turbine. For a two-bladed horizontal axis wind turbine model, FAST considers 22 degrees of freedom (DOF). Counted degrees of freedom are: platform translation and rotation (6 DOF), tower flexibility (4 DOF), nacelle yaw (1 DOF), variable generator and rotor speeds (2 DOF), blade teetering (1 DOF), blade flexibility (6 DOF), rotor furl (1 DOF), and tail furl (1 DOF). For the three-bladed horizontal axis wind turbine model, FAST considers 24 degrees of freedom: platform translation and rotation (6 DOF), tower flexibility (4 DOF), nacelle yaw (1 DOF), variable generator and rotor speeds (2 DOF), blade flapwise (6 DOF), blade displacement (3 DOF), rotor furl (1 DOF), and tail furl (1 DOF).

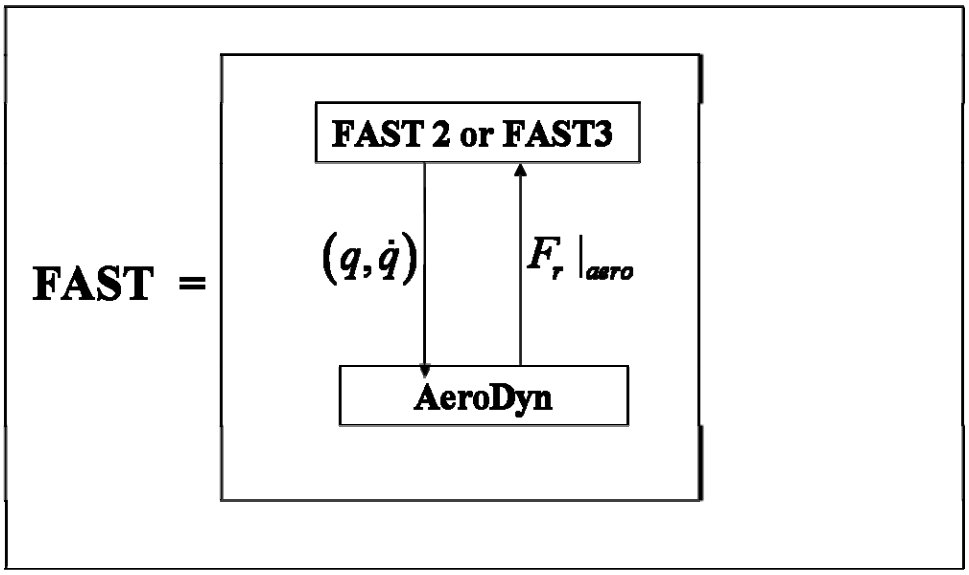

Figure 2-1 Structure of FAST

To model dynamic responses of wind turbines, FAST is constructed by two parts: the dynamic analysis routine (FAST2, and FAST3), and the aerodynamic loads calculation routine (AeroDyn). The structure of FAST is shown in figure 2.1. To simulate the dynamics of the wind turbine, there are two steps. First, the aerodynamic loads calculation routine (AeroDyn) computes the aerodynamic load $\left(F_r|_{aero}\right)$ at each blade element based on a generated flow model and displacement and velocity of the blades $(q,\dot{q})$, which is calculated by the dynamic analysis routine (FAST3, and FAST3). Second, the dynamic analysis routine (FAST2, FAST3) determines the dynamic response of the conventional horizontal axis wind turbines under the aerodynamic load$\left(F_r|_{aero}\right)$. More information about FAST can be found in the FAST User's Guide (Jonkman, Jason, and Buhl, 2004).

2.3 The concept of coupled model of floating offshore wind turbine

2.3.1 Introduction

In this section, physical and numerical backgrounds of the model are presented. The equations of motion of each model are introduced. In addition, detailed procedures of coupling are presented.

2.3.2 Process of time domain coupling simulation

In this research, a model of a fully-coupled dynamic system for the offshore floating wind turbine system is proposed based on the existing numerical models - CHARM3D and FAST.

Practical models of the floating body and the wind turbine are employed to develop a fully-coupled dynamic model of an offshore floating wind turbine system. For the time domain coupling calculation between the floating body and mooring lines, hydrodynamic coefficients are obtained by a panel-based 3D diffraction and radiation program, WAMIT. The results of a panel-based 3D diffraction and radiation program are RAOs (Response amplitude operator), added mass, radiation–damping coefficients, wave force linear transfer function, and drift forces.

In a floating wind turbine, many dynamic phenomena are expected. Above the floating body, there is a huge rotating rotor; it can produce a lot of dynamic loads and can affect the global motion of the floating body. Also, the motion of floating body can affect turning rotor and wind turbine. The equation of motion of the wind turbine's

floating body is solved in the time domain. For the wind turbine dynamics, the resulting floating body motion and velocity are used as inputs. Also for floating body motion dynamics, the resulting wind turbine dynamic loads are used as an external force in the floating body's governing equation of motion. This basic concept of coupling is shown in figure 2-2.

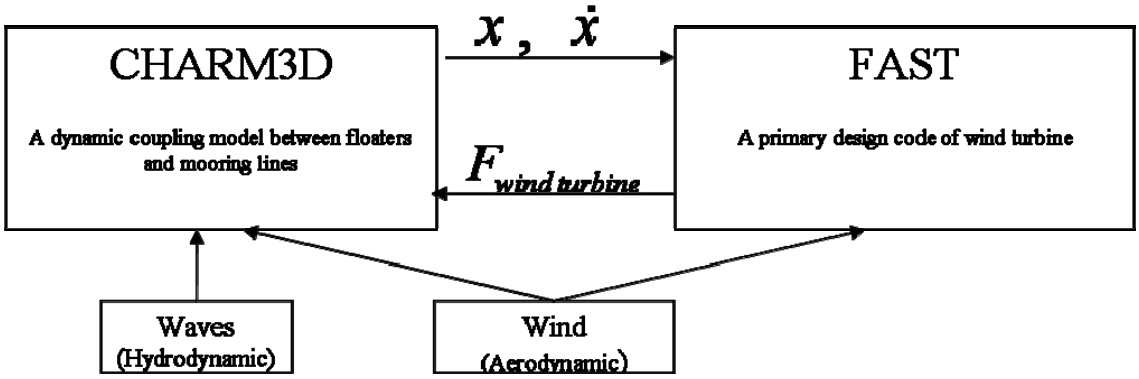

Figure 2-2 Basic computational concept of coupling analysis

2.3.3 Numerical model for the coupled floating wind turbine in the time domain

Because of the high nonlinearity in wind turbine motion and force, the equation of motion of the floating wind turbine is formulated in the time domain. Based on the small angle hypothesis, linear assumptions are made about the floating wind turbine and hydrodynamic loads. The transient motion of the floating body is mathematically represented by the use of an impulse response function and wave exciting force calculated from the 3D frequency domain panel method. The equation of motion of the floating body is given by equation (2.6).

$$\left(\mathbf{M}+\delta\mathbf{M}(\infty)\right)\ddot{\boldsymbol{\xi}}+\int_{-\infty}^{t}\mathbf{R}(t-\tau)\dot{\boldsymbol{\xi}}(\tau)d\tau+\mathbf{b}\dot{\boldsymbol{\xi}}+\mathbf{K}\boldsymbol{\xi}=\mathbf{f} \tag{2.6}$$

where, $\mathbf{M}$ is the mass matrix of the floating body, $\delta\mathbf{M}(\infty)$ is the added mass of the floating body, $\mathbf{R}$ is the retardation function matrix, $\mathbf{b}$ is the linear damping matrix, $\mathbf{K}$ is the restoring matrix from hydrostatics and moorings, $\mathbf{f}$ is the external forces (hydrodynamic and aerodynamic loads) on the floating body, ξ is the degrees of freedom of floating body, $\dot{\xi}$ is the first time derivatives of the degrees of freedom, $\ddot{\xi}$ is the second time derivatives of the degrees of freedom.

The retardation function, $R(t)$, is given by equation (2.7)

$$R(t) = \frac{2}{\pi}\int_0^\infty b(\omega)\cos(\omega t)\,d\omega \tag{2.7}$$

The complete nonlinear aeroelastic equation of motion for the wind turbine is equation (2.8)

$$\mathbf{M}_{ij}(q,u,t)\ddot{q}_j + \mathbf{f}_i(q,\dot{q},u,t) = 0 \tag{2.8}$$

where, $\mathbf{M}_{ij}$ is the *(i,j)* component of the inertia mass matrix, $\mathbf{f}$ is the forcing function, u is the set of wind turbine control inputs, q is the degrees of freedom of the wind turbine, $\dot{q}$ is the first time derivative of degrees of freedom, $\ddot{q}$ is the second time derivatives of degree of freedom, and t is the time. Based on the FAST manual, we can rewrite eq (2.9) as following:

$$\mathbf{F}_r^* + \mathbf{F}_r = 0 \quad (r = 1,2,...,P) \tag{2.9}$$

where, P is the number of degrees of freedom, and $\mathbf{F}_r^*$ is the generalized inertia forces, and $\mathbf{F}_r$ is the generalized active forces which includes everything except inertia forces. In the wind turbine model in FAST, the masses of the tower, nacelle, hub, and blades

contribute to the total generalized inertia forces:

$$F_r^* = F_r^*\Big|_{Tower} + F_r^*\Big|_{Nacelle} + F_r^*\Big|_{Hub} + F_r^*\Big|_{blades} \tag{2.10}$$

We can describe in detail follows:

$$F_r^*\Big|_{Tower} = -\int_0^H \mu_T(h)\, {}^E v_r^T \cdot {}^E a^T dh \tag{2.11}$$

where, $\mu_T(h)$ is the tower's distributed lineal density, ${}^E v_r^T$ is the r^{th} partial velocity associated with point T in the tower, and ${}^E a^T$ is the acceleration of the same point in the inertial frame.

$$F_r^*\Big|_{Nacelle} = {}^E v_r^D \cdot \left(-m_N\, {}^E a^D\right) + {}^E \omega_r^N \cdot \left(-{}^E \dot{H}^D\right) \tag{2.12}$$

where, ${}^E v_r^D$ is the r^{th} partial velocity associated with the center of mass (point D) of the nacelle, m_N is the mass of the nacelle, ${}^E a^D$ is the acceleration of the center of mass of the nacelle in the inertial frame, ${}^E \omega_r^N$ is the r^{th} partial angular velocity associated with the nacelle, and ${}^E \dot{H}^D$ is the time derivative of angular momentum of the nacelle about its center of mass in the inertial frame,

$$F_r^*\Big|_{Hub} = {}^E v_r^C \cdot \left(-m_H\, {}^E a^C\right) + {}^E \omega_r^H \cdot \left(-{}^E \dot{H}^C\right) \tag{2.13}$$

where, ${}^E v_r^C$ is the r^{th} partial velocity associated with the center of mass (point C) of the hub mass, ${}^E a^C$ is the acceleration of the center of mass of the hub in the inertial frame, ${}^E \omega_r^H$ is the r^{th} partial angular velocity associated with the hub, ${}^E \dot{H}^D$ is the time derivative of angular momentum of the hub about its center of mass in the inertial frame.

$$F_r^*\Big|_B = -\int_0^{R-R_H} \mu_B(r_1)\, {}^E v_r^{S_1} \cdot {}^E a^{S_1} dr_1 - \int_0^{R-R_H} \mu_B(r_2)\, {}^E v_r^{S_2} \cdot {}^E a^{S_2} dr_2 \tag{2.14}$$

where, $\mu_B(r)$ is the distributed lineal density of the blade, ${}^{E}v_r^{S_i}$ is the r^{th} partial velocity associated with point S in the blade *i* (*i* = 1, 2, and 3), ${}^{E}a^{S_i}$ is the acceleration of the same point in the inertial frame.

Also, the resultant of all applied forces action on elements of the wind turbine contributes to the total generalized active forces that govern the equation of motion. The forces include aerodynamic forces, elastic forces from the tower, blade, and drivetrain flexibility, gravitational forces, generator forces, and damping forces.

$$F_r = F_r\big|_{aero} + F_r\big|_{elastic} + F_r\big|_{gravity} + F_r\big|_{generator} + F_r\big|_{damp} \tag{2.15}$$

In equation (2.15), the first term of the equation is the aerodynamic loads which represent an external load (Jonkman, 2003). This is calculated by the aerodynamic subroutine, AeroDyn, based on wind speed and the blades' displacement and velocity, which are calculated by the dynamic analysis routine, FAST2 or FAST3. The second, third, and fourth terms of the equation are stiffness terms. The fifth term of the equation is a damping term. Details of each term are beyond the scope of this work and will not be covered here.

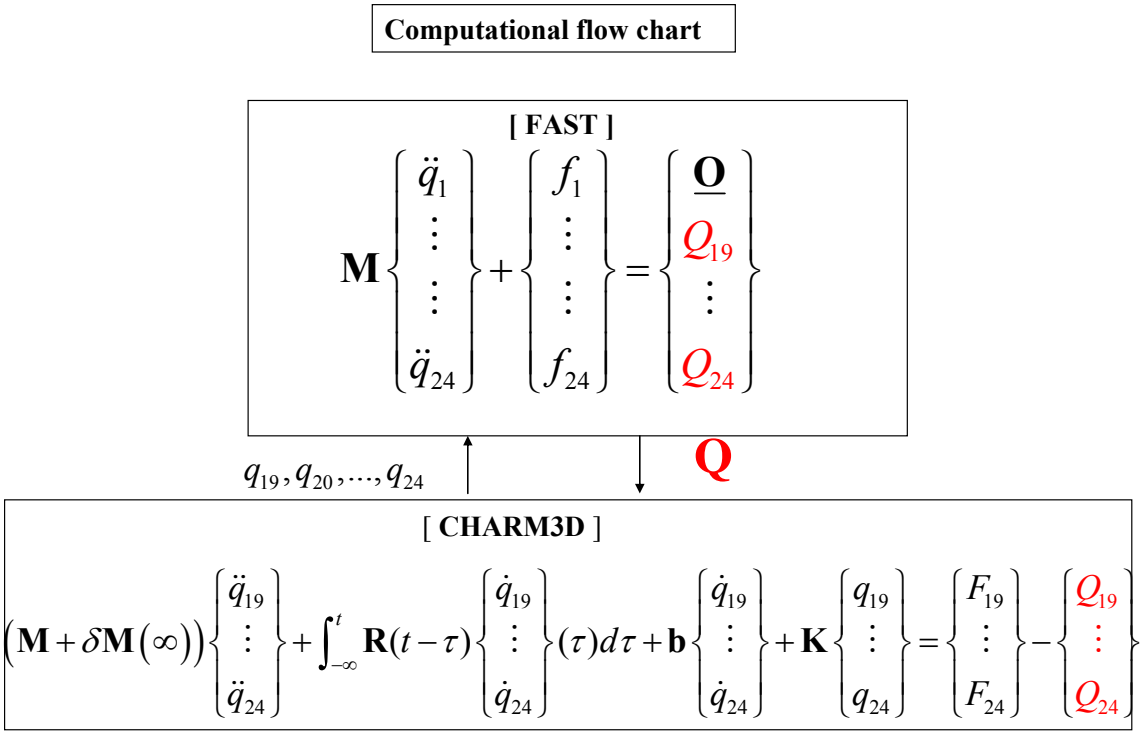

Figure 2-3 Detailed computational concept of coupling analysis

The computational model of this research is shown in figure 2-3. A developed model of a fully-coupled dynamic system for the offshore floating wind turbine system has two parts: CHARM3D (floating body part) and FAST (wind turbine part). To make a fully-coupled dynamic model, first, CHARM3D calculates six degrees of freedom of the floating body's motion based on solving the equation of motion. One of the external force terms (response forces of dynamics of the wind turbine, $Q_{19}, Q_{20}, \ldots, Q_{26}$) of the equation of motion comes from FAST. Second, FAST calculates the dynamics of a wind turbine based on the aerodynamic and dynamic analysis routines. For a three-bladed

horizontal axis wind turbine model, FAST has 24 degrees of freedom $(q_1, q_2, ..., q_{24})$, which includes six degrees of freedom $(q_{19}, q_{20}, ..., q_{24})$ from the floating body. These six degrees of freedom for the floating body are used as input when FAST analyzes that dynamics of a wind turbine. The output of a developed model of a fully coupled dynamic system for the offshore floating wind turbine system provides following: the wave elevation, the displacements, velocity, and acceleration of the floating body, the external forces, the nodal point of the legs, the nodal reaction forces of the legs, the nodal axial tension of the legs, the top tension of the legs in the time domain, and the dynamic reaction forces of the wind turbine.

3. CASE STUDIES

The wind turbines used in the case studies are the 1.5 MW Baseline wind turbine and the modified Baseline wind turbine. They are three horizontal axis wind turbines, and all the models are obtained from the National Renewable Energy Laboratory (NREL). This wind turbine was evaluated by FAST and certified by NREL. A part of the design concept of the floating body was obtained from Massachusetts Institute of Technology (MIT). There was a joint research of the offshore wind turbine between the NREL and MIT. The first part of the case studies is performed on the 1.5 MW Base line wind turbine with different wind speeds: 5m/s, 8m/s, 11m/s. The second part of the case study is performed on the modified Baseline wind turbine. The modified Baseline wind turbine represents same mass, stiffness, and damping properties as the 1.5 MW Base line wind turbine but large size blades with less density are introduced.

3.1 Pre-process: floating body motion analysis in frequency domain

3.1.1 Introduction

In this section, pre-process is performed by WAMIT. A frequency domain analysis of the floating body which has the mass of the wind turbine is presented. 3-D panel program, WAMIT, is used to perform frequency domain analysis. Added mass, damping, exciting force, drift force, and RAOs (Response Amplitude Operator) are obtaining using WAMIT. In the frequency analysis, 0 degree wave heading is considered based on 16

wave frequencies from 0.05 to 1.5 (rad/s) with 0.1 (rad/s) intervals. The total system (floating body + wind turbine) mass matrix is used. The external stiffness which represents 4 tethers is applied. In case studies, high modulus polyethylene (HMPE) is used as a material type of tethers. Table 3-1 and 3-2 shows mass matrix information of floating body and wind turbine.

Table 3-1 Characteristics of the 1.5 MW baseline wind turbine

Power output (MW)	1.5	Blade mass (kg)	11756 kg
Hub height (m)	84.29	Nacelle Mass (kg)	51200 kg
Rotor Diameter (m)	70 m	Hub Mass (kg)	15100 kg
Number of blades	3	Tower mass (kg)	123003 kg
Initial rotational speed (rpm)	20	Number of tower segments	10
Ixx $\left(kg \cdot m^2\right)$	7.45E8	Number of elements of a blade	21
Iyy $\left(kg \cdot m^2\right)$	7.44E8	Izz $\left(kg \cdot m^2\right)$	1.82E6

Table 3-2 Characteristics of the TLP type floating body with water depth 200 m

Spar diameter (m)	10	Structure thickness (cm)	2.53
Spar length (m)	12	Mass of floating body (kg)	210435.4
Tower diameter (m)	8	Center of gravity of floating body (m)	-13.82
Tower draft (m)	5	Center of buoyancy (m)	-10.89
Spoke length (m)	20	Total submerged volume (m^3)	1270.57
Spoke width (m)	1	Number of tether (per spoke)	1
Spoke height (m)	1	Pretension of a tether (N)	2.0E6
Water depth (m)	200	Center of gravity of total system (wind turbine + floating system) (m)	16.98
Izz $\left(kg \cdot m^2\right)$	1.41E7	Ixx $\left(kg \cdot m^2\right)$ = Iyy $\left(kg \cdot m^2\right)$	4.39E7
Diameter of a tether (m)	0.104	Axial stiffness - EA (N)	9.94E8

3.1.2 RAO

In this study, sea-keeping analysis is performed using WAMIT, a panel-based 3D diffraction/radiation program based on potential theory. Response Amplitude Operator (RAO) is calculated for 16 wave frequencies from 0.05 to 1.5 (rad/s) with 0.1 (rad/s) intervals with 0 degree wave heading. The generated panel model is presented for WAMIT input in figure 3-1. RAOs in 6 degrees of freedom (surge, sway, heave, roll, pitch, and yaw) are shown in figures 3-2 to 3-7. The natural frequencies are obtained from mass, stiffness, and add mass. Surge and sway natural frequency is 0.18 rad/sec.

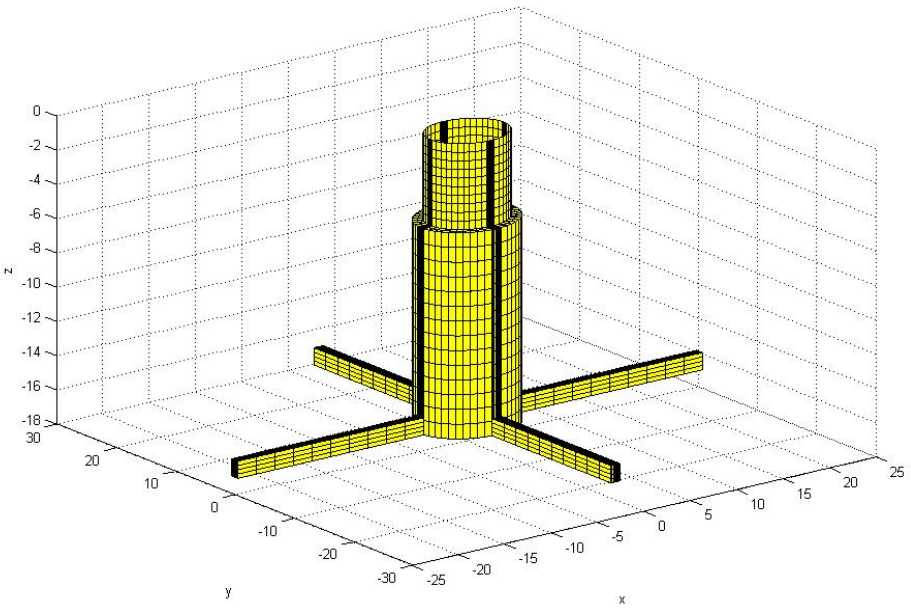

Figure 3-1 Mesh information for WAMIT (unit: meter)

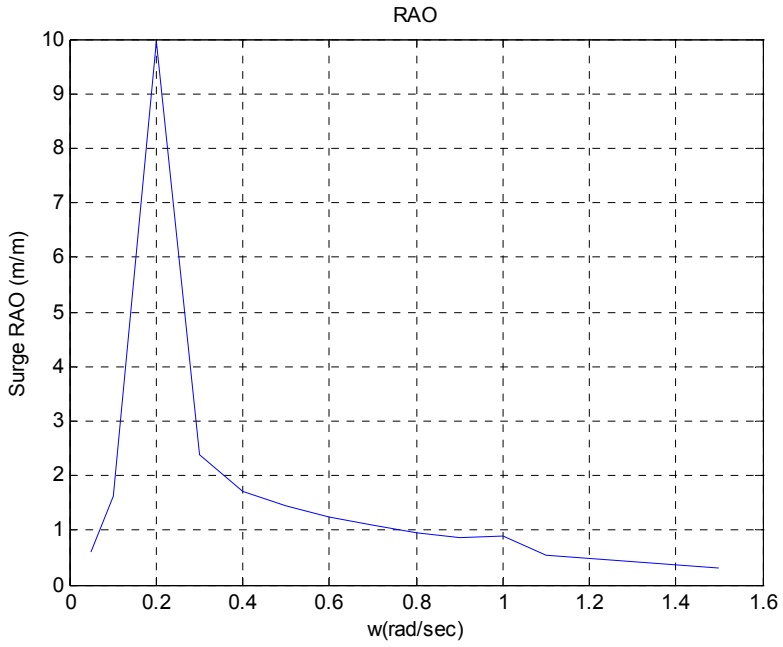

Figure 3-2 Surge RAO of the floating body of the offshore floating wind turbine in 0 degree wave heading

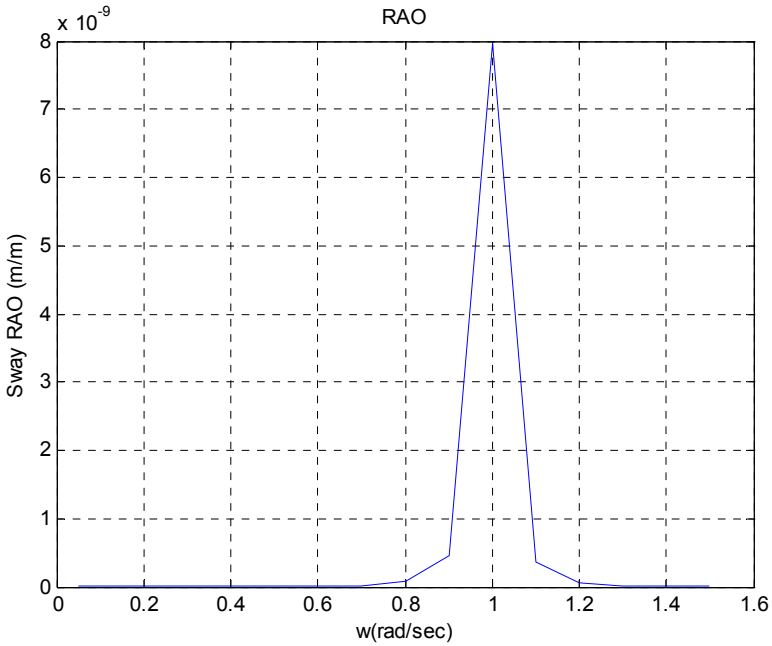

Figure 3-3 Sway RAO of the floating body of the offshore floating wind turbine in 0 degree wave heading

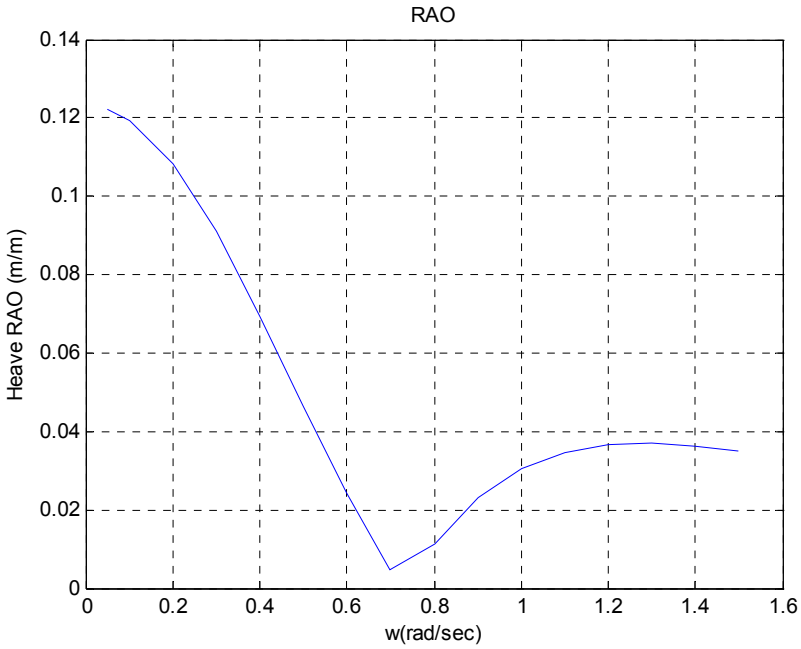

Figure 3-4 Heave of the floating body of the offshore floating wind turbine in 0 degree wave heading

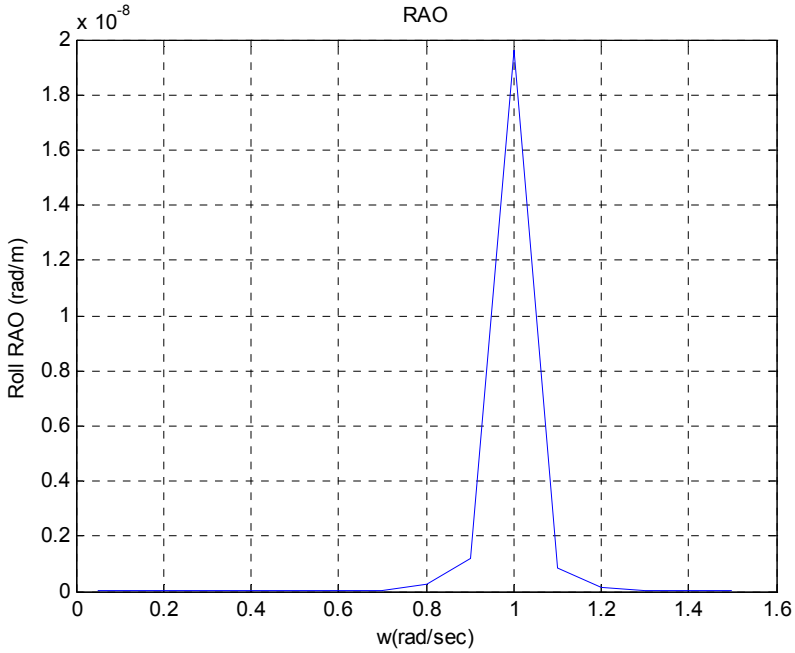

Figure 3-5 Roll of the floating body of the offshore floating wind turbine in 0 degree wave heading

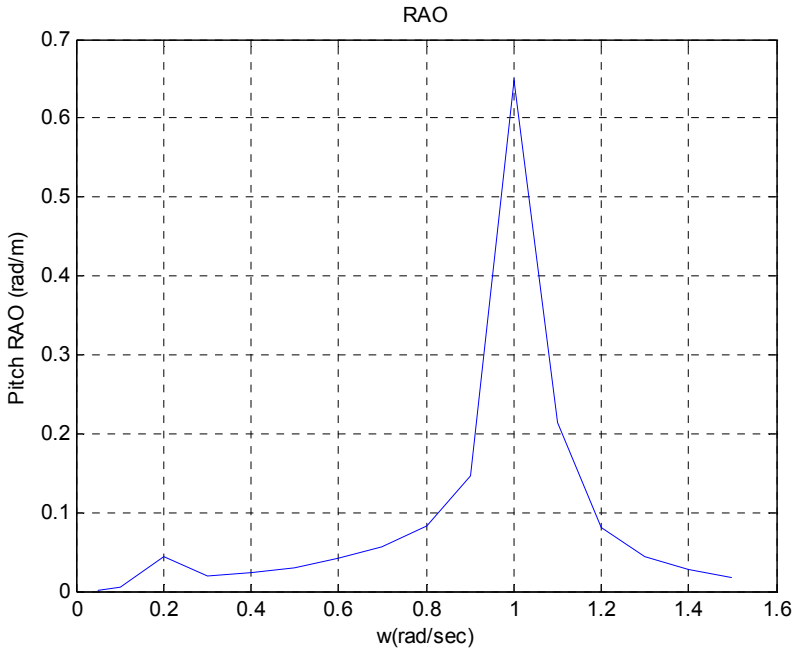

Figure 3-6 Pitch of the floating body of the offshore floating wind turbine in 0 degree wave heading

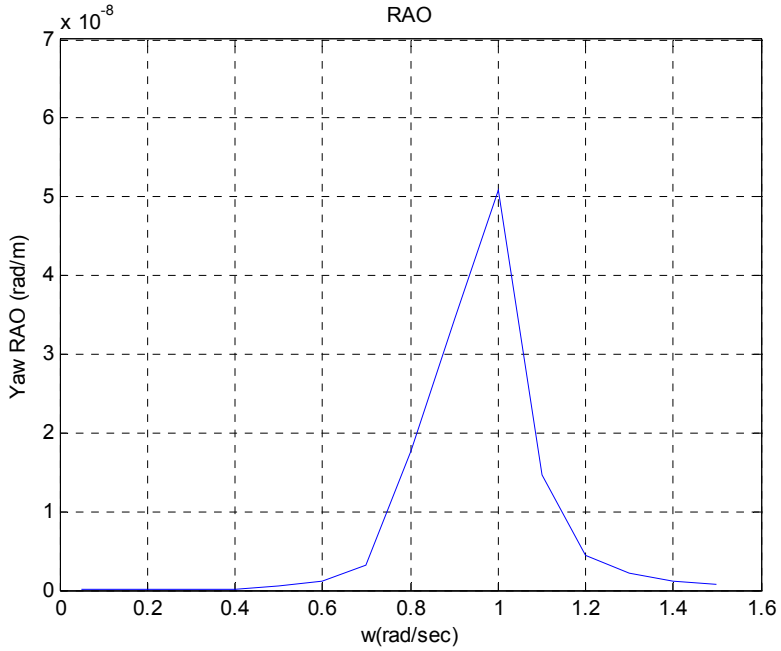

Figure 3-7 Yaw of the floating body of the offshore floating wind turbine in 0 degree wave heading

Since surge natural frequency is 0.18 rad/sec, a peak is observed in 0.2 rad/sec. Also since the incident wave angle is 0, sway, roll, and yaw RAO does not have a practical meaning. Magnitudes of RAOs are almost zero.

3.1.3 Added mass and damping coefficient

Added mass for the floating body of offshore floating wind turbine shows a spiky behavior at around 0.8 rad/sec. The added masses for the floating body are shown in figures 3-8 to 3-13. The damping coefficient gets a peak at around 1.2 rad/sec. The damping coefficients for the floating body are shown in figures 3-14 to 3-19.

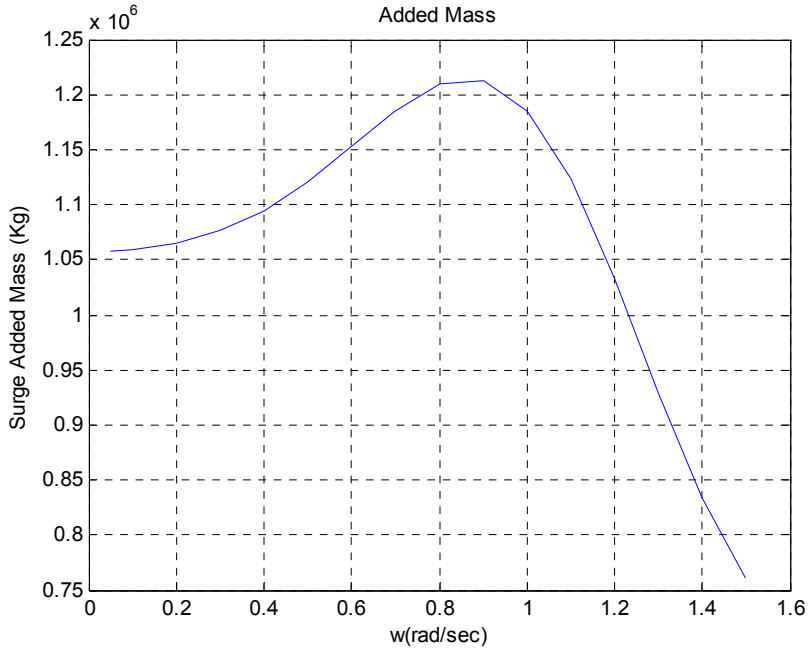

Figure 3-8 Surge added mass of the floating body of offshore floating wind turbine in 0 degree wave heading

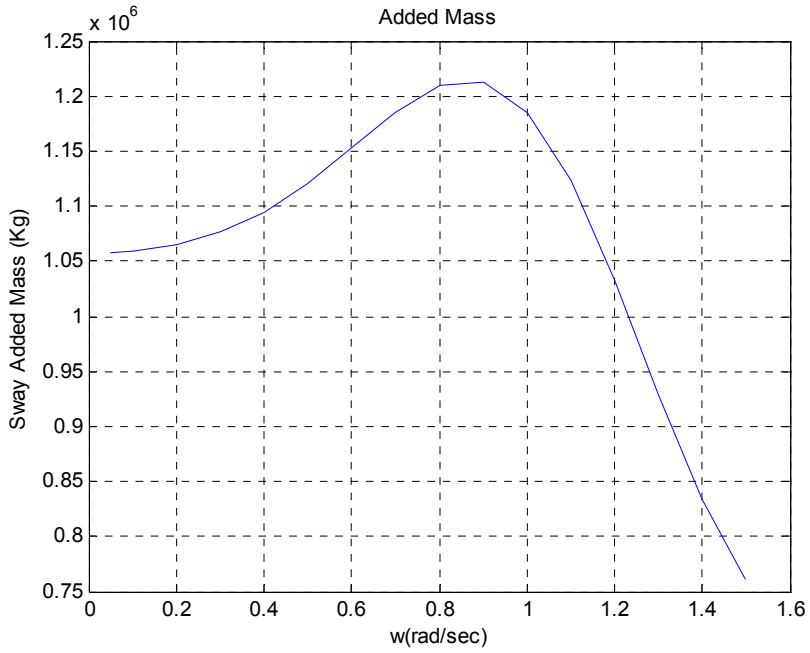

Figure 3-9 Sway added mass of the floating body of offshore floating wind turbine in 0 degree wave heading

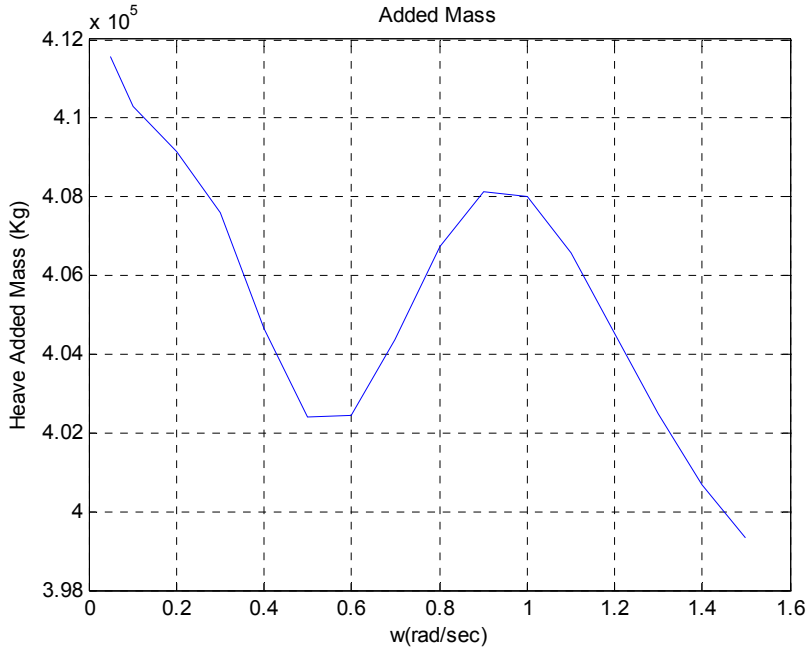

Figure 3-10 Heave added mass of the floating body of offshore floating wind turbine in 0 degree wave heading

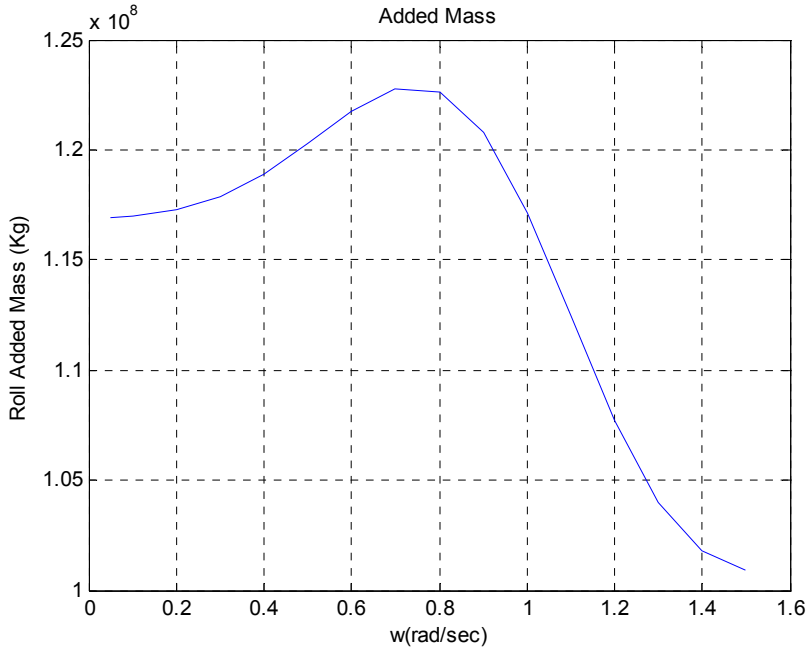

Figure 3-11 Roll added mass of the floating body of offshore floating wind turbine in 0 degree wave heading

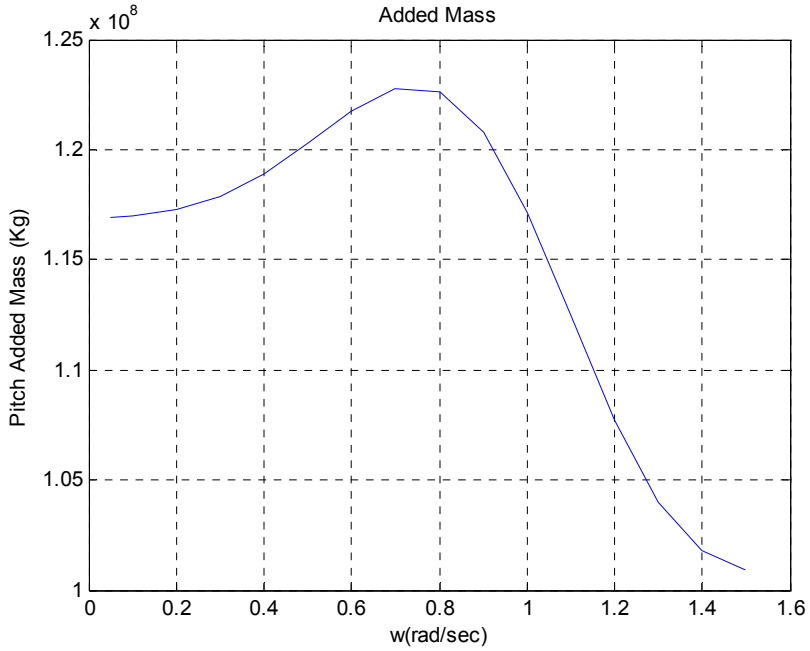

Figure 3-12 Pitch added mass of the floating body of offshore floating wind turbine in 0 degree wave heading

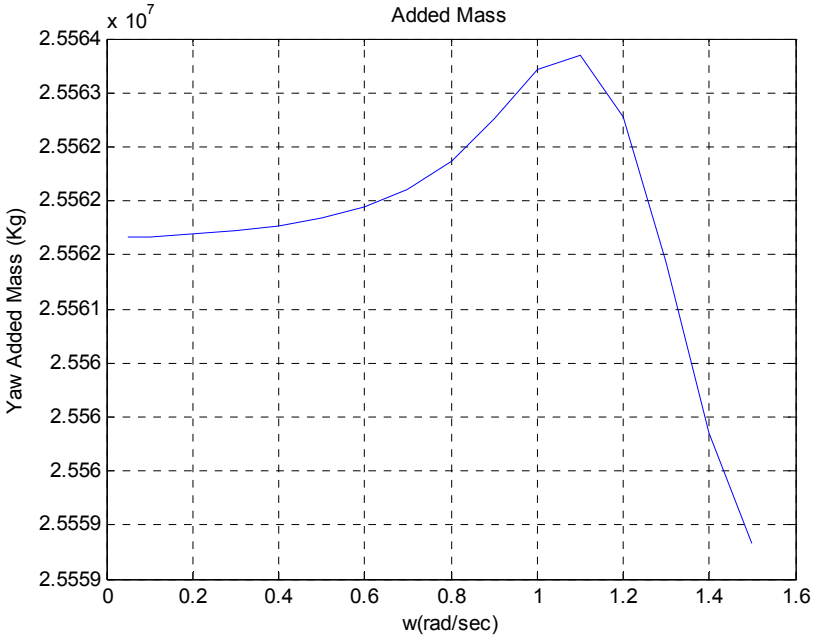

Figure 3-13 Yaw added mass of the floating body of offshore floating wind turbine in 0 degree wave heading

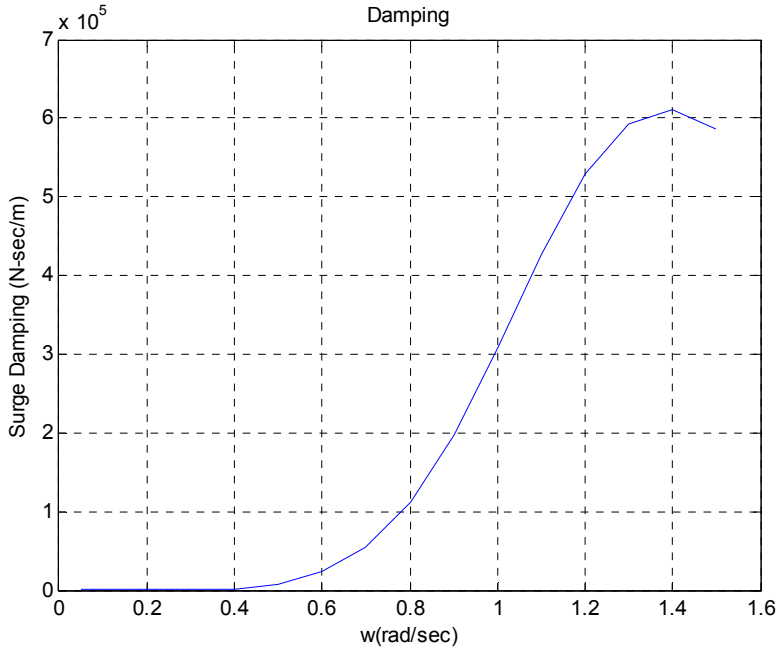

Figure 3-14 Surge damping coefficient of the floating body of the offshore floating wind turbine in 0 degree wave heading

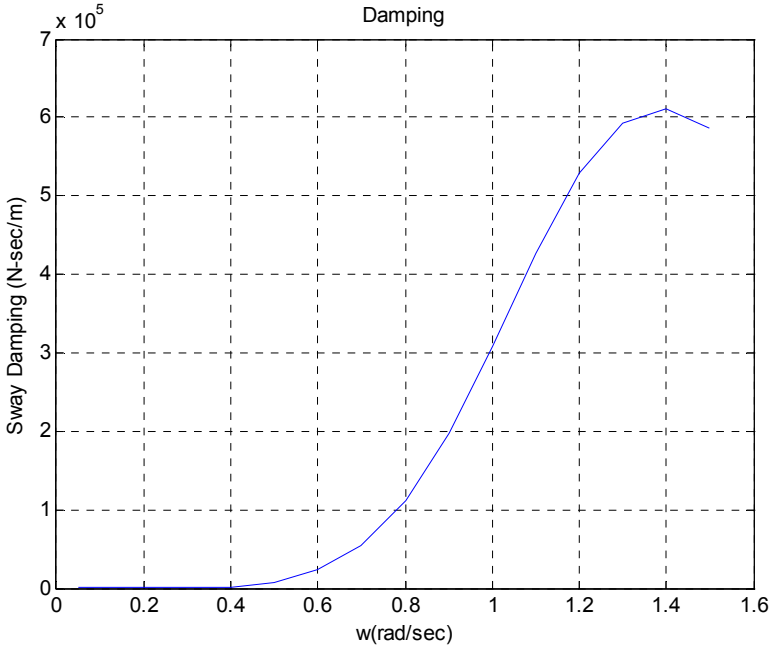

Figure 3-15 Sway damping coefficient of the floating body of the offshore floating wind turbine in 0 degree wave heading

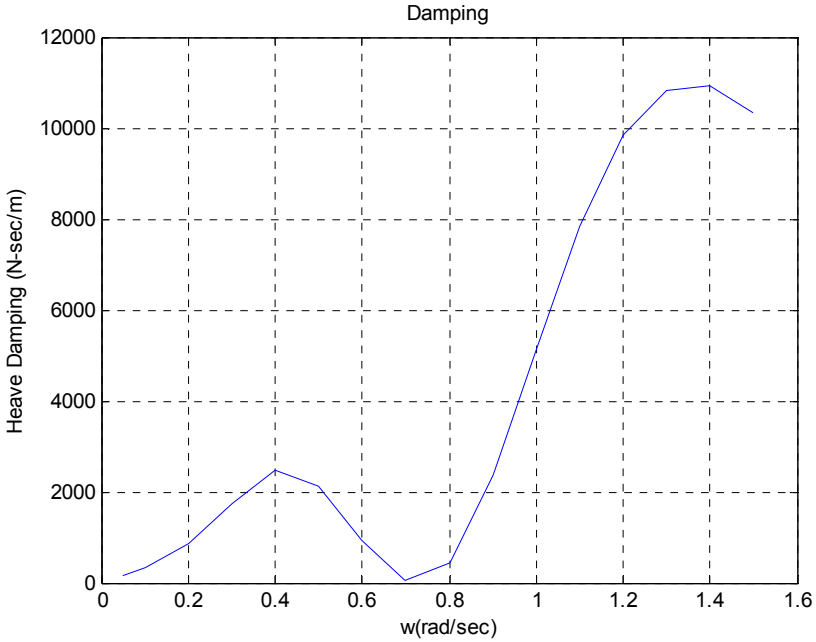

Figure 3-16 Heave damping coefficient of the floating body of the offshore floating wind turbine in 0 degree wave heading

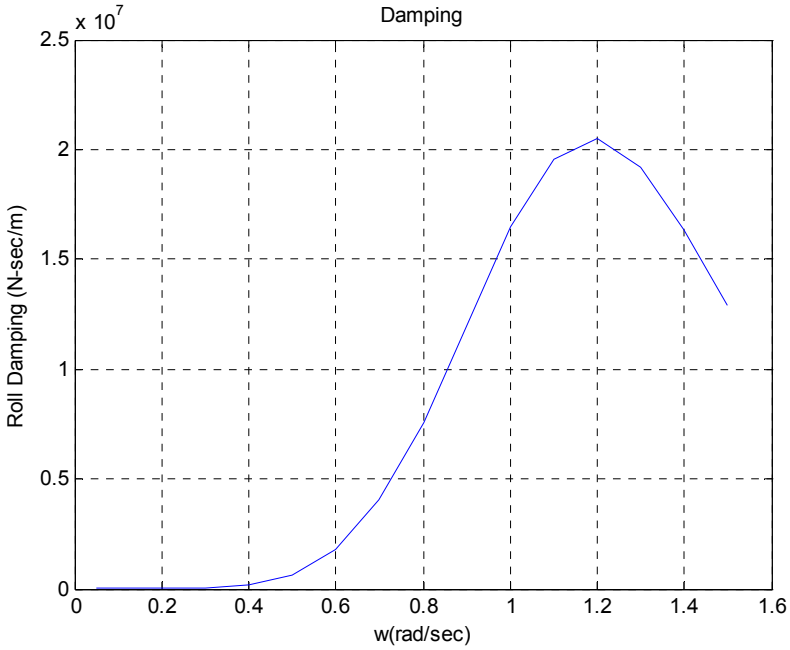

Figure 3-17 Roll damping coefficient of the floating body of the offshore floating wind turbine in 0 degree wave heading

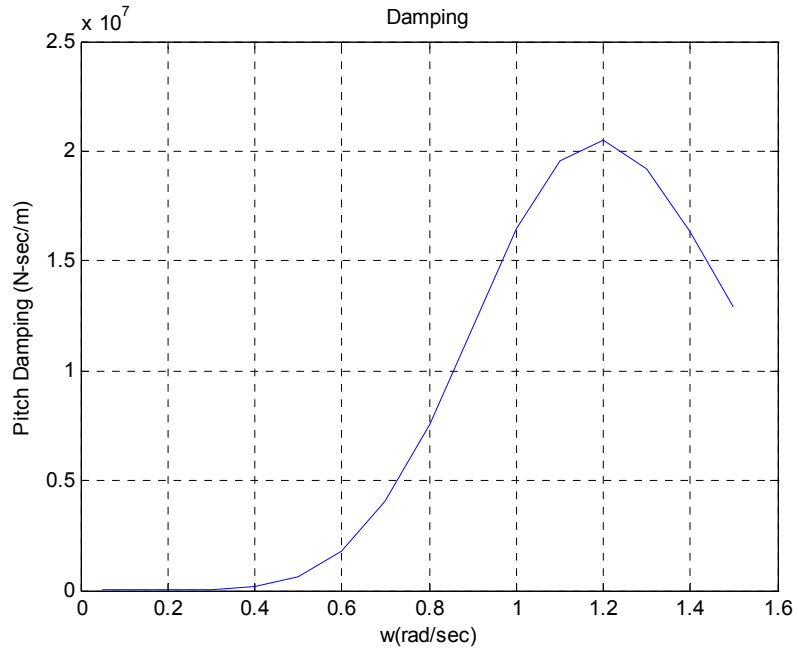

Figure 3-18 Pitch damping coefficient of the floating body of the offshore floating wind turbine in 0 degree wave heading

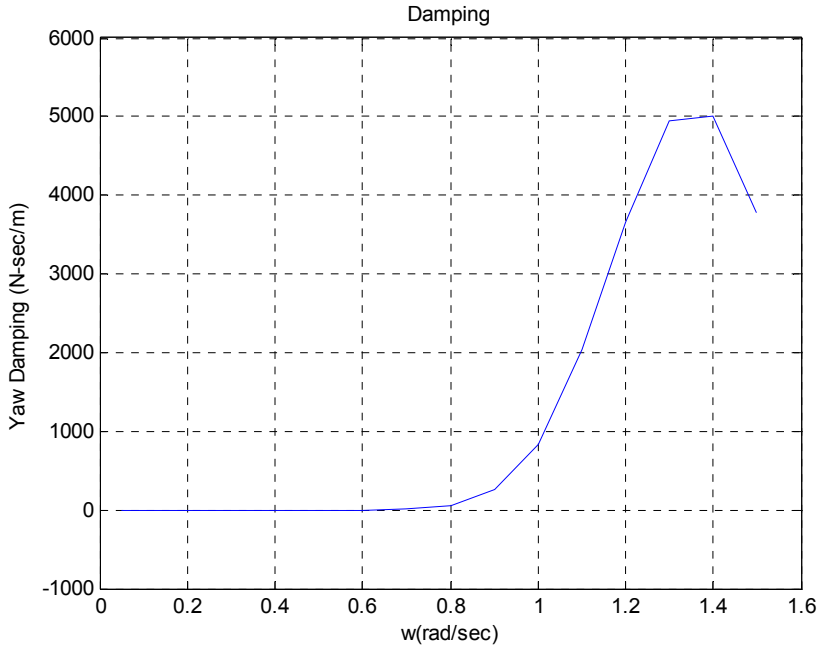

Figure 3-19 Yaw damping coefficient of the floating body of the offshore floating wind turbine in 0 degree wave heading

3.1.4 Exciting force and mean drift force

The wave exciting force and mean drift force on the floating body are also determined for 16 wave frequencies from 0.05 to 1.5 (rad/s) with 0.1 (rad/s) intervals with 0 degree wave heading. Since frequency-domain analysis is performed in 0 degree wave heading, we can only observe the wave exciting force in surge, heave and pitch. The wave exciting forces on the floating body of offshore floating wind turbine are shown in figure 3-20 to 3-22. The mean surge and sway drift force on the floating body of offshore floating wind turbine is shown in figures 3-23 and 3-24. Since the incident wave angle is zero, sway drift force are small and dose not have a practical meaning.

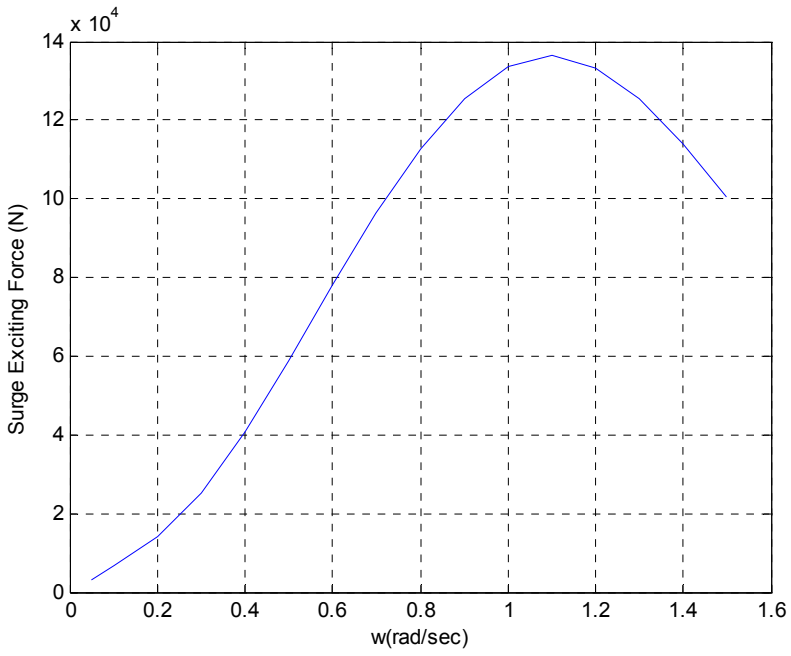

Figure 3-20 Surge wave exciting force on the floating body of the offshore floating wind turbine in 0 degree wave heading

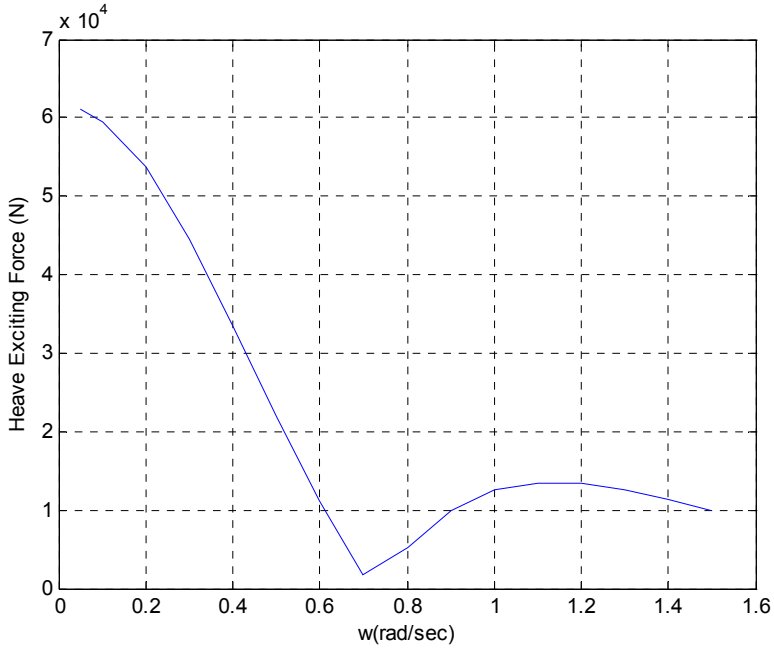

Figure 3-21 Heave wave exciting force on the floating body of the offshore floating wind turbine in 0 degree wave heading

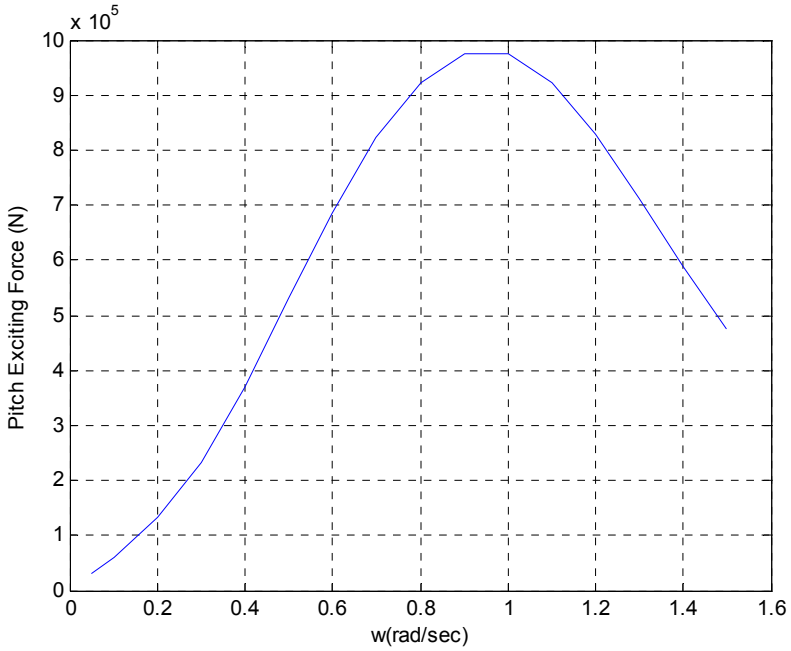

Figure 3-22 Pitch wave exciting force on the floating body of the offshore floating wind turbine in 0 degree wave heading

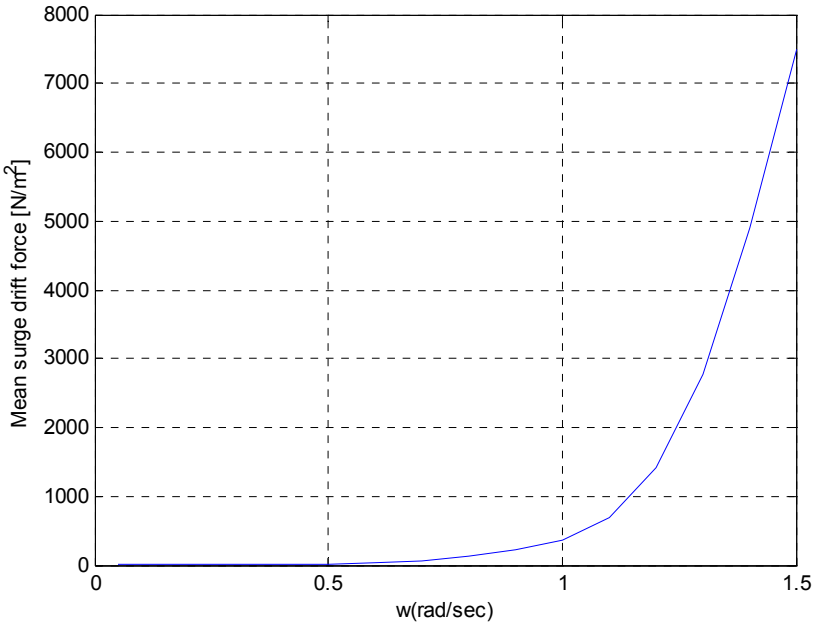

Figure 3-23 Surge mean drift force on the floating body of the offshore floating wind turbine in 0 degree wave heading

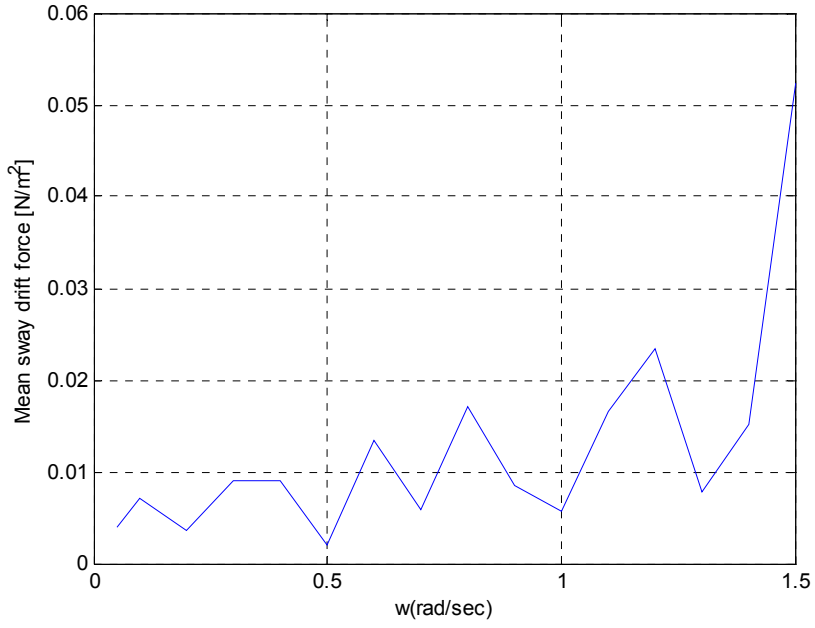

Figure 3-24 Sway mean drift force on the floating body of the offshore floating wind turbine in 0 degree wave heading

3.2 Coupling simulation for floating wind turbine with the in time domain

In time domain simulation, several simulations are performed on different wind speeds: 5m/s, 8m/s, and 11m/s. At each wind speed, a comparison study is performed between the coupled and uncoupled case. In this simulation it can be inferred from the uncoupled case that there is an offshore floating wind turbine that blades that are not rotating. Therefore, we only consider the wind loads of the projected area on blades in the simulation. Also, it can be inferred from the coupled case that we consider a floating wind turbine fully coupled which has every load on the rotating blade and inertia loads. Figure 3-25 shows an offshore floating wind turbine that is used in these case studies. Figure 3-26 represents the numbering of the leg of the floating body and the environmental forces' direction in the case studies. The running time of the simulation is 7500 sec (2.08 hours) with 0.05 sec interval.

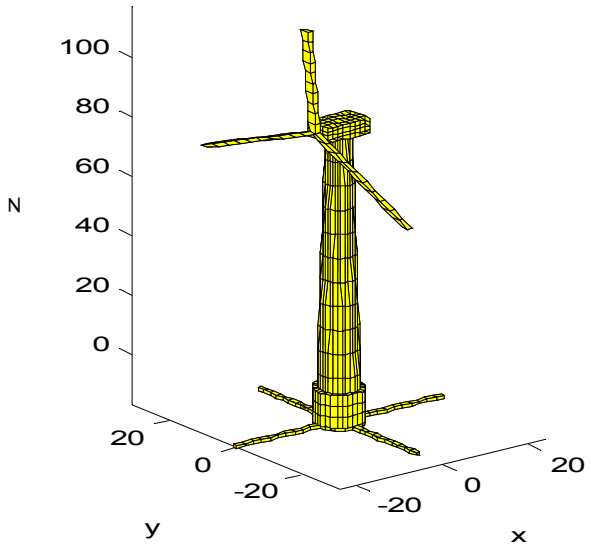

Figure 3-25 A model of the offshore floating wind turbine (unit: meter)

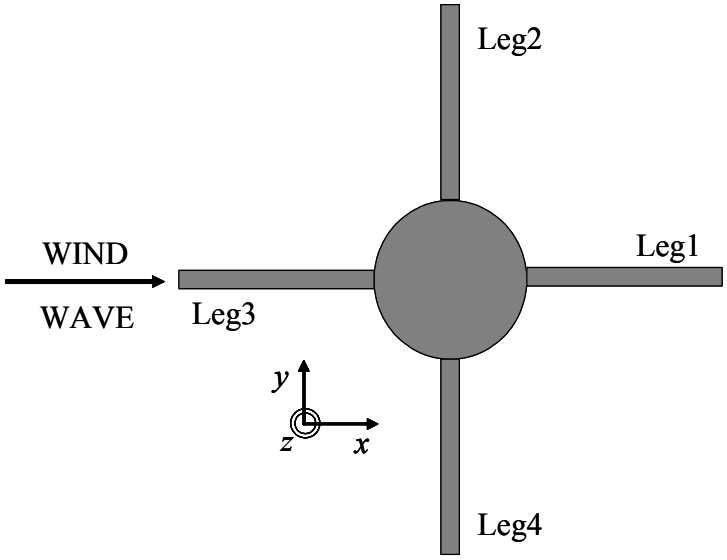

Figure 3-26 Numbering of legs and environmental forces' direction

Environmental condition is determined by table 3-3. In the case studies, we simulate three different environmental conditions. Wave elevation time series and spectrum are shown in figure 3-27. In these case studies, JONSWAP is used. Also wind force time history and spectrum of 11 m/s wind speed are shown in figure 3-28.

Table 3-3 Environmental condition

Wave heading: 0 degree			
Wind Input		Wave Input	
Reference Wind Speed (m/s)	Mean Wind Speed (hub) (m/s)	Significant Wave Height - $H_{1/3}$ (m)	Mean Wave Period - T_1 (seconds)
5	6.53	5.0	8.688
8	10.44	5.0	8.688
11	14.36	5.0	8.688

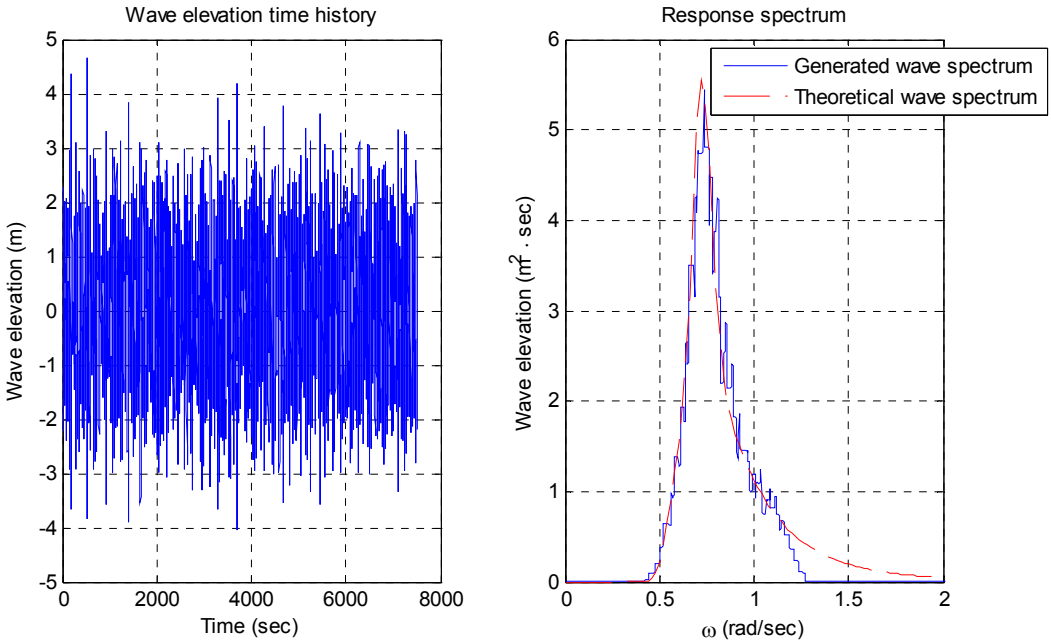

Figure 3-27 Wave elevation time series, spectrum, and theoretical input spectrum (Hs=5m, Tp=8.7 sec and Gamma=2.4)

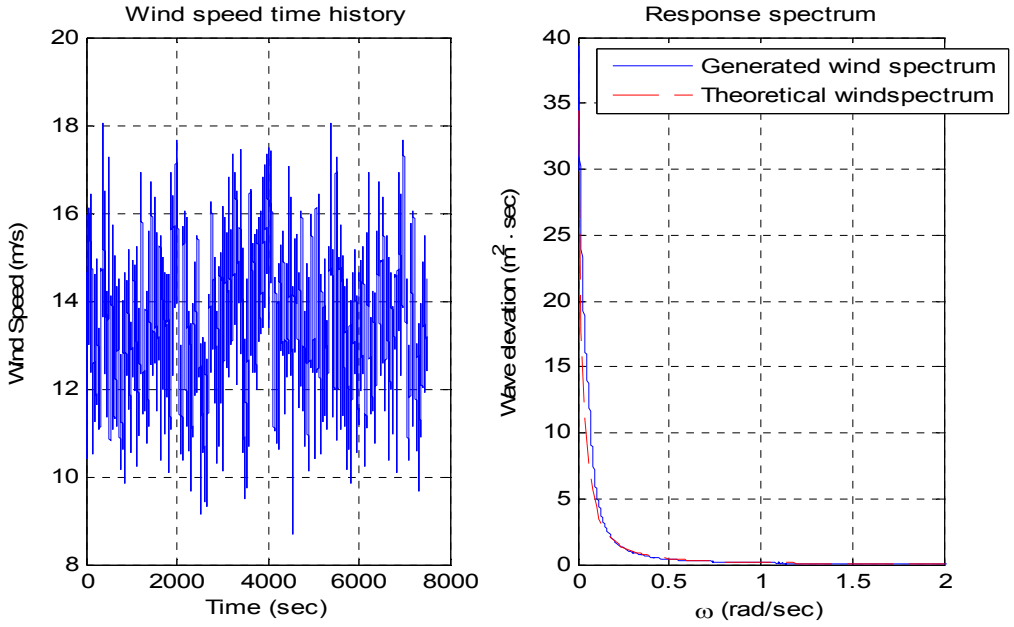

Figure 3-28 Wind force time history, spectrum, and theoretical API input spectrum (V10=11 m/s, V(z) = 14.38 m/s)

3.2.1 Wind speed 5m/s case

3.2.1.1 Uncoupled case in wind speed 5 m/s

3.2.1.1.1 External forces of the coupled case in wind speed 5 m/s

In uncoupled time domain analysis the time histories and spectra of two decomposed external forces are shown in figure 3-29. In uncoupled time domain simulation, the wind force and the wave force are external forces on the floating body.

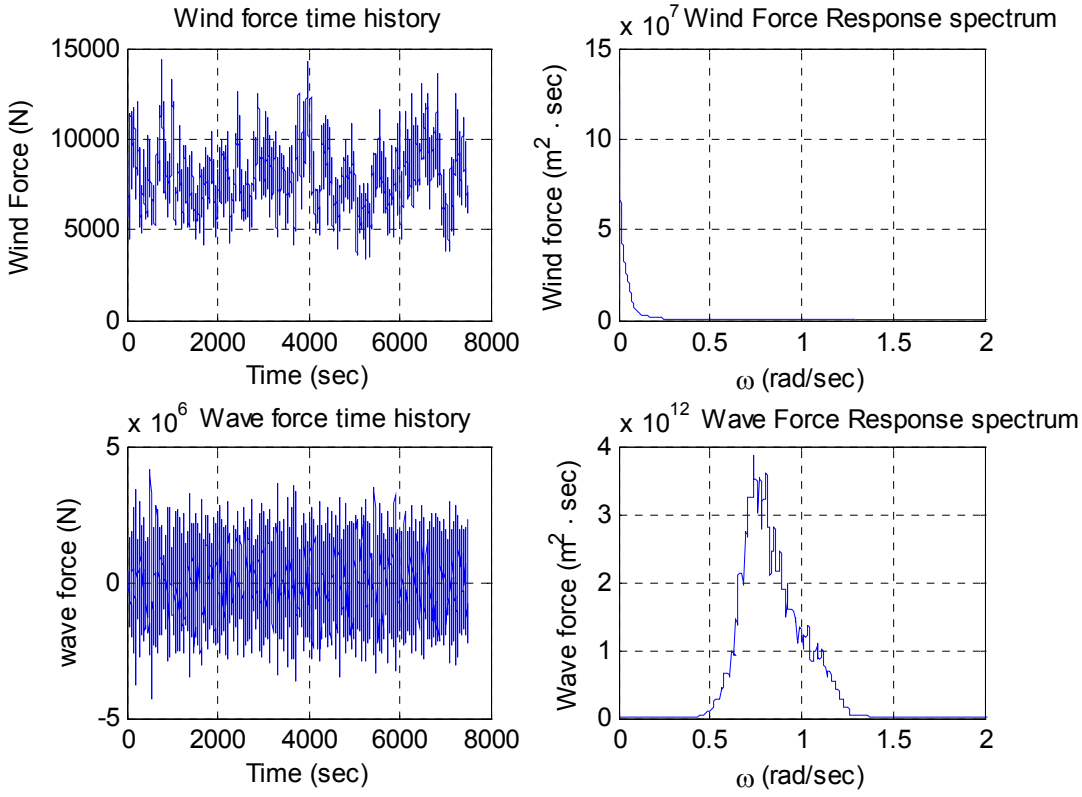

Figure 3-29 External forces time histories and spectra on the floating body of the uncoupled case in wind speed 5m/s

3.2.1.1.2 Time series and spectra of uncoupled case in wind speed 5 m/s

Time series and spectra of top tensions of a tether are shown in figure 3-30. Motion time histories and spectra of the floating body of the uncoupled case in wind speed 5m/s are shown in figure 3-31. In surge, sway, and roll we can observe a peak in low frequency..

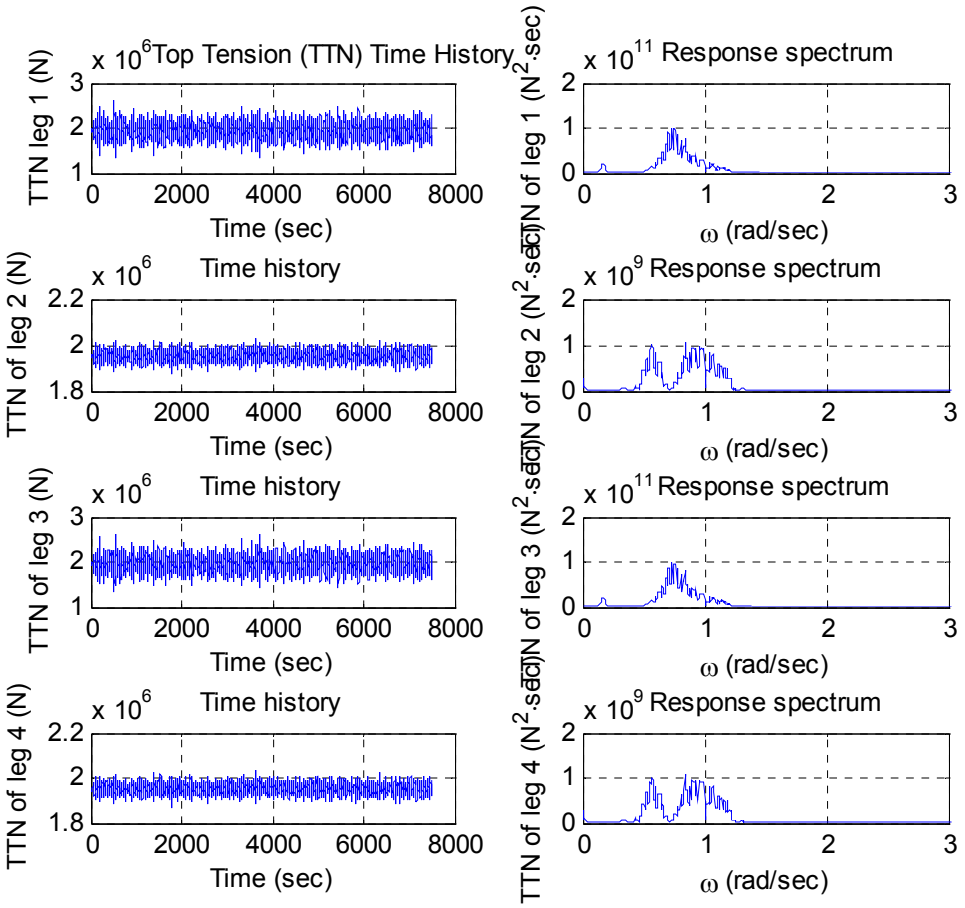

Figure 3-30 Top tension time series and spectra of the uncoupled case in wind speed 5m/s

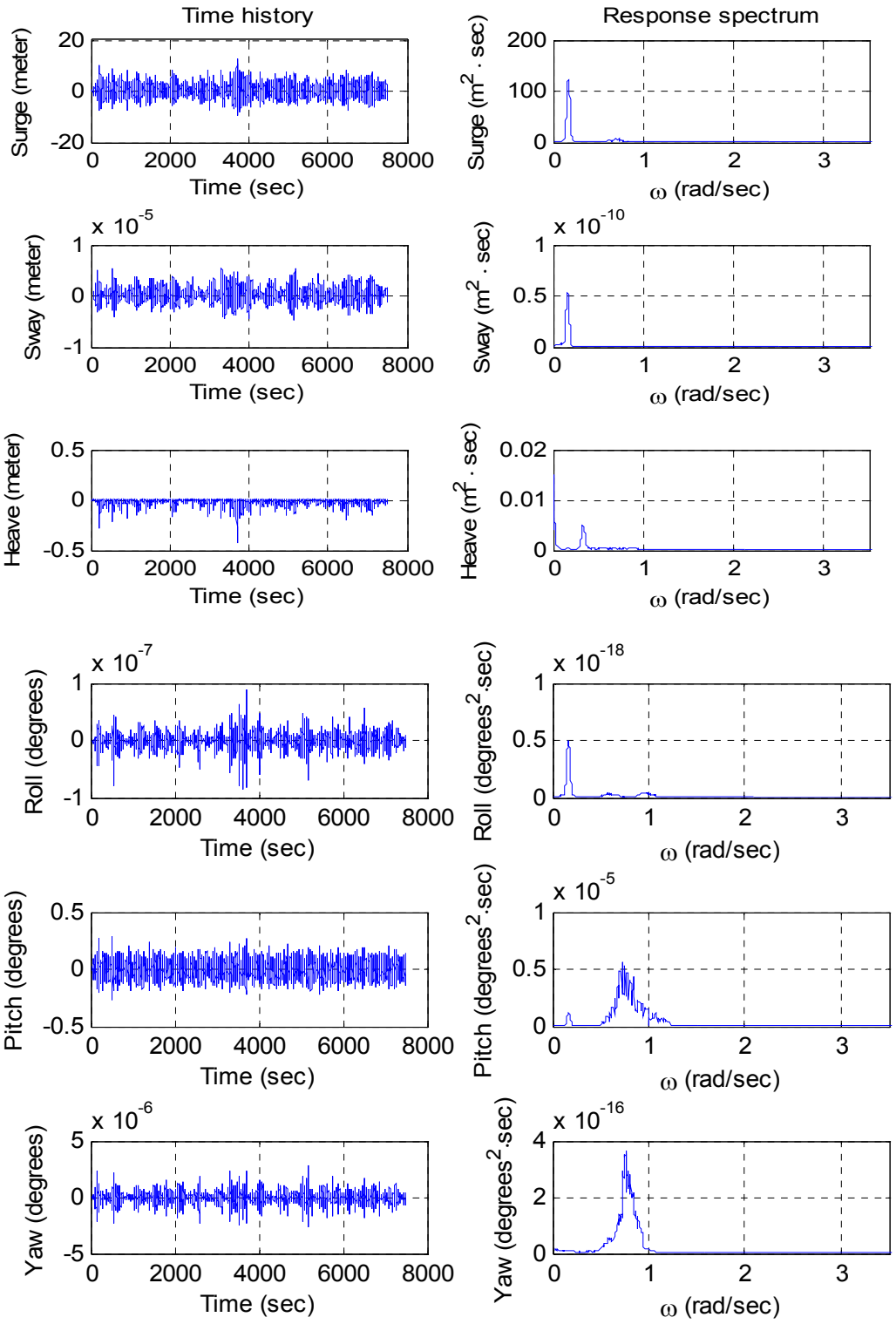

Figure 3-31 Motion time history and spectra of the uncoupled case in wind speed 5m/s

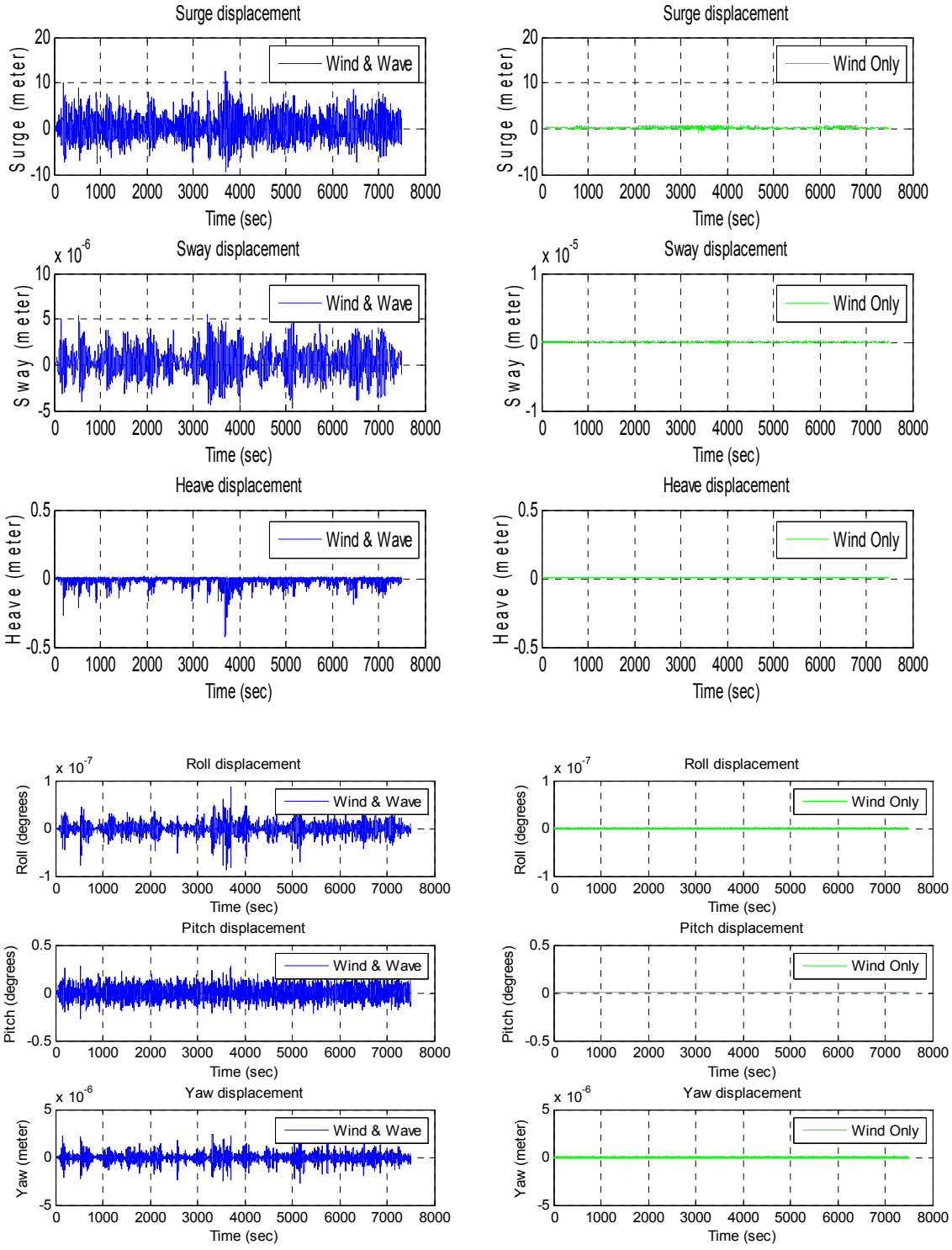

Figure 3-32 Motion time series comparison between wave + wind case and wind only case in wind speed 5m/s

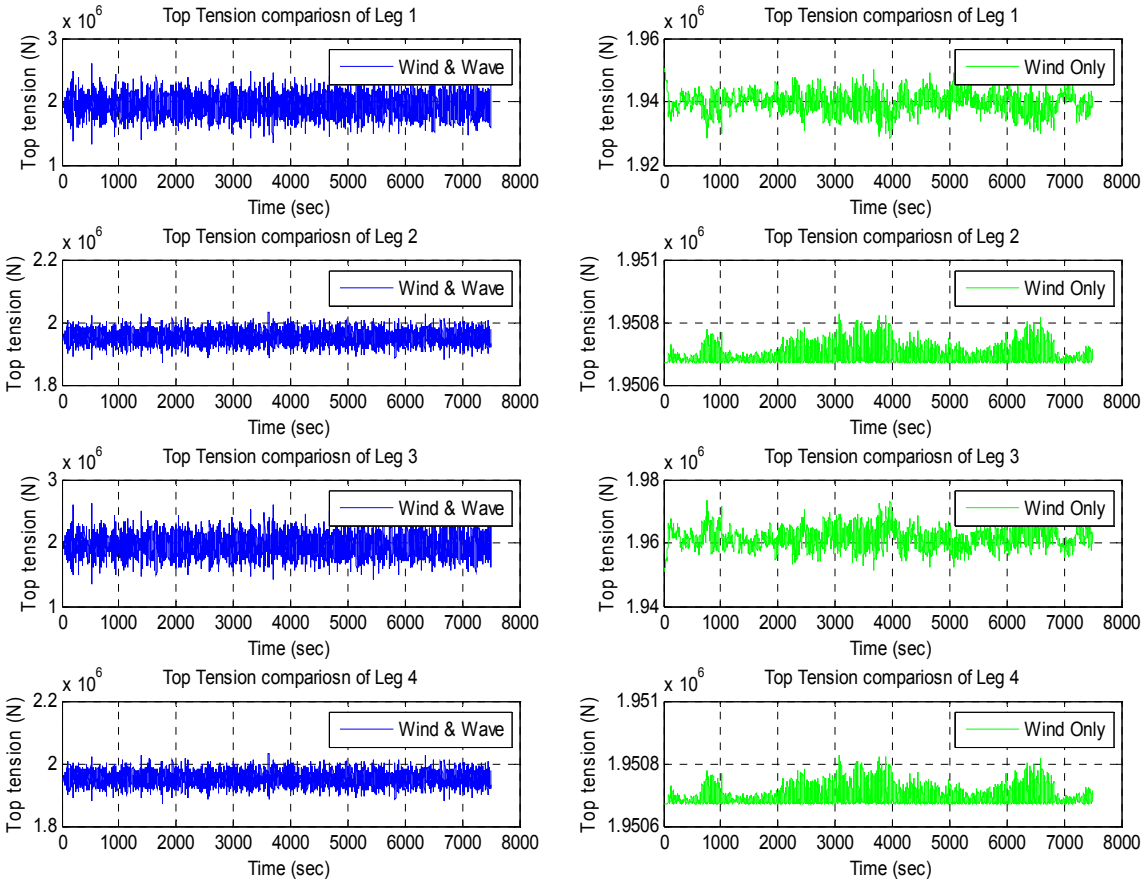

Figure 3-33 Top tension of tethers comparison between wave+wind case and wind only case in wind speed 5m/s

Figures 3-32 and 3-33 show time series comparisons of offshore floating wind turbine body and top tension of tethers between wind only case and wind + wave case. Naturally, wind only case shows less motion and top tension than that of wind + wave case.

3.2.1.2 Coupled case in wind speed 5 m/s

3.2.1.2.1 External forces of the coupled case in wind speed 5 m/s

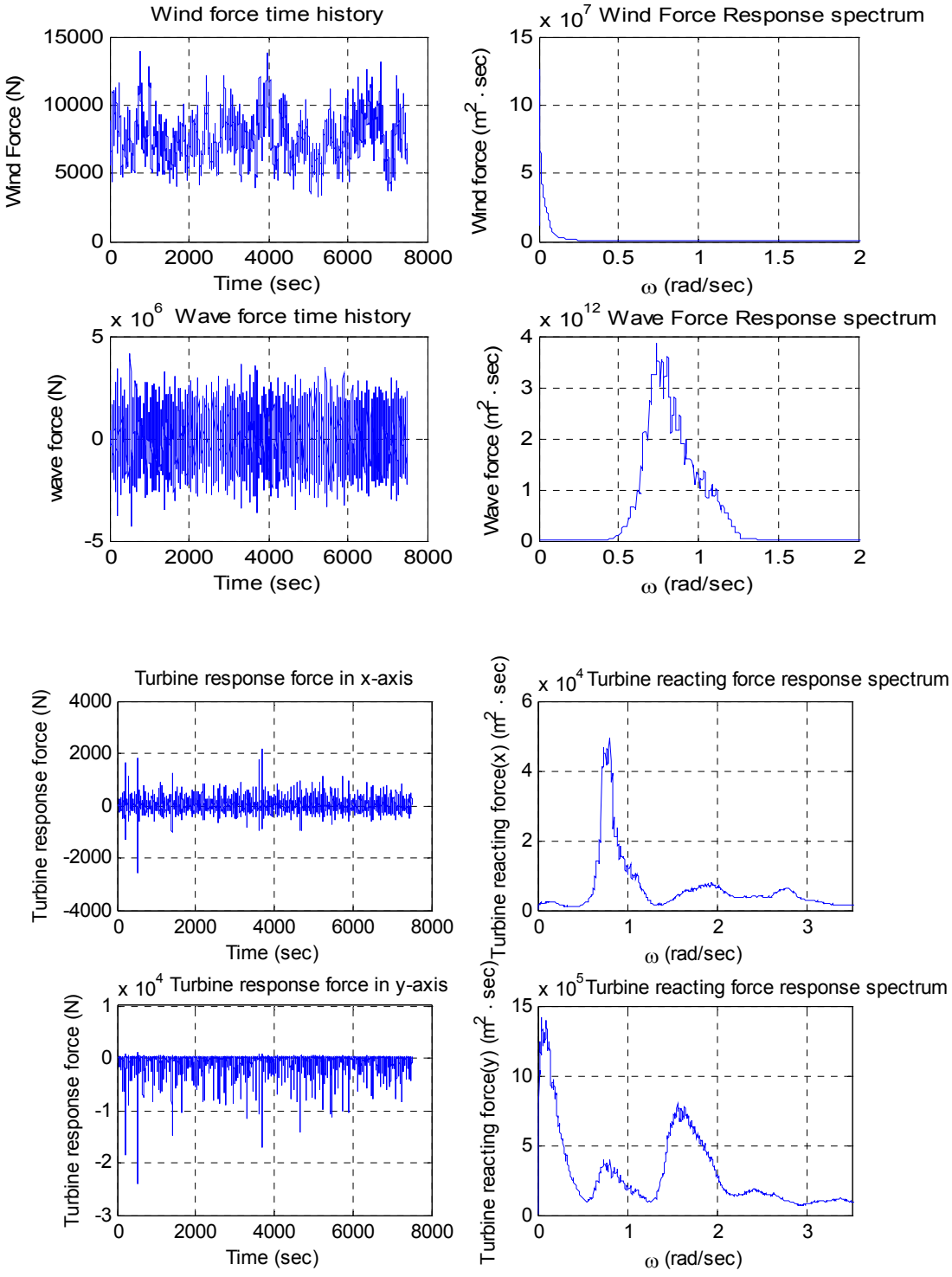

Figure 3-34 External forces time series and spectra on the floating body of the coupled case in wind speed 5m/s

In the coupled time domain analysis the time histories and spectra of four decomposed external forces are shown in figure 3-34. In the coupled time domain simulation we have wind force, wave force, and reaction forces from dynamics of the wind turbine as external forces on the floating body.

3.2.1.2.2 Time series and spectrum of coupled case in wind speed 5 m/s

Figures 3-35 and 3-36 show the coupled motion time histories and spectra of the floating body in wind speed 5m/s. In surge and sway we can observe a peak in low frequency. In roll, a peak is monitored in high frequency. Figure 3-37 shows time series and spectrum of top tension of a tether.

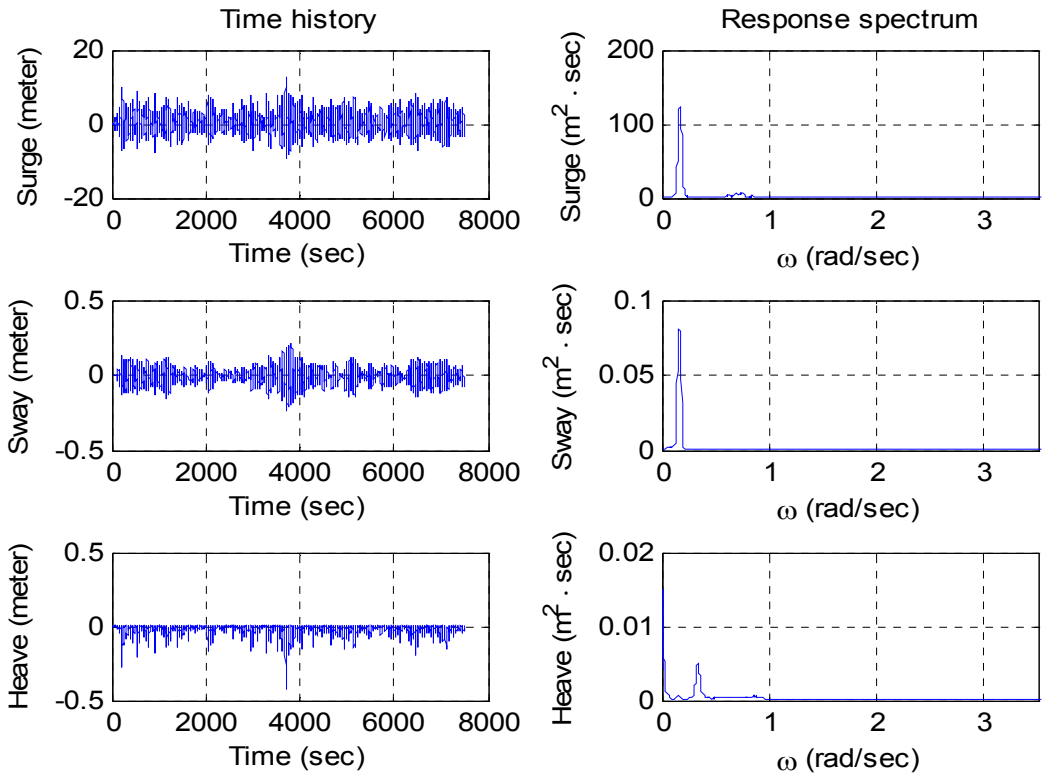

Figure 3-35 Axial motion time history and spectra of the coupled case in wind speed 5m/s

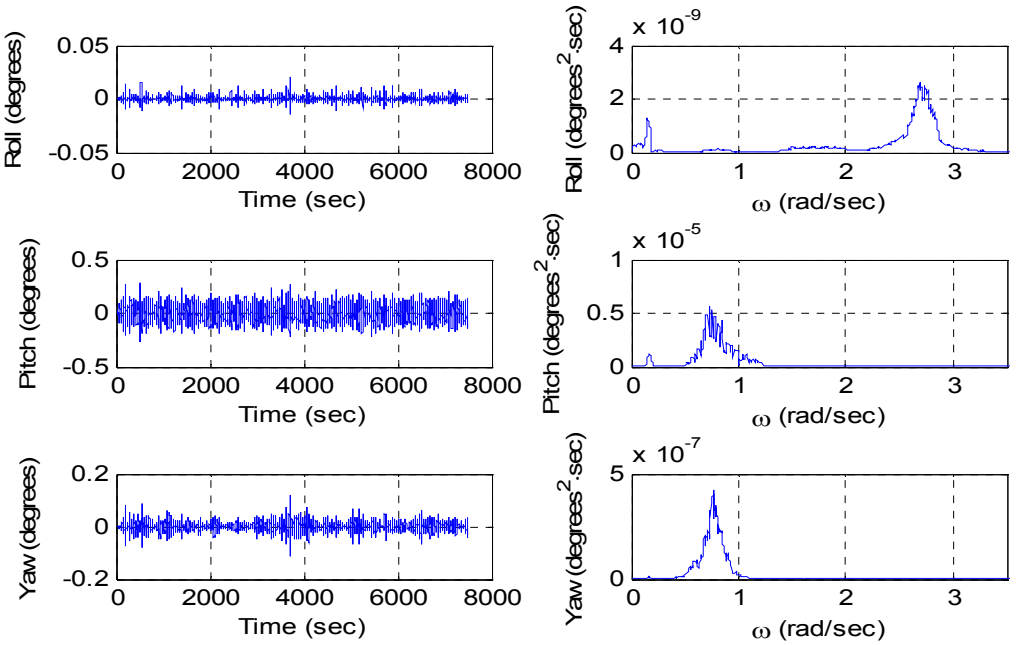

Figure 3-36 Rotational motion time history and spectra of the coupled case in wind speed 5m/s

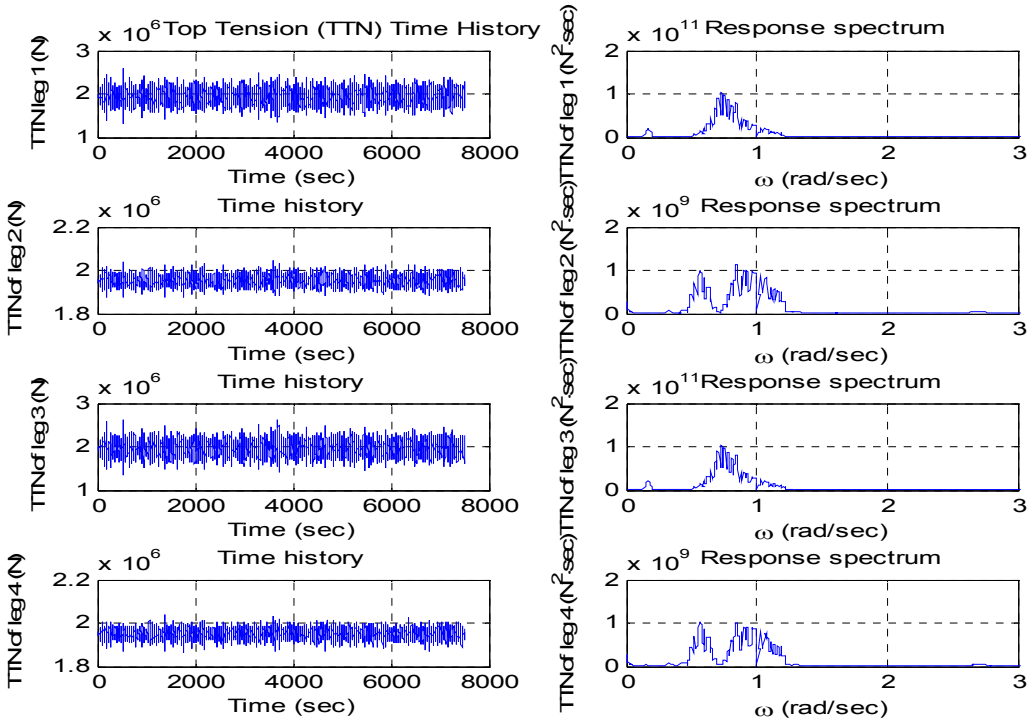

Figure 3-37 Top tension time series and spectra of the coupled case in wind speed 5m/s

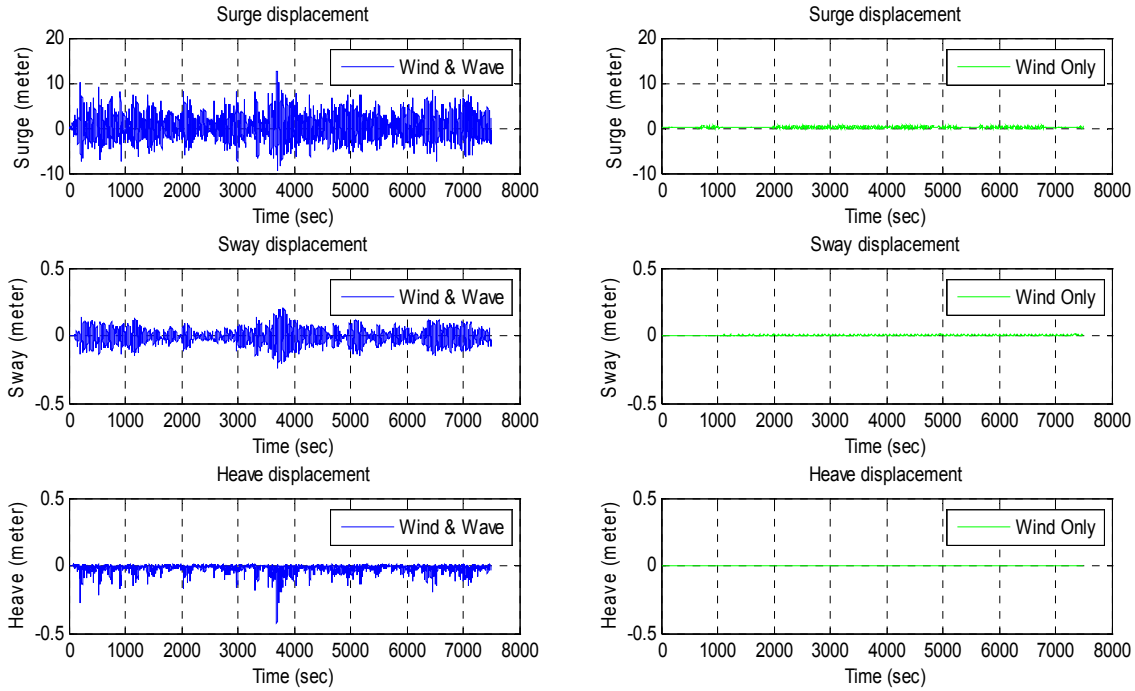

Figure 3-38 Axial **motion time series comparison between wind + wave case and wind only case in wind speed 5m/s**

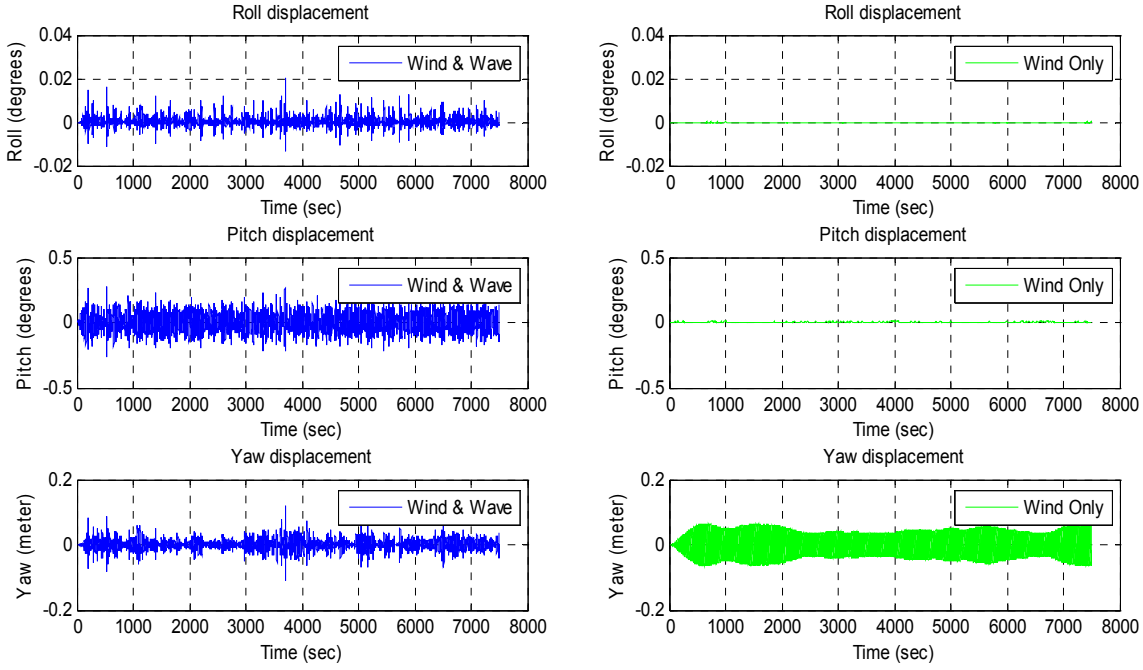

Figure 3-39 Rotational motion time series comparison between wind + wave case and wind only case in wind speed 5m/s

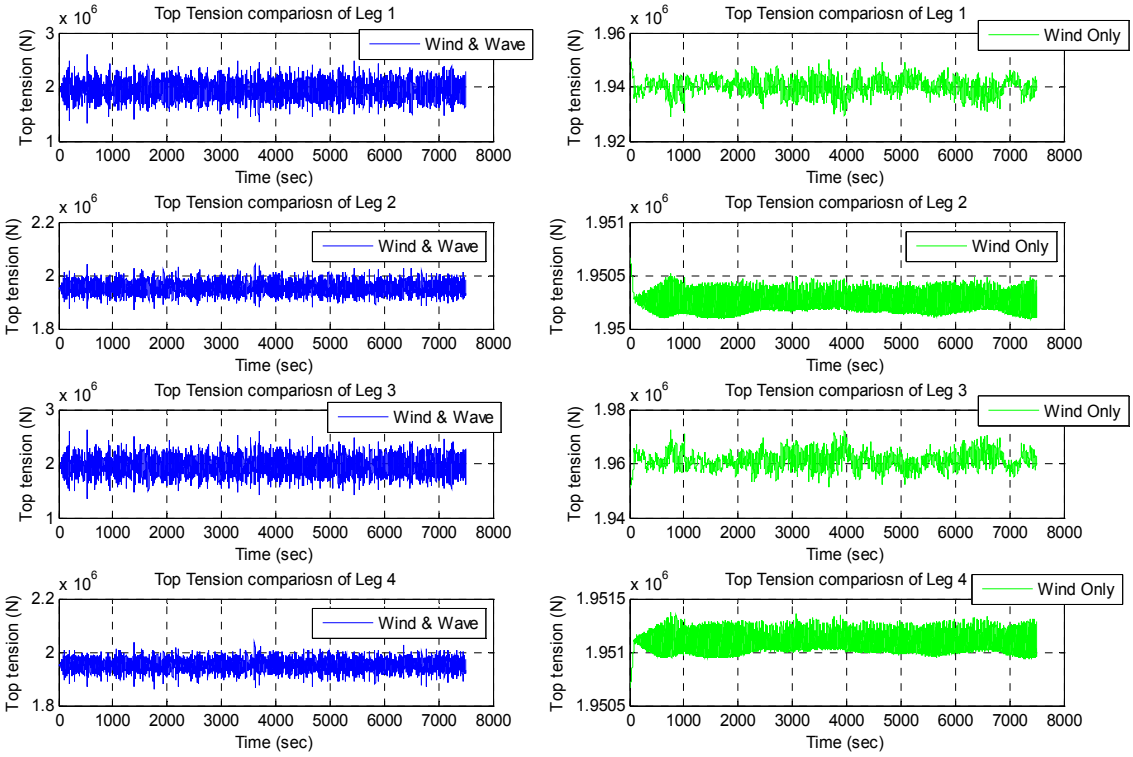

Figure 3-40 Top tension time history comparison between wind + wave case and wind only case in wind speed 5m/s

Figures 3-38 to 3-40 show comparisons of floating offshore floating body motion and top tension of tethers between wind only case and wind + wave case.

3.2.1.3 Coupled VS Uncoupled in wind speed 5 m/s

As mentioned in section 2, huge dynamic loads from the wind turbine are expected in coupled case. For the comparison between coupled and uncoupled cases the global motion of floating body and top tension of tether is examined. The motion time series and the spectra of all six degrees of freedom are shown in figures 3-41. It is clearly shown that a coupled motion analysis gives bigger values in sway, roll, and yaw than uncoupled analysis.

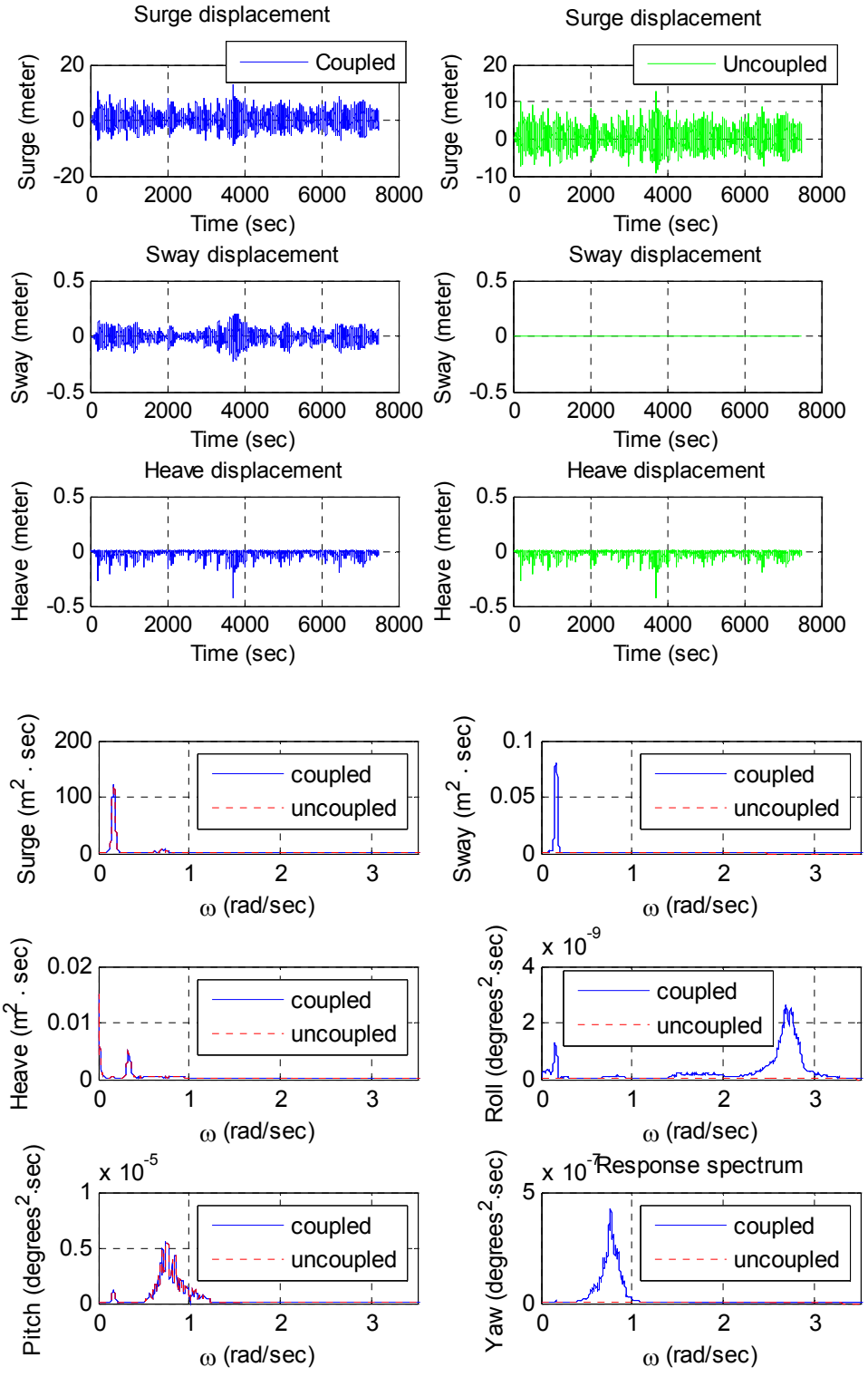

Figure 3-41 Motion time series and spectra comparison between coupled and uncoupled cases in wind speed 5m/s

The top tension time series and spectra of 4 legs are shown figures 3-42 and 3-43.

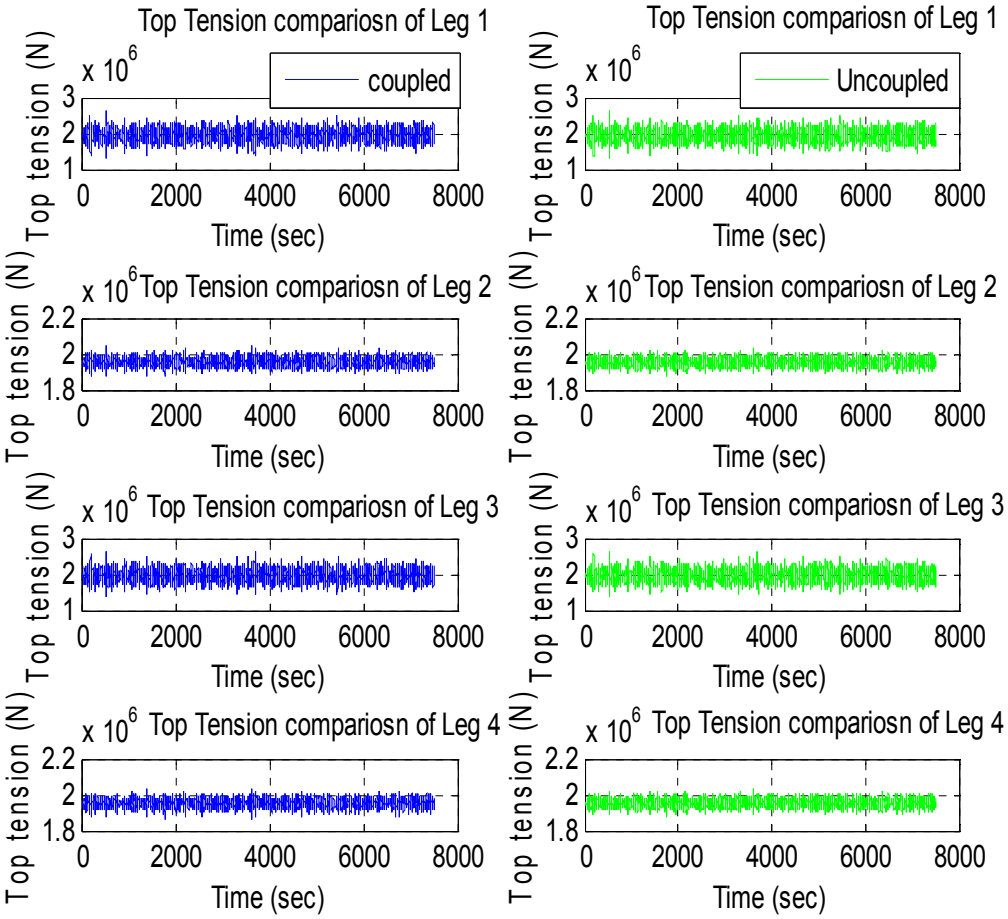

Figure 3-42 Top tension time series comparison between coupled and uncoupled case in wind speed 5m/s

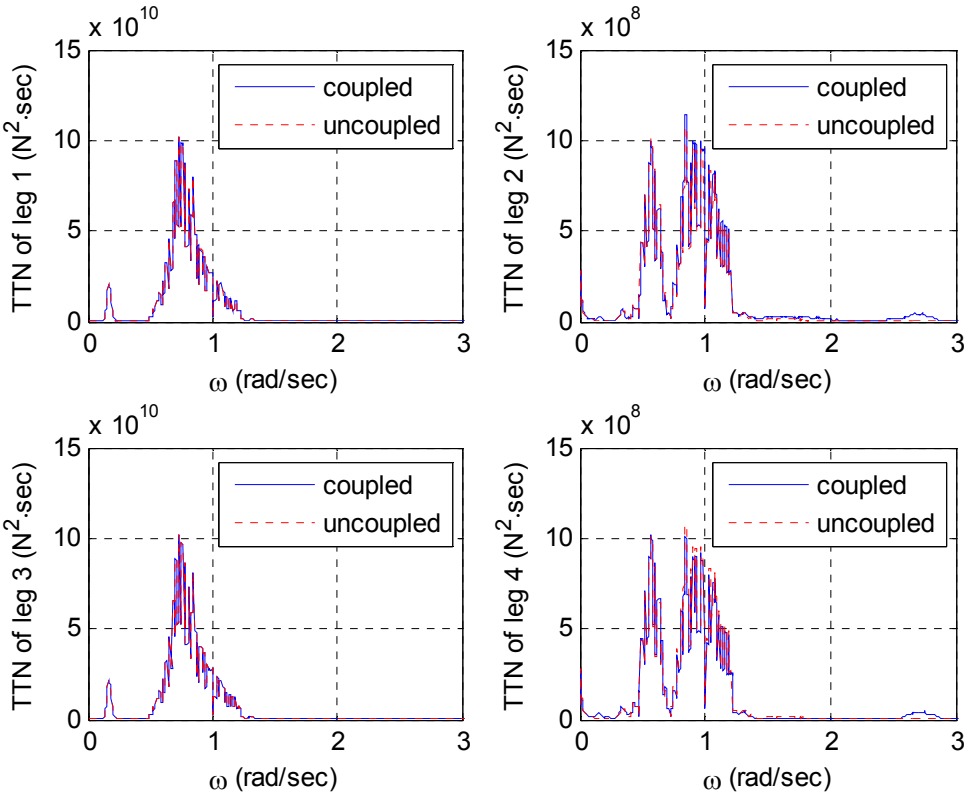

Figure 3-43 Top tension spectra comparison between coupled and uncoupled case in wind speed 5m/s

3.2.2 Wind speed 8m/s case

3.2.2.1 Uncoupled case in wind speed 8 m/s

3.2.2.1.1 External forces of the uncoupled case in wind speed 8m/s

In uncoupled time domain analysis, the time histories of two decomposed external forces are shown in figure 3-44. In uncoupled time domain simulation we have wind forces and wave force as external forces on the floating body. Bigger external forces than that of wind speed 5 m/s case can be observed.

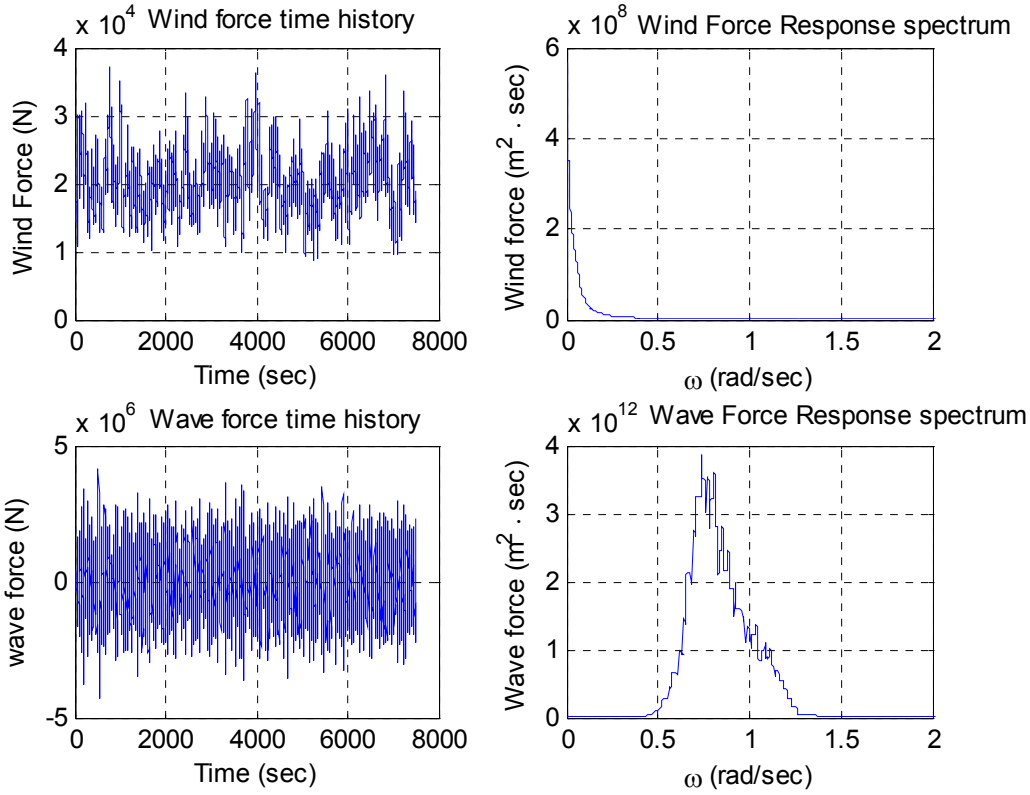

Figure 3-44 External force time series and spectra on the floating body of the uncoupled case in wind speed 8m/s

3.2.2.1.2 Time series and spectra of uncoupled case in wind speed 8 m/s

Figure 3-45 shows the uncoupled case's motion time histories and spectra of the floating body in wind speed 8m/s. In surge, sway, and roll we can also observe a peak in low frequency. Figure 3-46 shows time series and spectrum of top tension of a tether. Since there are bigger motions and top tension than that of wind speed 5 m/s case, the magnitude of spectra is increased. In surge, sway, roll, and spectra of motion we can find a peak in low frequency around 0.2 rad/sec.

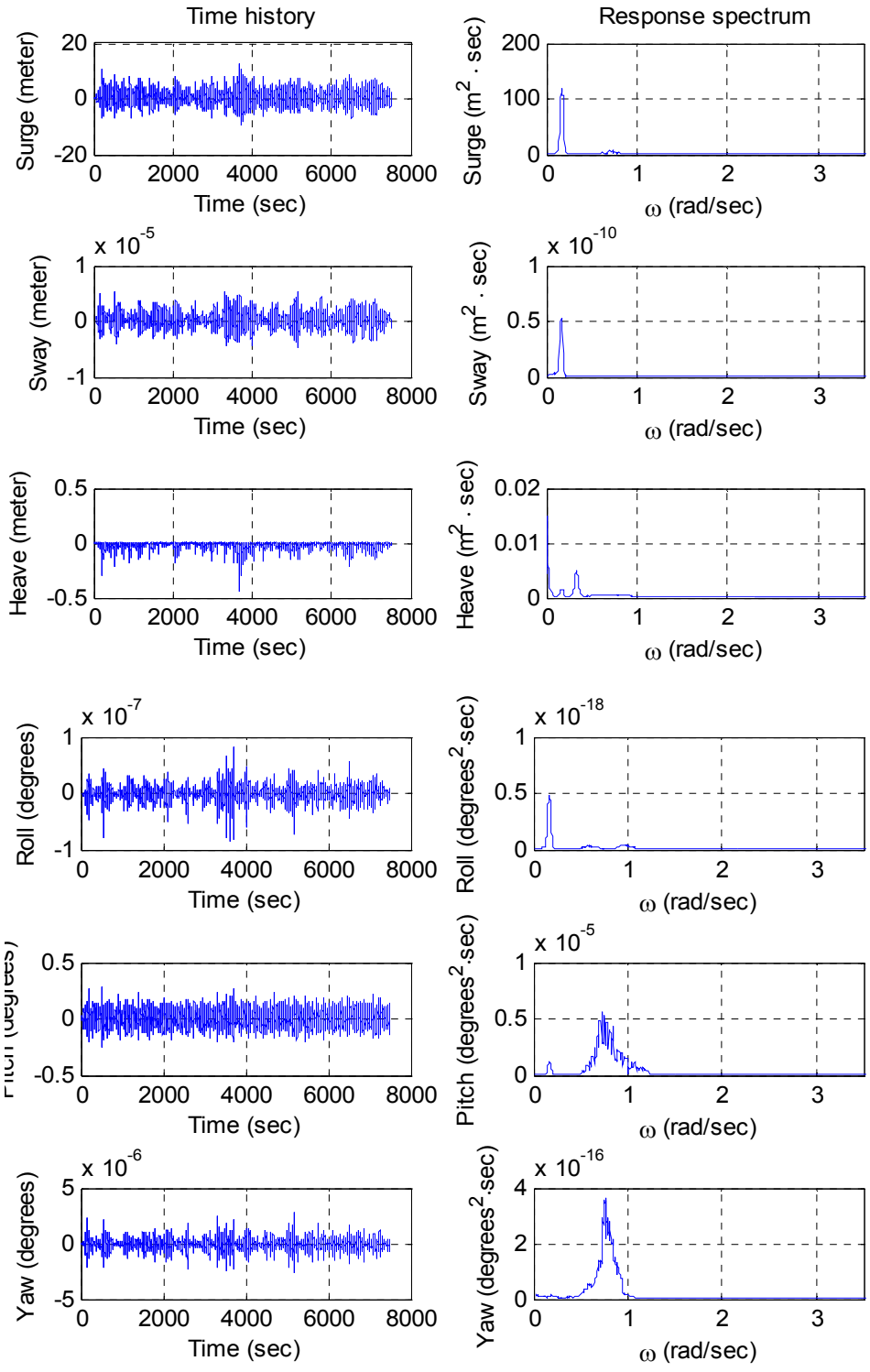

Figure 3-45 Motion time history and spectra of the uncoupled case in wind speed 8m/s

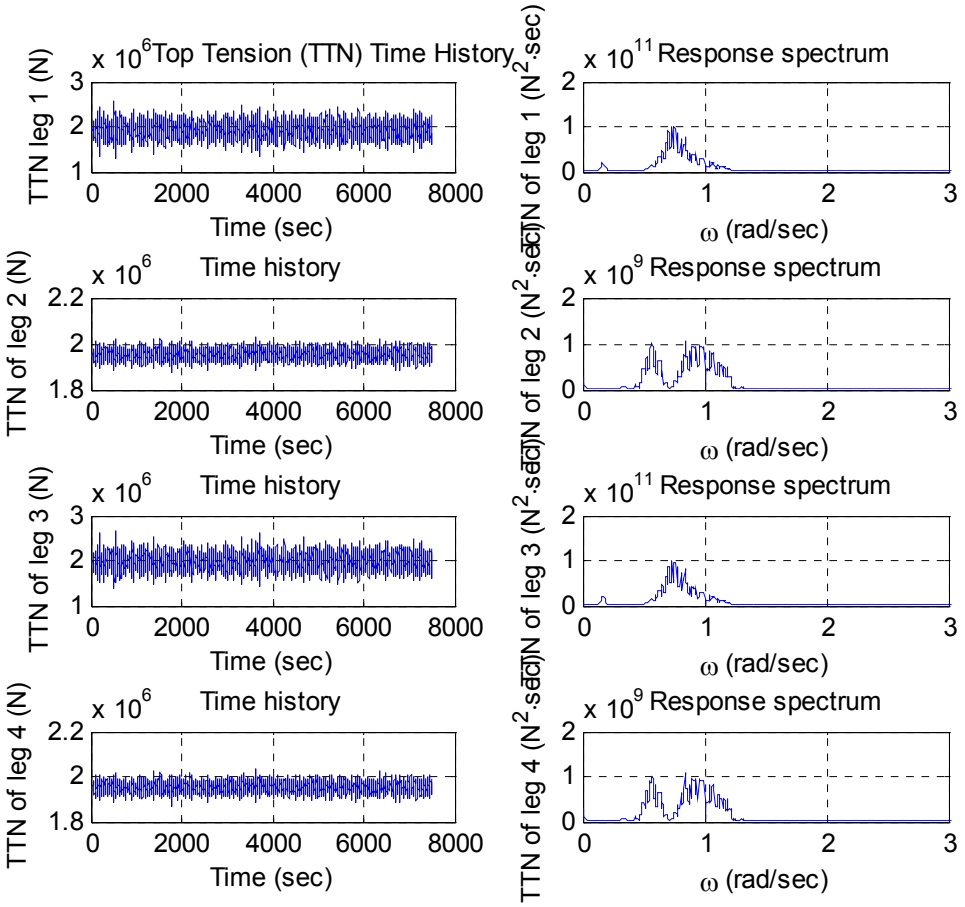

Figure 3-46 Top tension time series and spectra of uncoupled case in wind speed 8m/s

3.2.2.2 Coupled case in wind speed 8 m/s

3.2.2.2.1 External forces of the coupled case in wind speed 8 m/s

In coupled time domain analysis the time histories and spectra of four decomposed external forces are shown in figure 3-47. In coupled time domain simulation we have wind force, wave force, and reaction forces from dynamics of the wind turbine as external forces on the floating body.

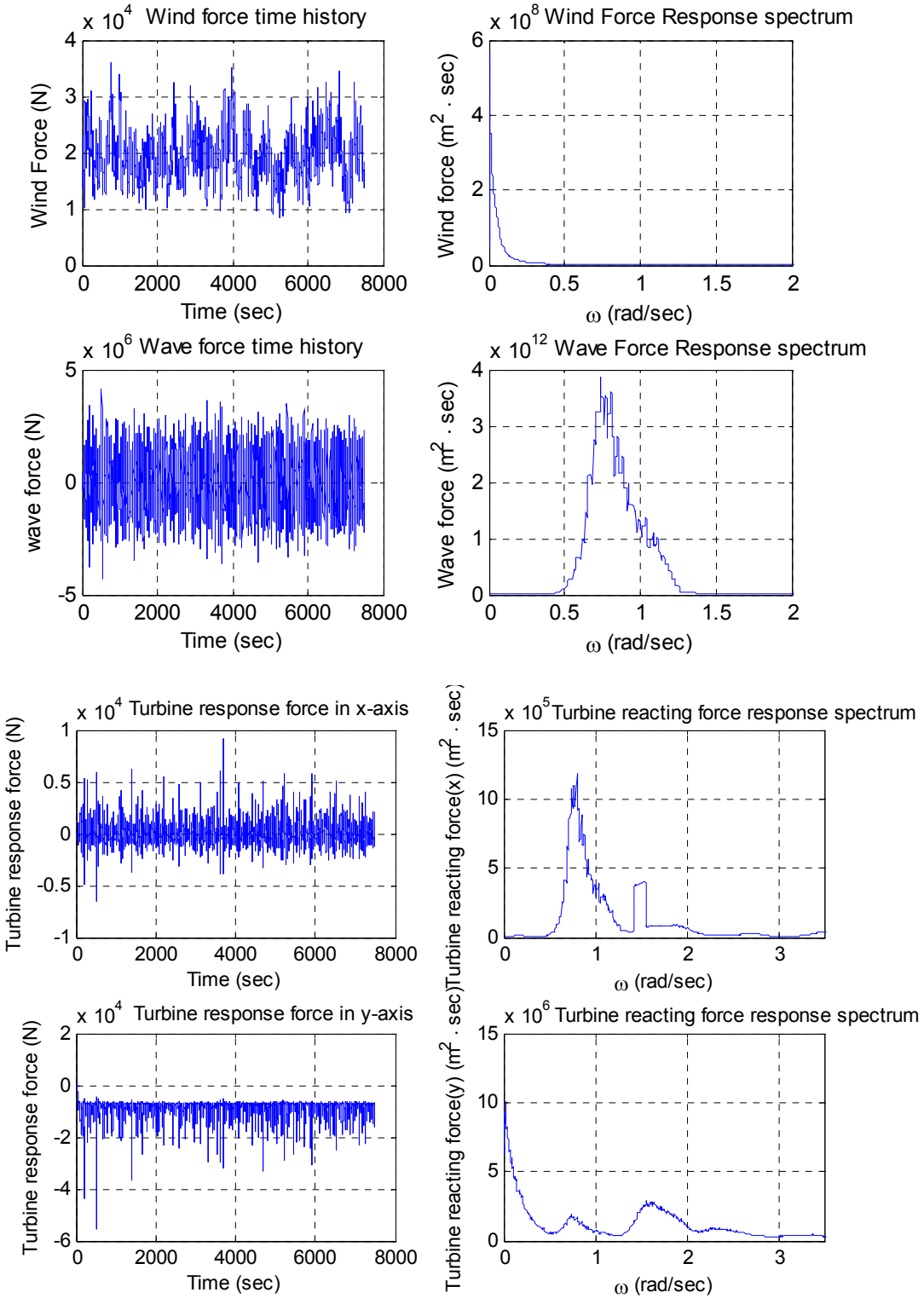

Figure 3-47 External forces time series and spectra on the floating body of coupled case in wind speed 8m/s

3.2.2.2.2 Time series and spectrum of the coupled case in wind speed 8 m/s

Figures 3-48 and 3-49 show coupled case's motion time histories and spectra of floating body in wind speed 8m/s. In surge and sway we can observe a peak in low frequency. In roll, a peak is monitored in high frequency. Figure 3-50 shows time series and spectra of top tension of a tether. Since there are bigger motions than that of wind speed 5 m/s case, the magnitude of spectra is increased.

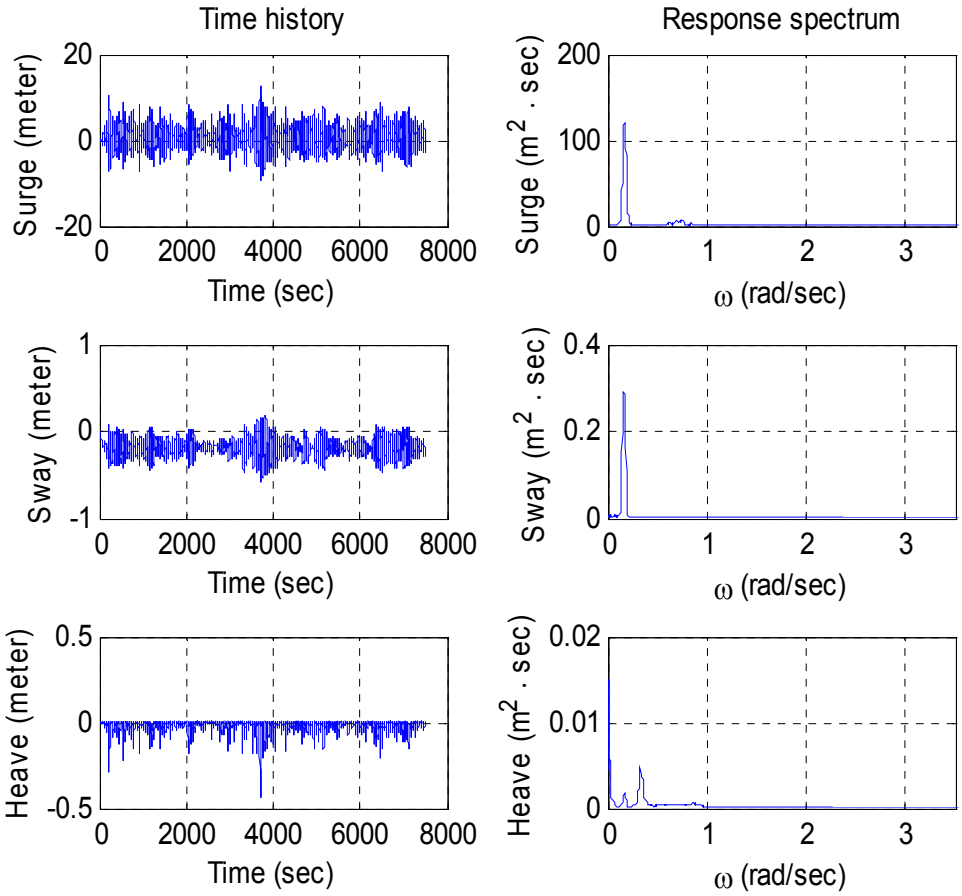

Figure 3-48 Axial motion time history and spectra of the coupled case in wind speed 8m/s

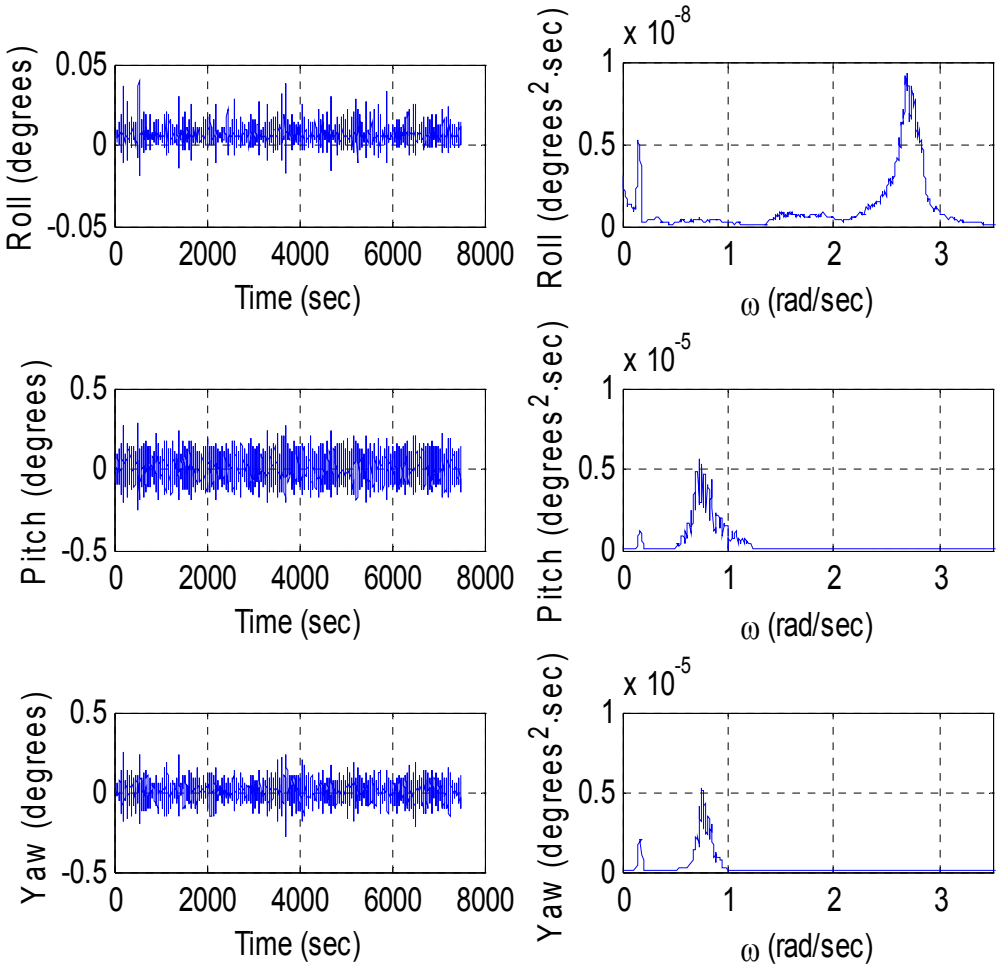

Figure 3-49 Rotational motion time history and spectra of the coupled case in wind speed 8m/s

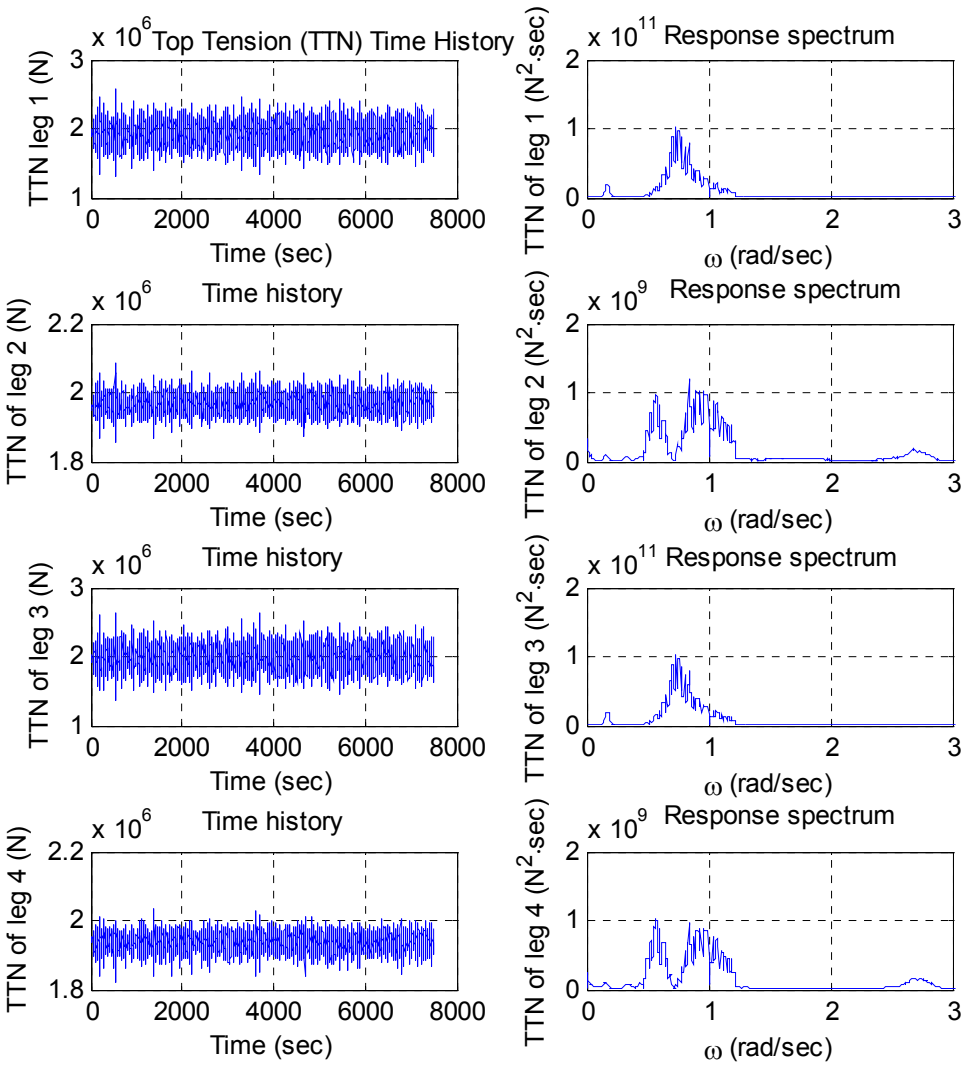

Figure 3-50 Top tension time series and spectra of the coupled case in wind speed 8m/s

3.2.2.3 Coupled VS Uncoupled in wind speed 8 m/s

The motion time series and the spectra of all six degrees of freedom are shown in figures 3-51 to 3-53. It is clearly shown that a coupled motion analysis gives bigger values in

sway, roll, and yaw than uncoupled analysis. In the spectra comparison a peak is observed in high frequency in roll motion. Also, the top tension time series and spectra of 4 legs are shown in figures 3-54 and 3-55. As expected, bigger motions are observed in the coupled cases, especially in sway, roll, and yaw.

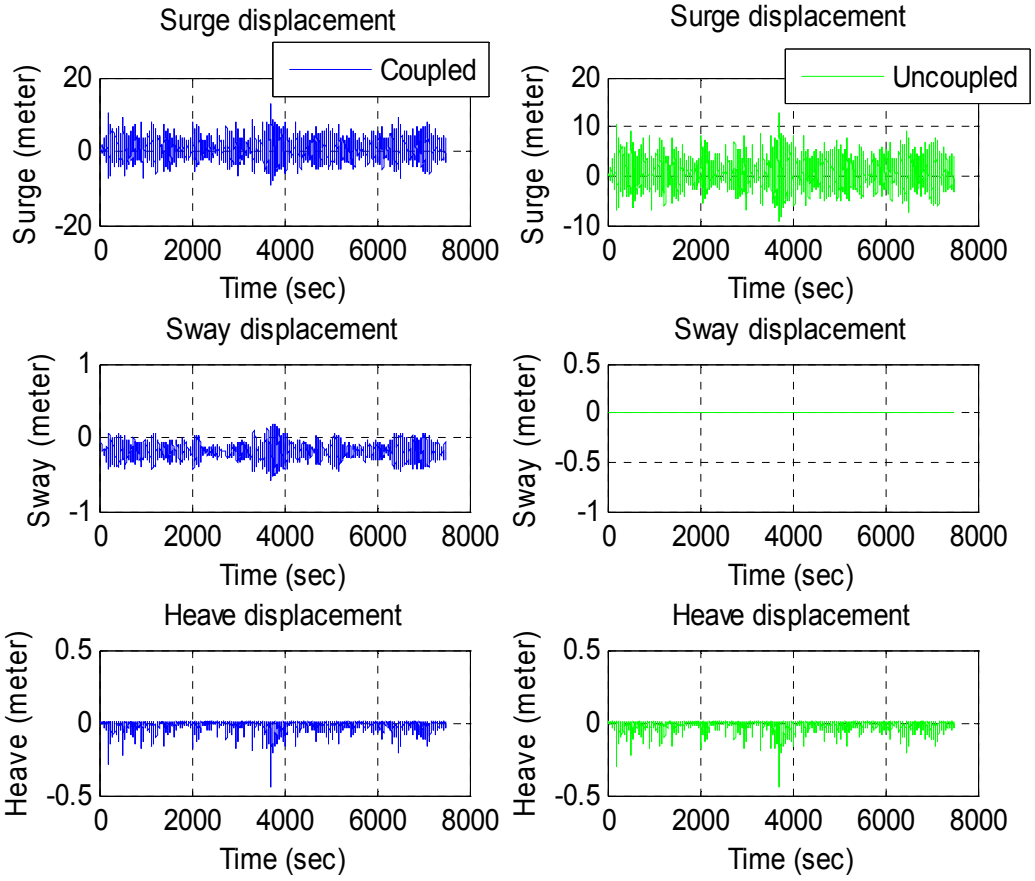

Figure 3-51 Axial motion time series comparison between coupled and uncoupled cases in wind speed 8m/s

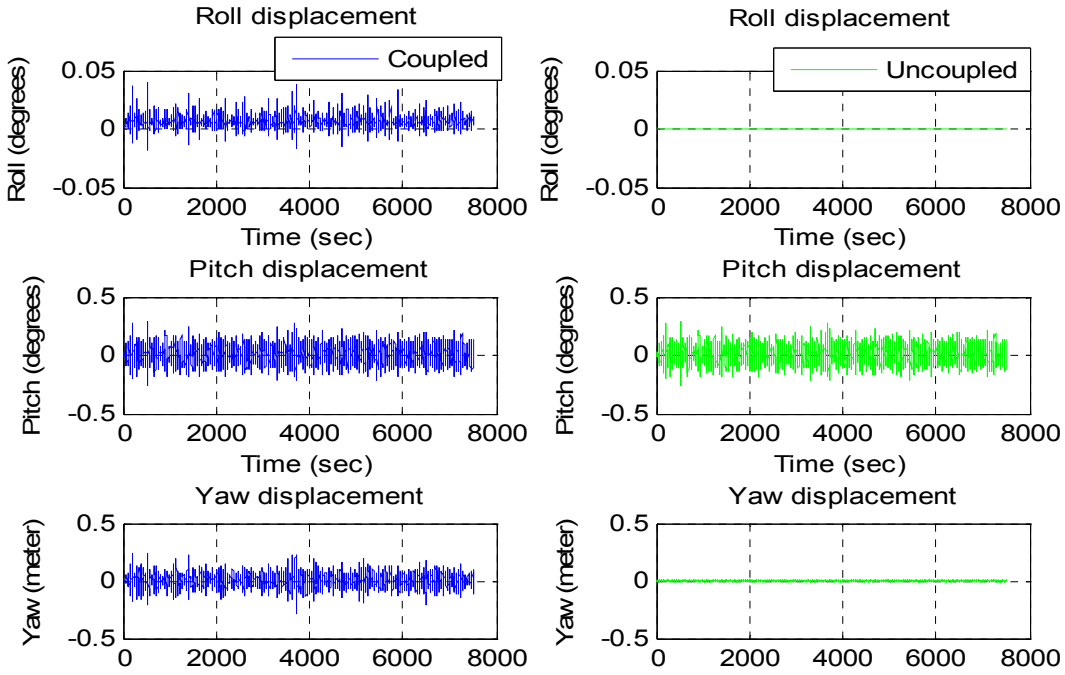

Figure 3-52 Rotational motion time series comparison between coupled and uncoupled cases in wind speed 8m/s

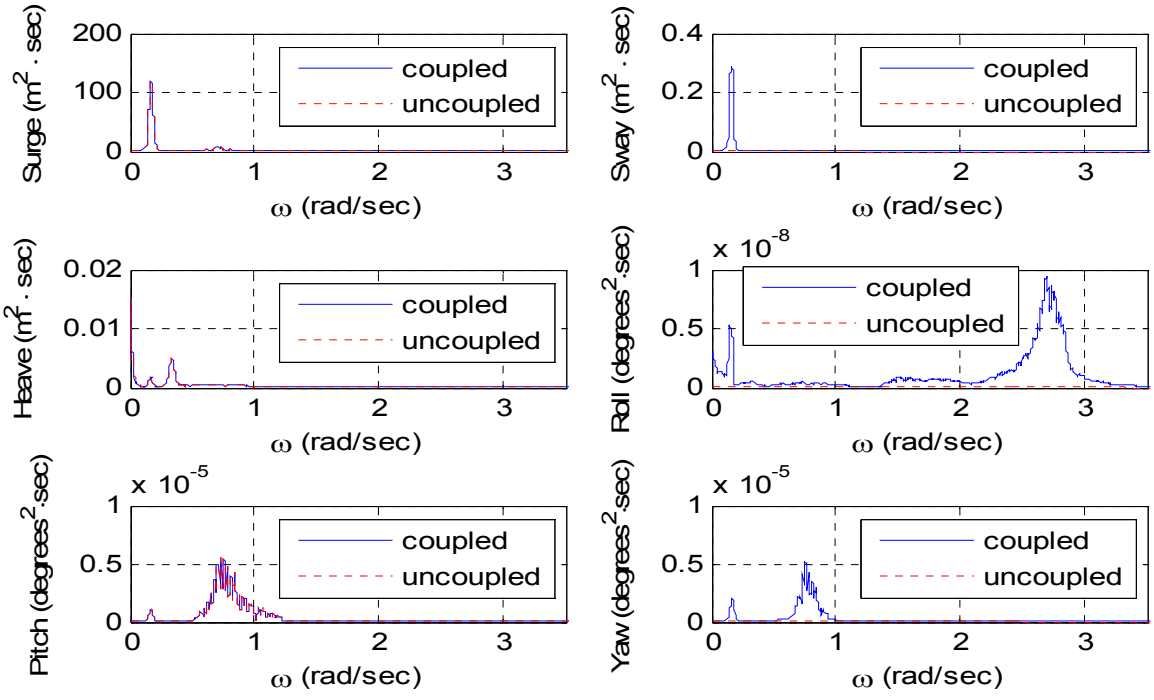

Figure 3-53 Motion spectra comparison between coupled and uncoupled case in wind speed 8m/s

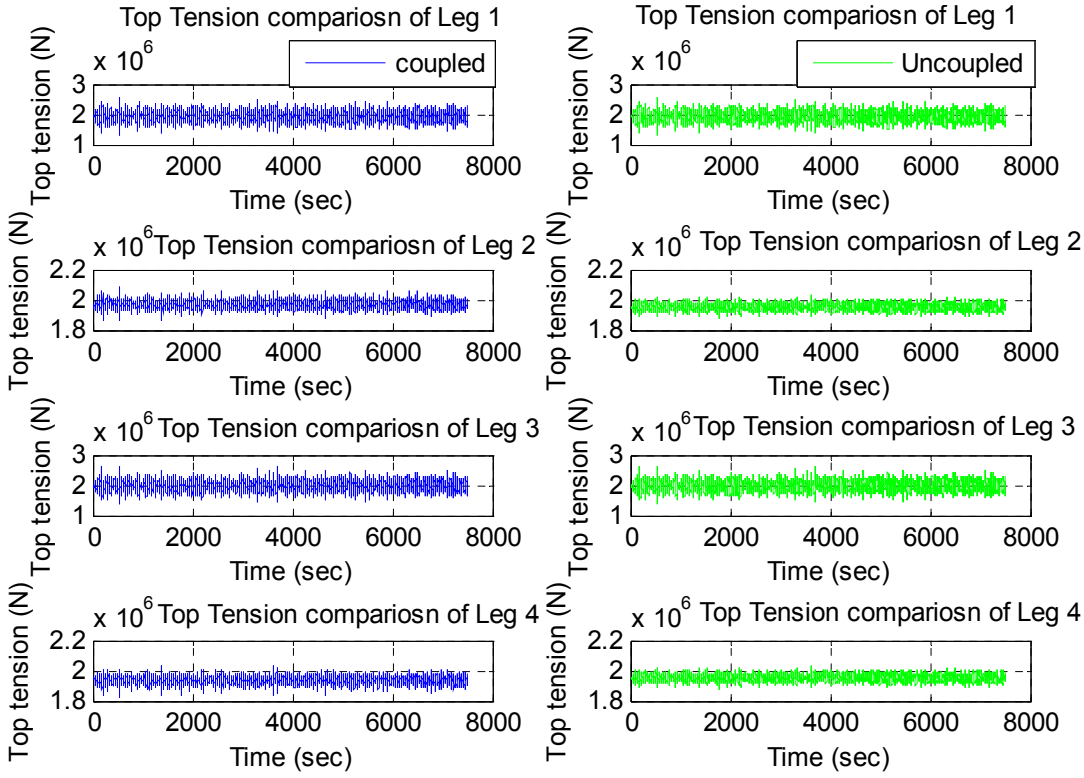

Figure 3-54 Top tension time history comparison between coupled and uncoupled case in wind speed 8 m/s

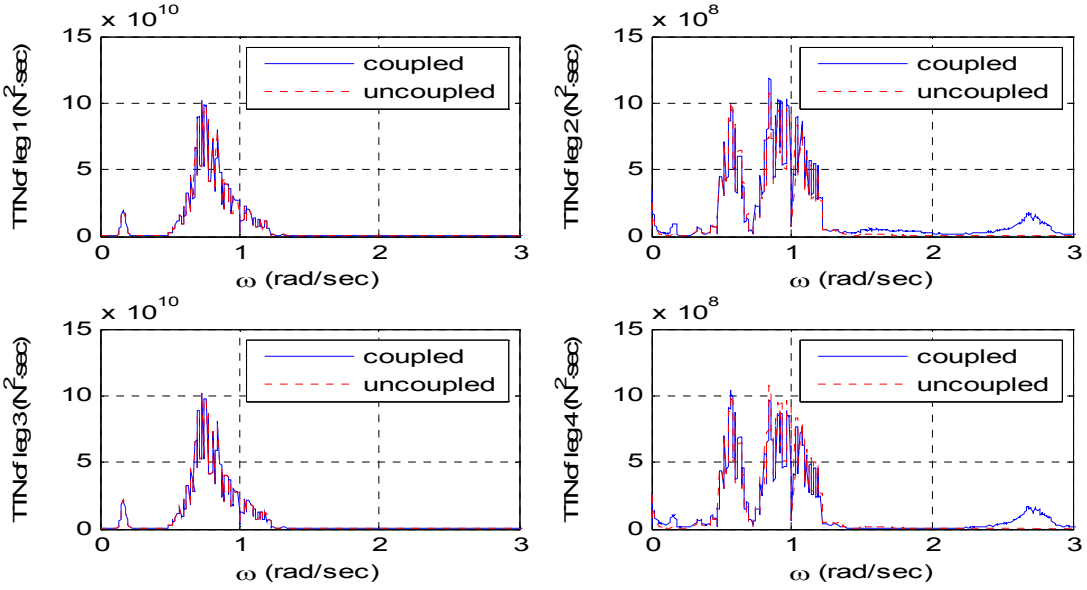

Figure 3-55 Top tension spectra comparison between coupled and uncoupled case in wind speed 8m/s

3.2.3 Wind speed 11m/s case

3.2.3.1 Uncoupled case in wind speed 11 m/s

3.2.3.1.1 External forces of uncoupled case in wind speed 11 m/s

In uncoupled time domain analysis, the time histories of two decomposed external forces are also show in figure 3-56. Wind force and wave force are external forces on the floating body in uncoupled time domain simulation.

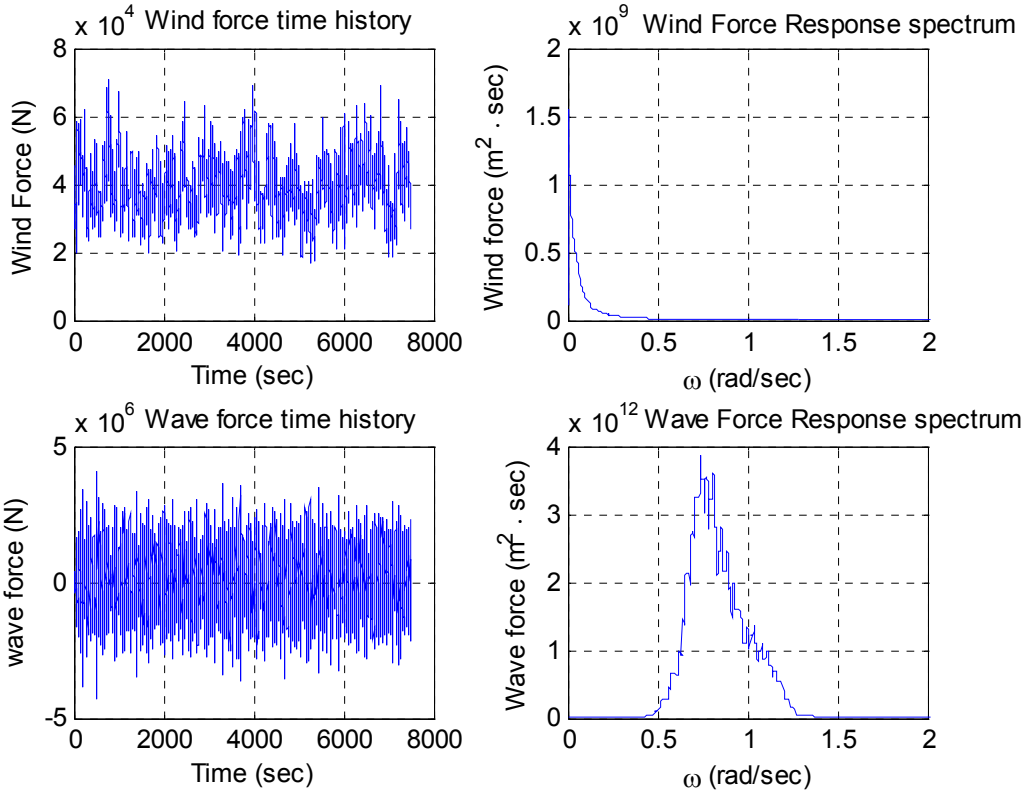

Figure 3-56 External force time series and spectra on the floating body of the uncoupled case in wind speed 11m/s

3.2.3.1.2 Time series and spectra of uncoupled case in wind speed 11 m/s

Figure 3-57 shows time series and spectra of top tension of a tether. Figure 3-58 shows the uncoupled motion time histories and spectra of the floating body in wind speed 11m/s. In surge, sway, and roll a peak is observed in low frequency. There are bigger motions and top tensions than that of wind speed 8 m/s. The trend of spectra is the same, but bigger magnitude is observed.

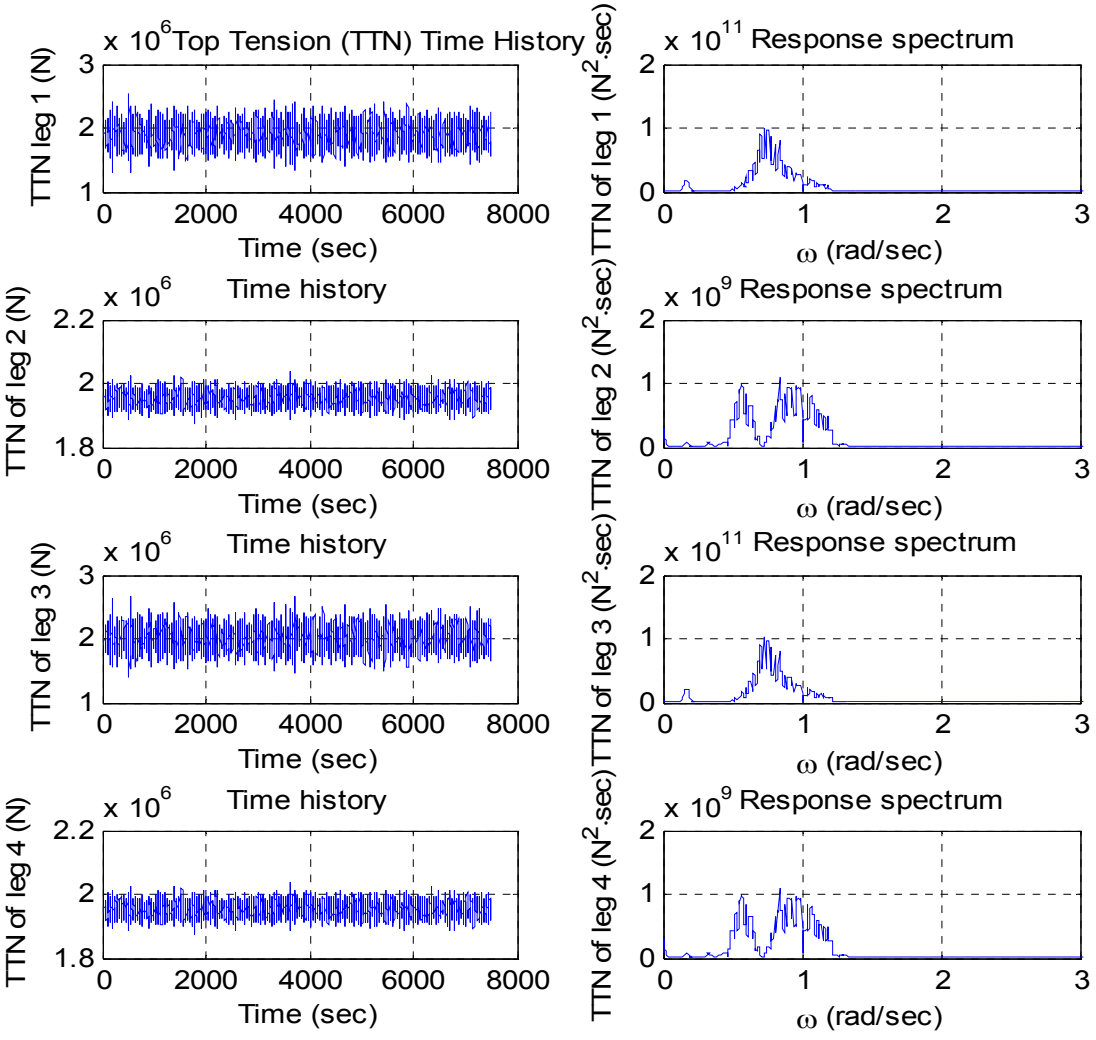

Figure 3-57 Top tension time series and spectrum of the uncoupled case in wind speed 11 m/s

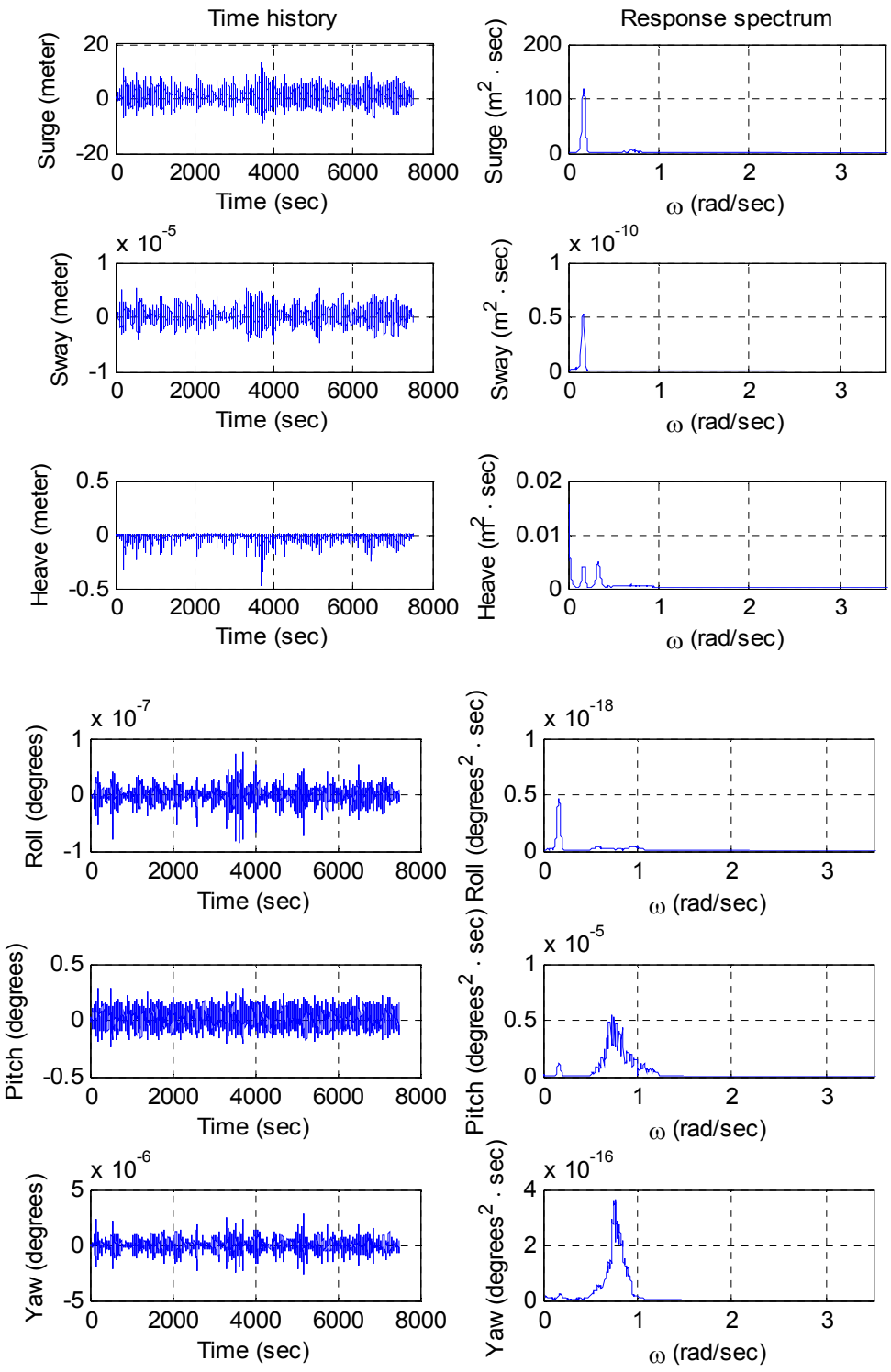

Figure 3-58 Motion time history and spectra of the uncoupled case in wind speed 11m/s

3.2.3.2 Coupled case in wind speed 11 m/s

3.2.3.2.1 External forces of coupled case in wind speed 11 m/s

In coupled time domain analysis the time histories of four decomposed external forces are shown in figures 3-59 and 3-60.

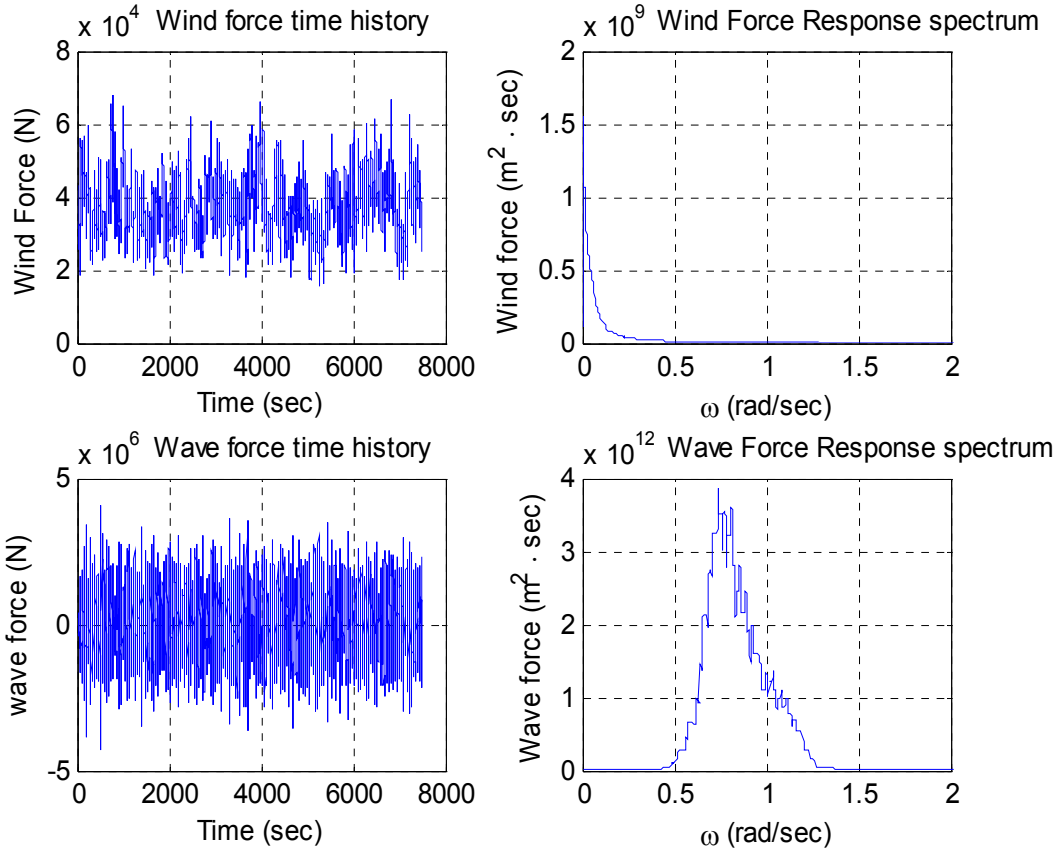

Figure 3-59 Environmental forces time series and spectra on the floating body of coupled case in wind speed 11m/s

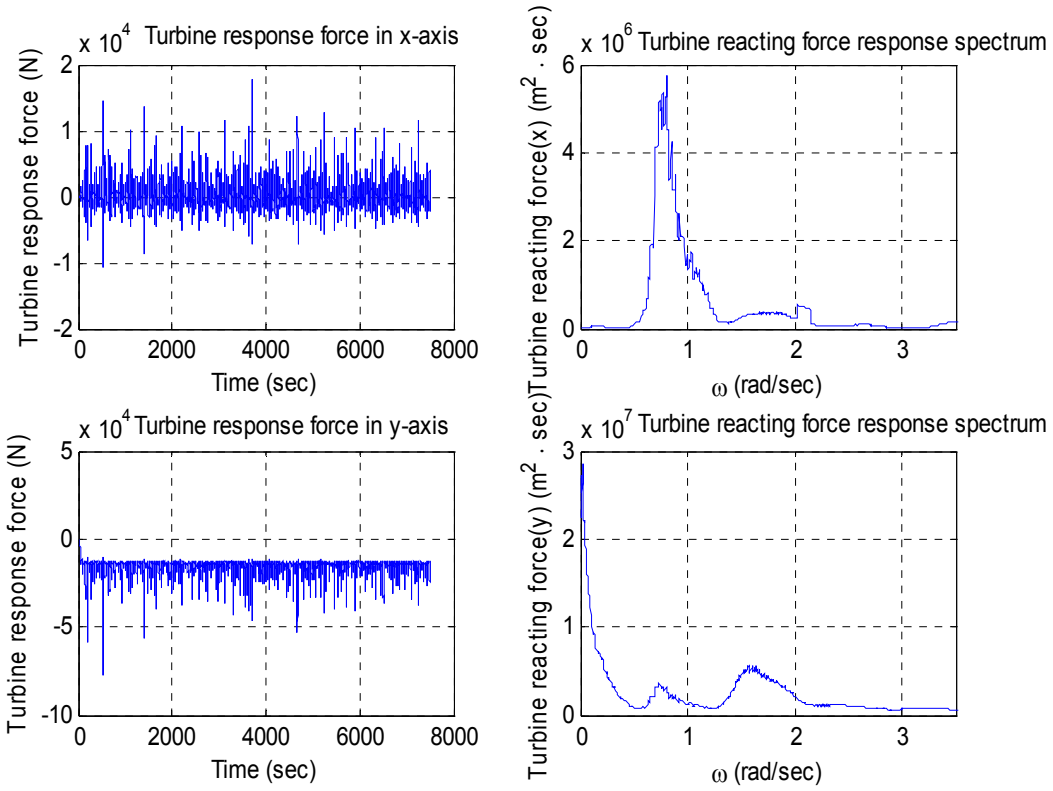

Figure 3-60 Turbine forces time series and spectra on the floating body of coupled case in wind speed 11m/s

3.2.3.2.2 Time series and spectra of coupled case in wind speed 11 m/s

We can observe same trends of time histories and spectra with wind speed 5 m/s and 8 m/s coupled case. Figure 3-61 shows time series and spectra of top tension of a tether. Figure 3-62 shows the coupled case's motion time histories and spectra of the floating body in wind speed 8m/s. In surge and sway we can observe a peak in low frequency. In roll, however, a peak is monitored in high frequency. We observe bigger motions and top tensions than that of wind speed 8 m/s.

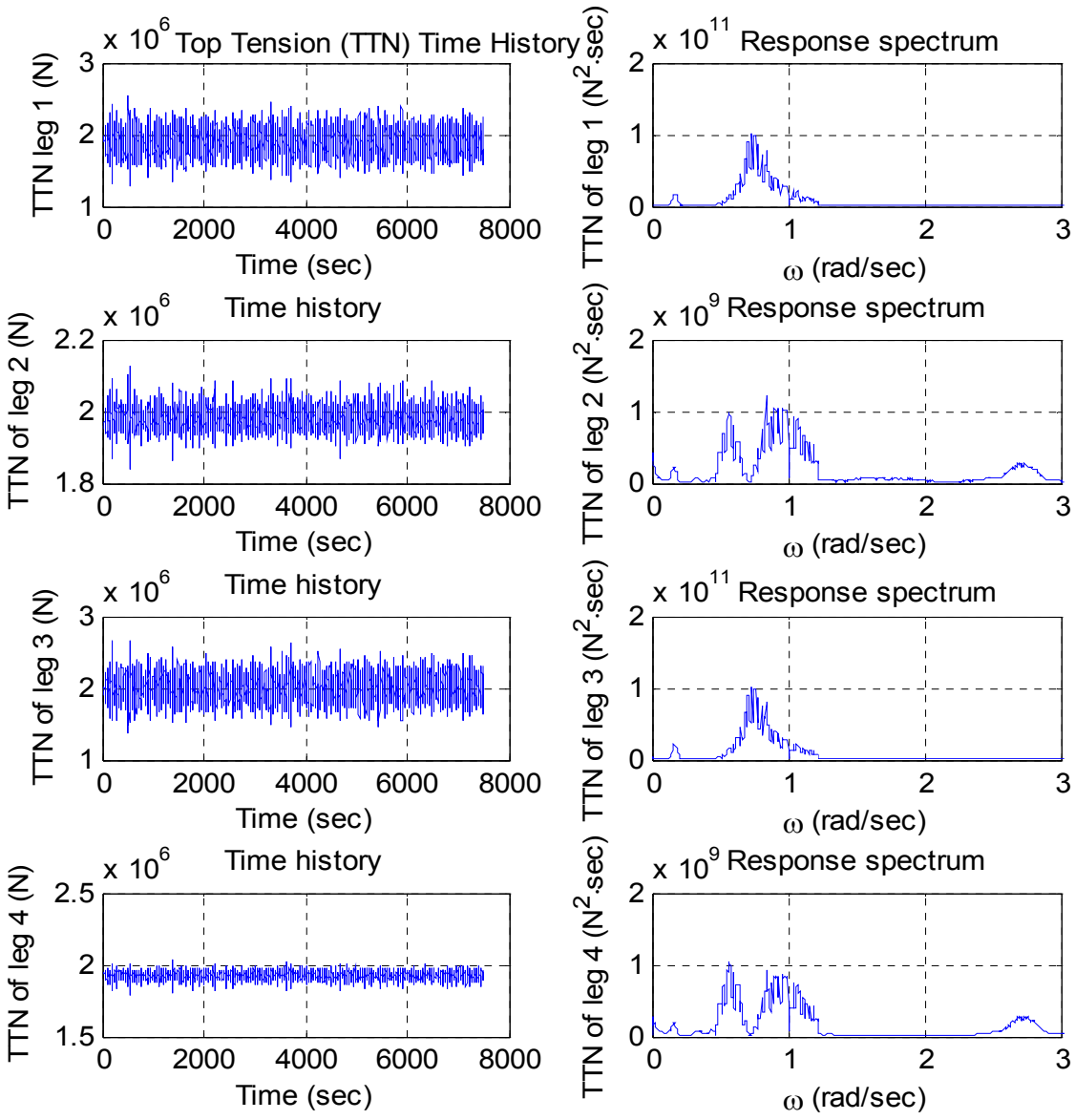

Figure 3-61 Top tension time series and spectra of the coupled case in wind speed 11 m/s

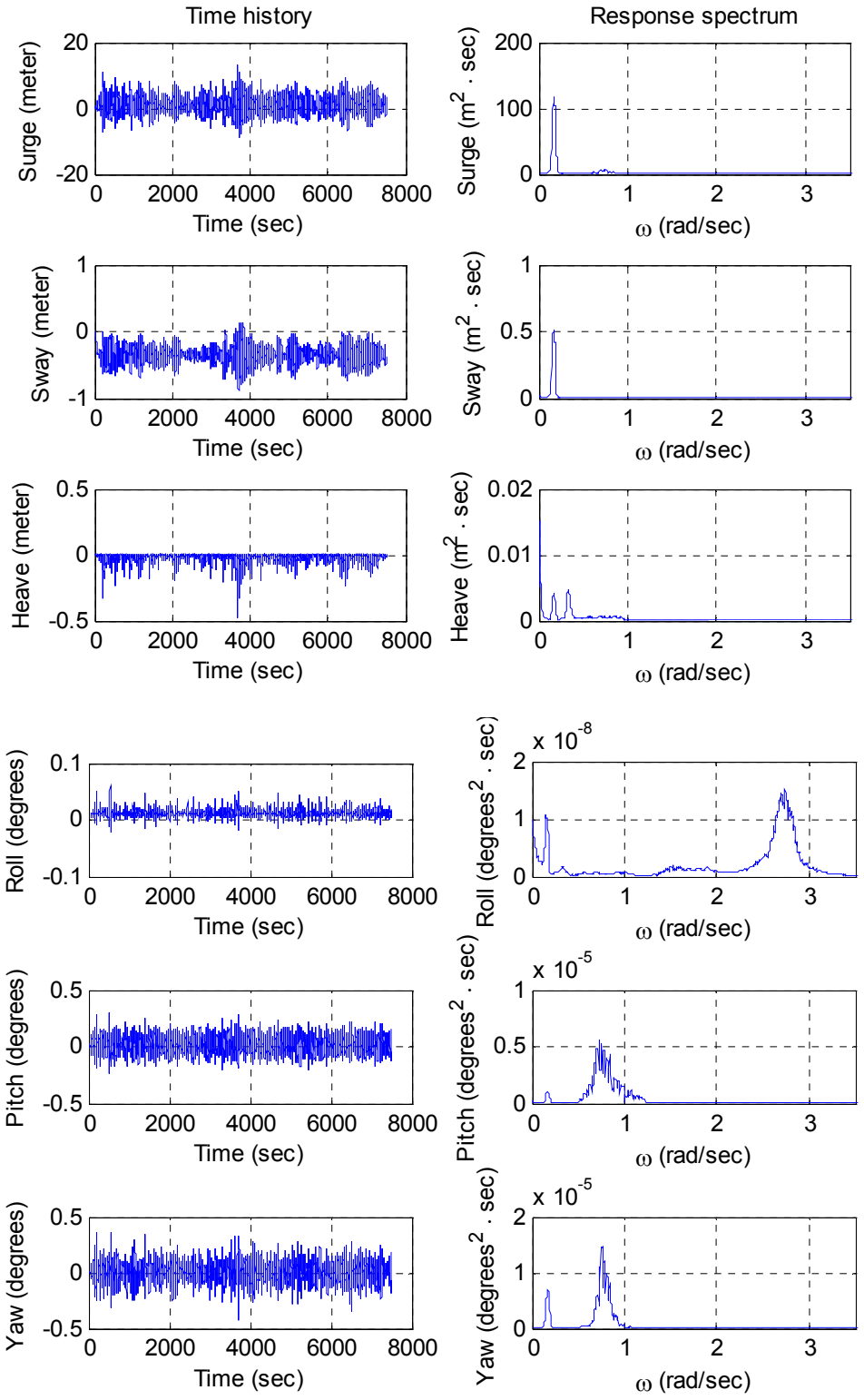

Figure 3-62 Motion time history and spectra of coupled case in wind speed 11 m/s

3.2.3.3 Coupled VS Uncoupled in wind speed 11 m/s

Same trends of time histories and spectra with wind speed 5 m/s and 8 m/s coupled and uncoupled cases are observed. The motion time series and the spectra of all six degrees of freedom are shown in figures 3-63 to 3-65. Like other cases, it is also clearly shown that a coupled motion analysis gives bigger values in sway, roll, and, yaw than uncoupled analysis. Also, bigger spectra are observed in the coupled cases. Comparisons of top tension time series and spectra of tethers at 4 legs are shown in figures 3-66 to 3-67.

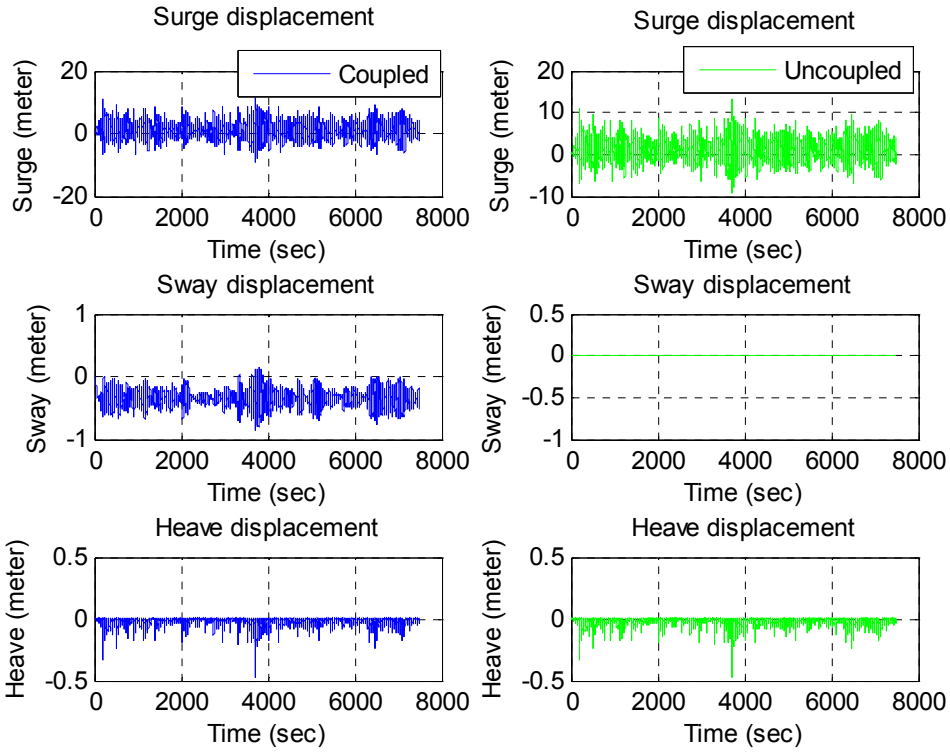

Figure 3-63 Axial motion time series comparison between coupled and uncoupled case in wind speed 11 m/s

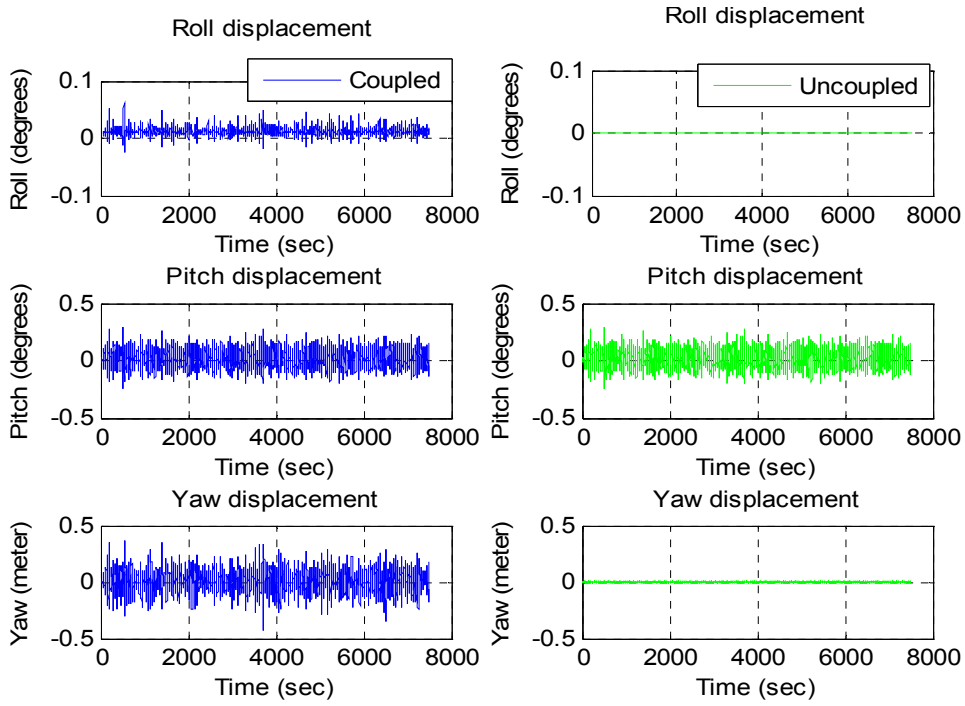

Figure 3-64 Rotational motion time series comparison between coupled and uncoupled case in wind speed 11 m/s

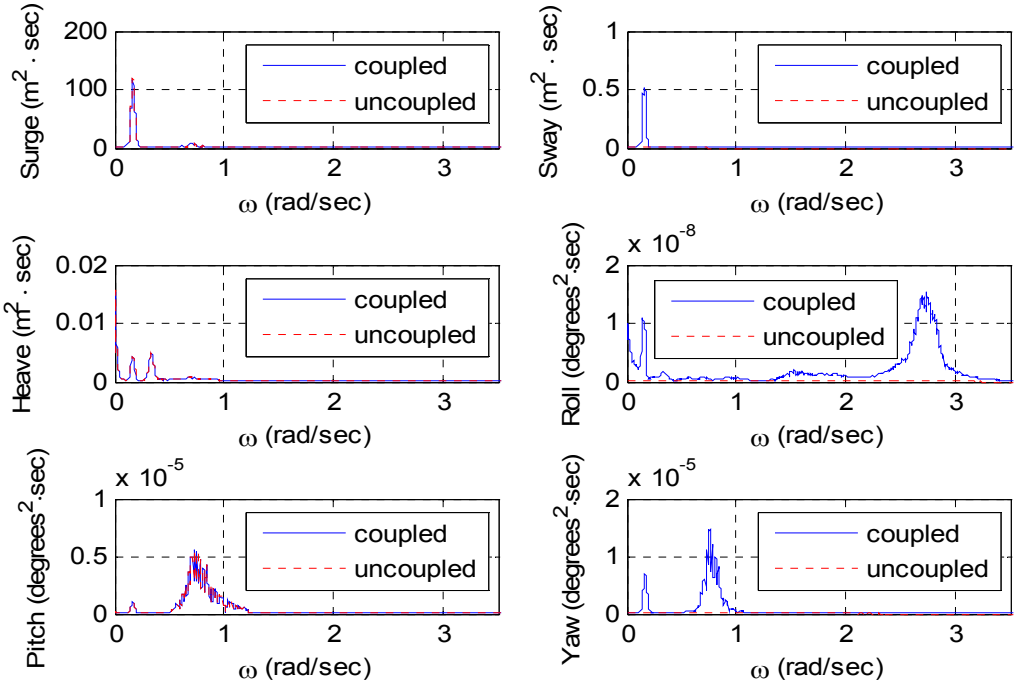

Figure 3-65 Motion spectra comparison between coupled and uncoupled case in wind speed 11 m/s

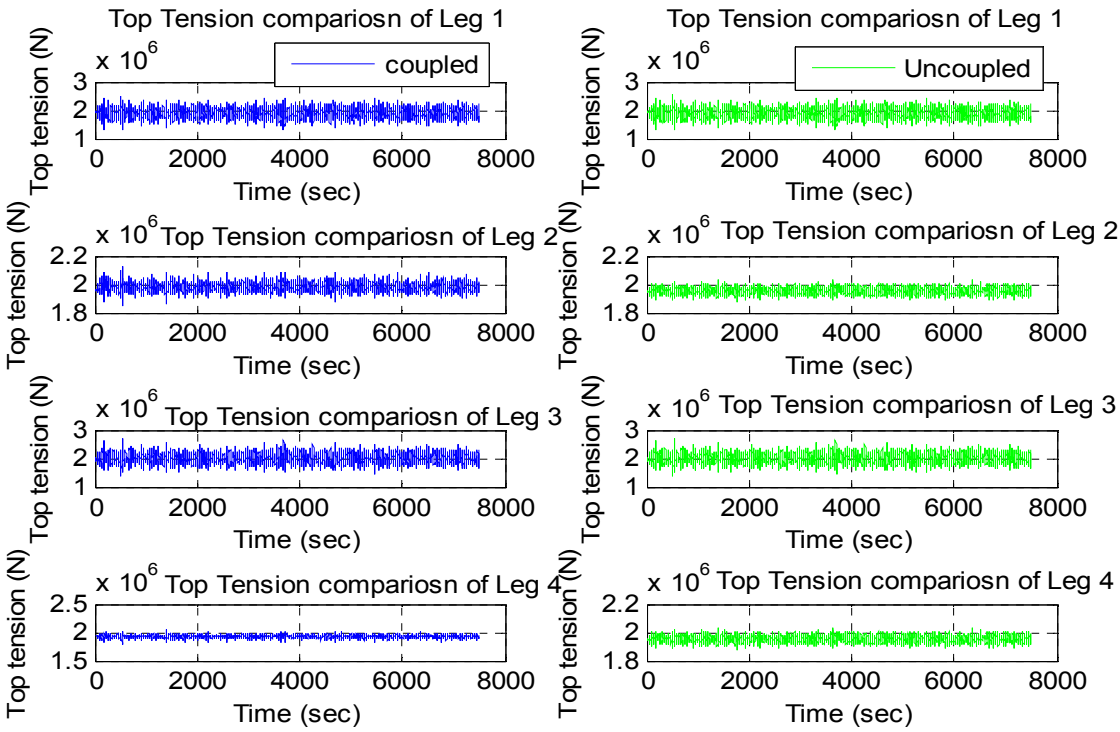

Figure 3-66 Top tension time history comparison between coupled and uncoupled case in wind speed 11 m/s

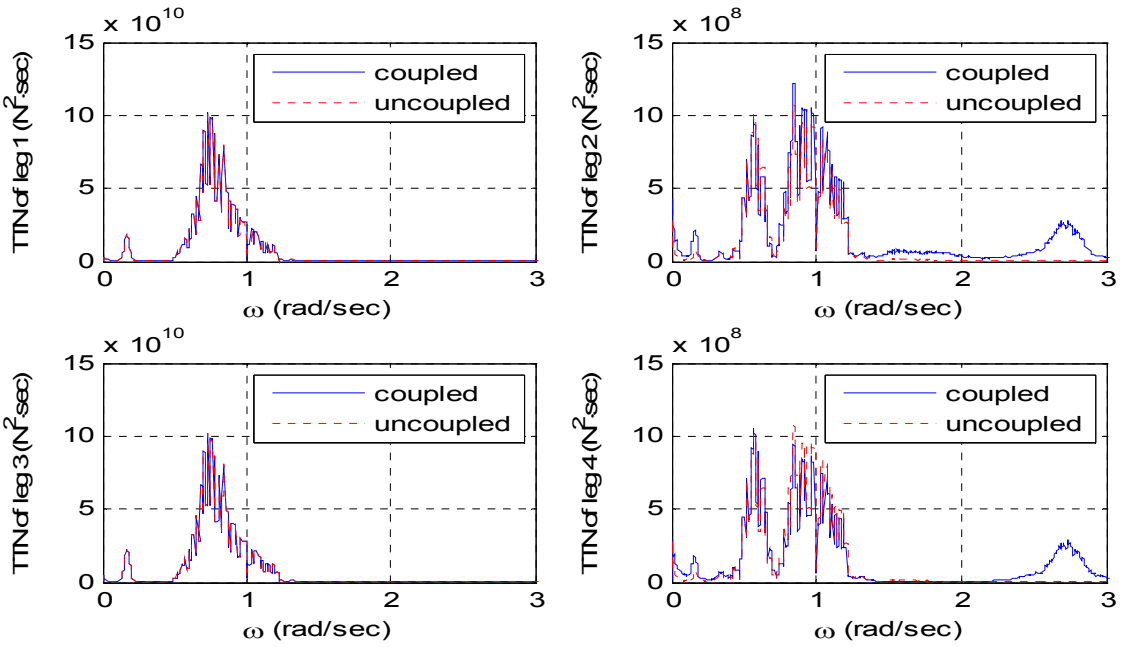

Figure 3-67 Top tension spectra comparison between coupled and uncoupled case in wind speed 11 m/s

Based on these results, we might find that coupling with floating body, mooring, and wind turbine case yields more magnitude of motion and top tension than that of coupling with floating body and mooring only. Especially, in sway, roll, and yaw case, motions and spectra of coupled cases are significantly bigger than that of uncoupled cases. Also, larger standard deviation is observed in tethers at leg 2 and leg 4. It should be effect on fatigue life of tethers. Table 3-4 and table 3-5 show the average of RPM of blades and the statistics of the top tensions of each leg, respectively. We can find that average rpm is increased by high wind speed.

Table 3-4 Average rpm of blades in each wind speed

Wind Speed	Average RPM
5 m/s	7.4482
8 m/s	14.2220
11 m/s	19.8992

Table 3-5 Top tension comparison between coupled and uncoupled in wind speed 11 m/s

		Max.	Min.	Mean	STDEV
Top Tension of Tether at **Leg 1 (N)**	Uncoupled	2.546e6	1.286e6	1.895e6	1.549e5
	Coupled	2.554e6	1.285e6	1.897e6	1.546e5
Top Tension of Tether at **Leg 2 (N)**	Uncoupled	2.036e6	1.870e6	1.953e6	**2.023e4**
	Coupled	2.125e6	1.841e6	1.979e6	**2.392e4**
Top Tension of Tether at **Leg 3 (N)**	Uncoupled	2.668e6	1.389e6	2.011e6	1.566e5
	Coupled	2.671e6	1.378e6	2.009e6	1.565e5
Top Tension of Tether at **Leg 4 (N)**	Uncoupled	2.036e6	1.870e6	1.953e6	**2.023e4**
	Coupled	2.044e6	1.788e6	1.926e6	**2.195e4**

3.3 Coupling simulation for the modified floating wind turbine in the time domain

Case studies of the modified Baseline wind turbine are performed. The modified Baseline wind turbine is the same as the previous floating wind turbine, but larger sized blades (126 m diameter blade) with less density are introduced. We assume that total mass is same as the previous simulation, but we have bigger blades. It is not a really practical study, but we can seek dynamic phenomena with big blades. Based on previous simulations, we observed that more dynamics are observed at high wind speed (11 m/s). In these case studies, we present only a high speed wind speed case (11m/s) and two different wave headings (0 degree and 45 degrees)

3.3.1 Wind speed 11 m/s with 0 degree wave and wind heading

3.3.1.1 Modified uncoupled case in wind speed 11 m/s with 0 degree wave and wind heading

3.3.1.1.1 External forces of the modified uncoupled case in wind speed 11 m/s with 0 degree wave and wind heading

In uncoupled time domain analysis the time histories of two decomposed external forces are shown in figure 3-68. In uncoupled time domain simulation we have wind force and wave force as external forces on the floating body. In this case, since we have a bigger size of blades, we observe bigger wind force on the floating wind turbine.

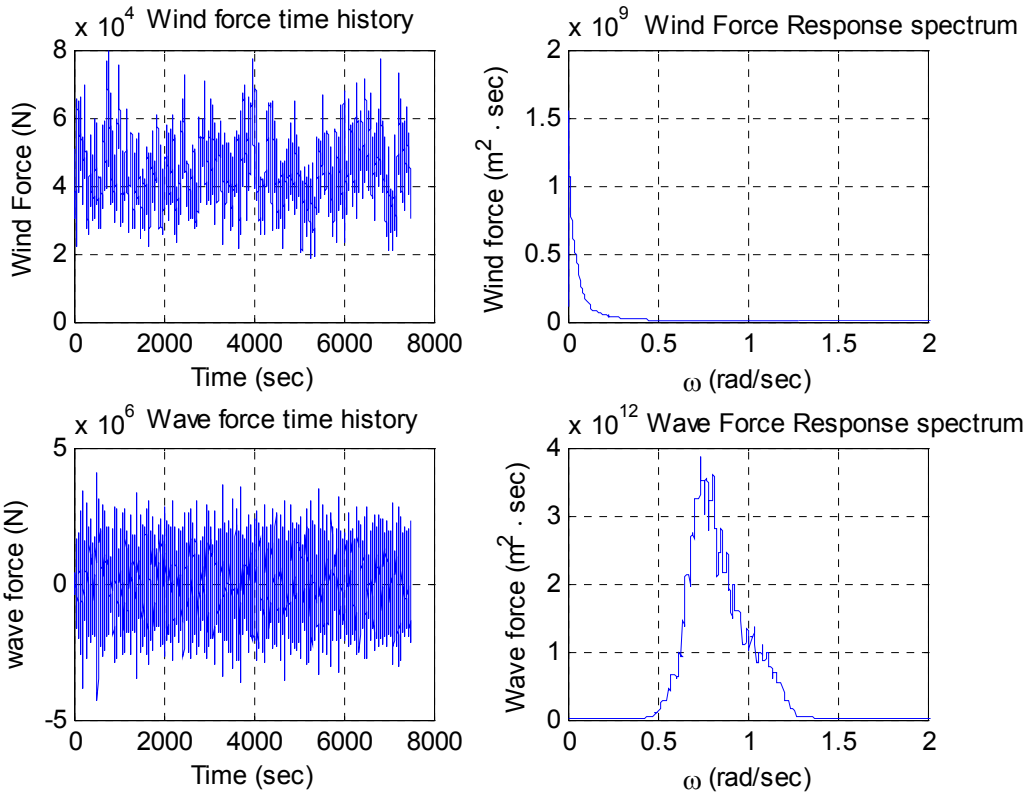

Figure 3-68 External force time series and spectra on the floating body of the modified uncoupled case in wind speed 11m/s with 0 degree wave and wave heading

3.3.1.1.2 Time series and spectra of the modified uncoupled case in wind speed 11 m/s with 0 degree wave and wind heading

Figure 3-69 shows the uncoupled case's motion time history and spectra of the floating body in wind speed 11m/s with 0 degree wave and wind heading. Since we have bigger wind forces on blades, we can observe large motions and spectra than that of previous simulations. Figure 3-70 shows time series and spectrum of top tension of a tether.

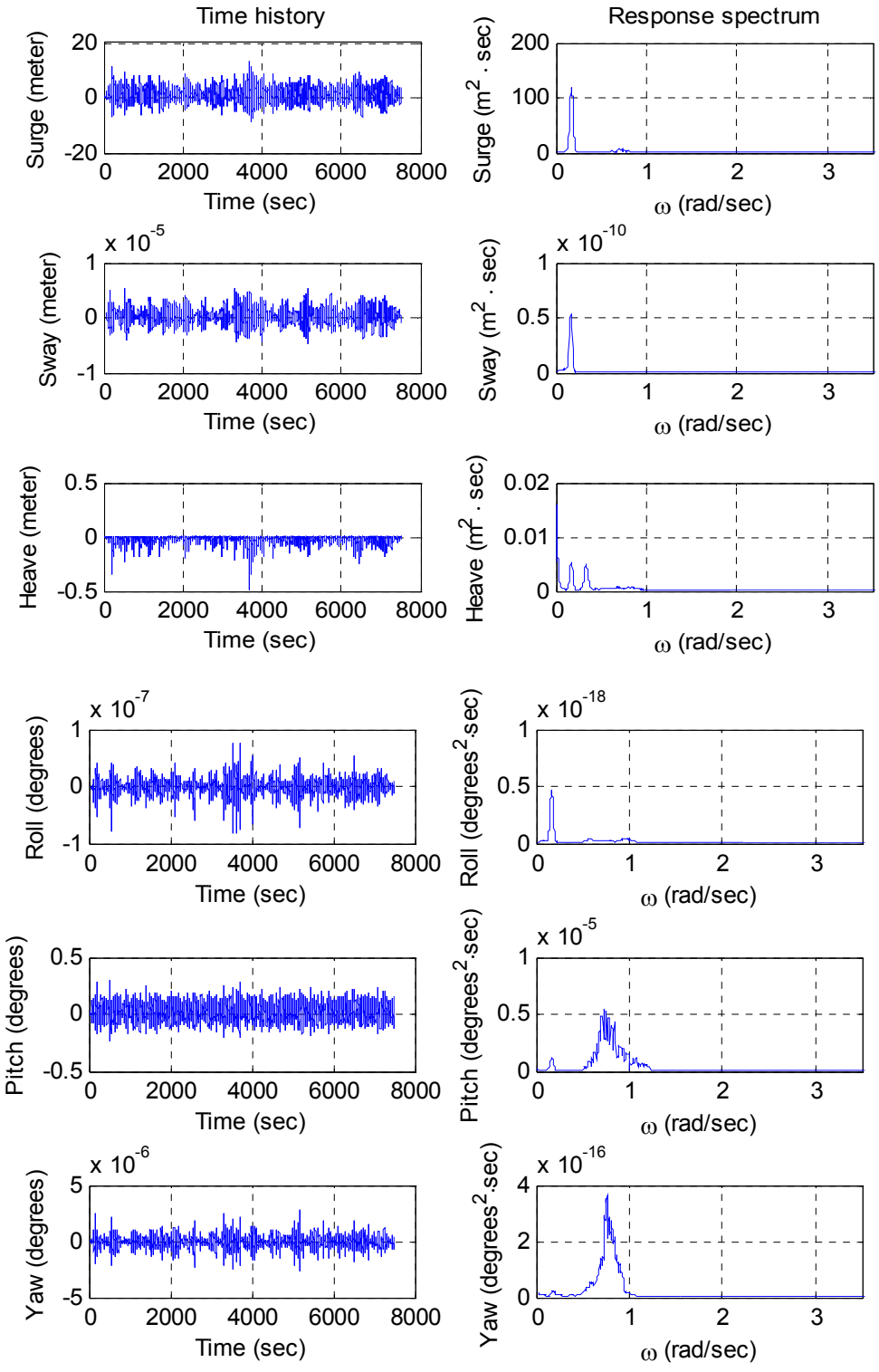

Figure 3-69 Motion time history and spectra of the modified uncoupled case in wind speed 11m/s with 0 degree wave and wind heading

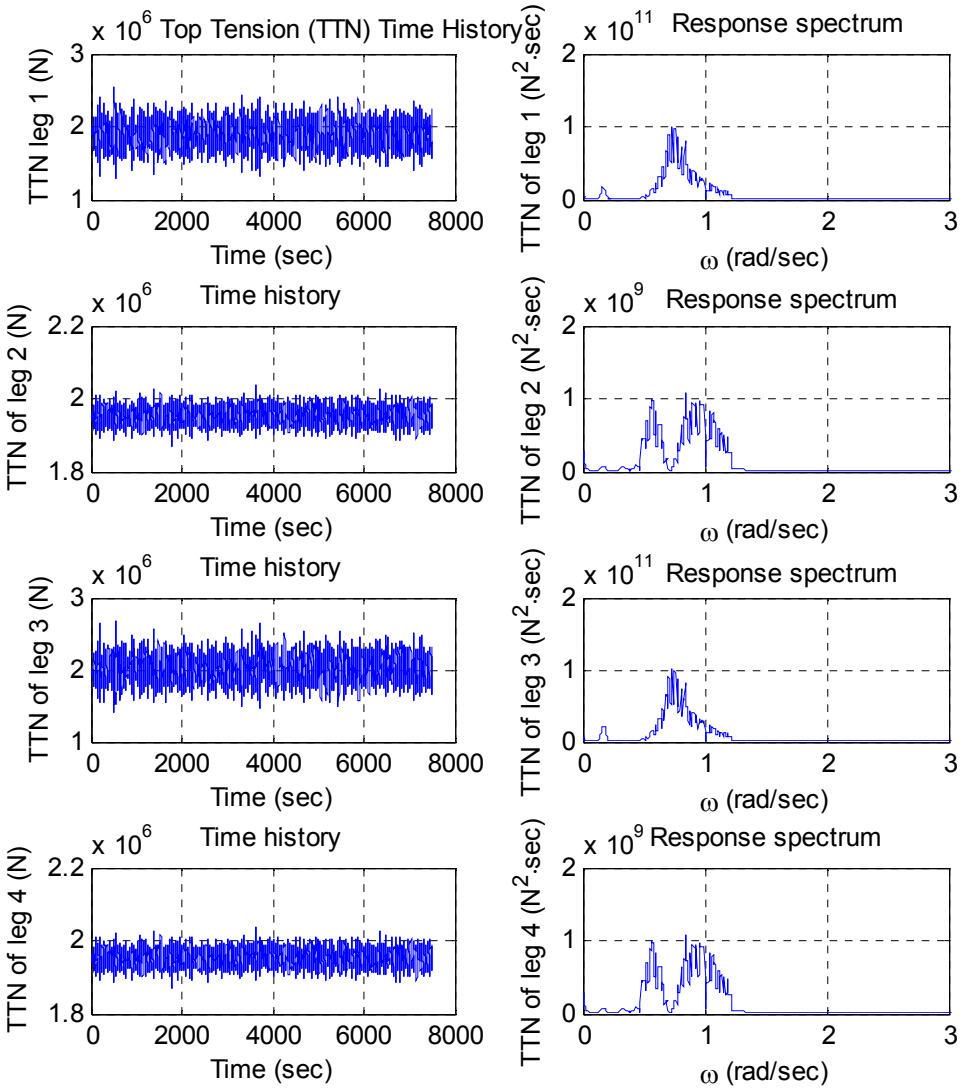

Figure 3-70 Top tension time series and spectra of the modified uncoupled case in wind speed 11m/s with 0 degree wave and wind heading

3.3.1.2 Modified coupled case in wind speed 11 m/s with 0 degree wave and wind heading

3.3.1.2.1 External forces of the modified coupled case in wind speed 11 m/s with 0 degree wave and wind heading

In the modified coupled time domain analysis, the time histories of four decomposed external forces are show in figures 3-71 and 3-72. In the modified coupled time domain simulation, we have wind force, wave force, and reaction forces from dynamics of wind turbine as external forces on the floating body.

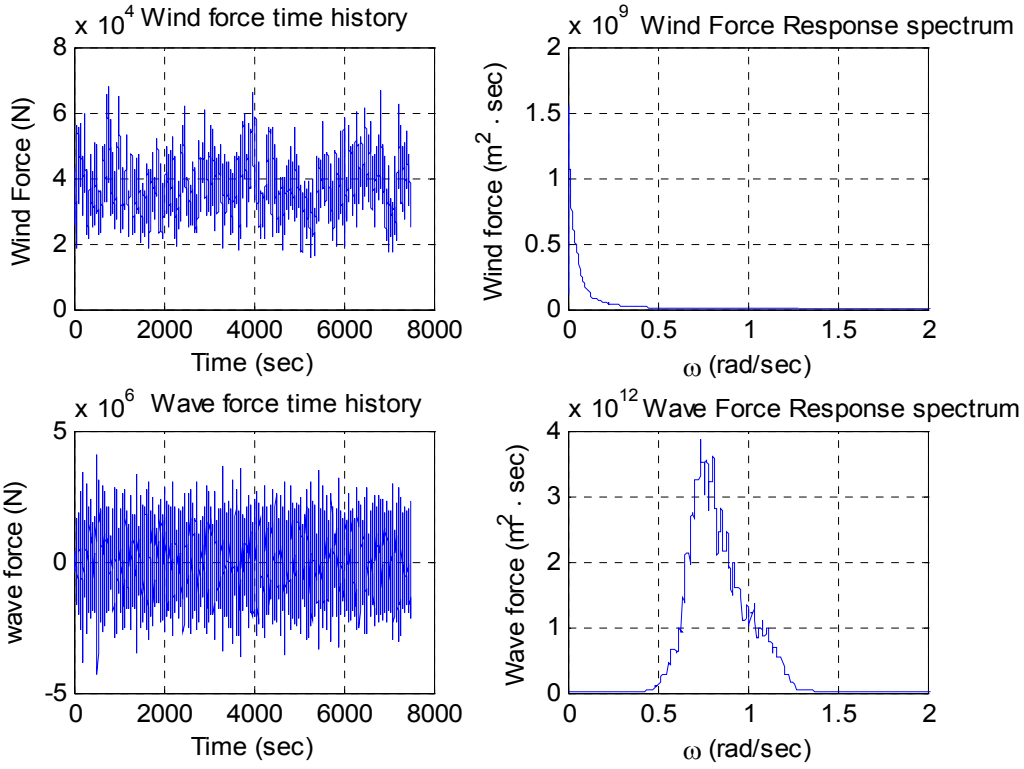

Figure 3-71 Environmental forces time series and spectra on the floating body of the modified coupled case in wind speed 11m/s with 0 degree wave and wind heading

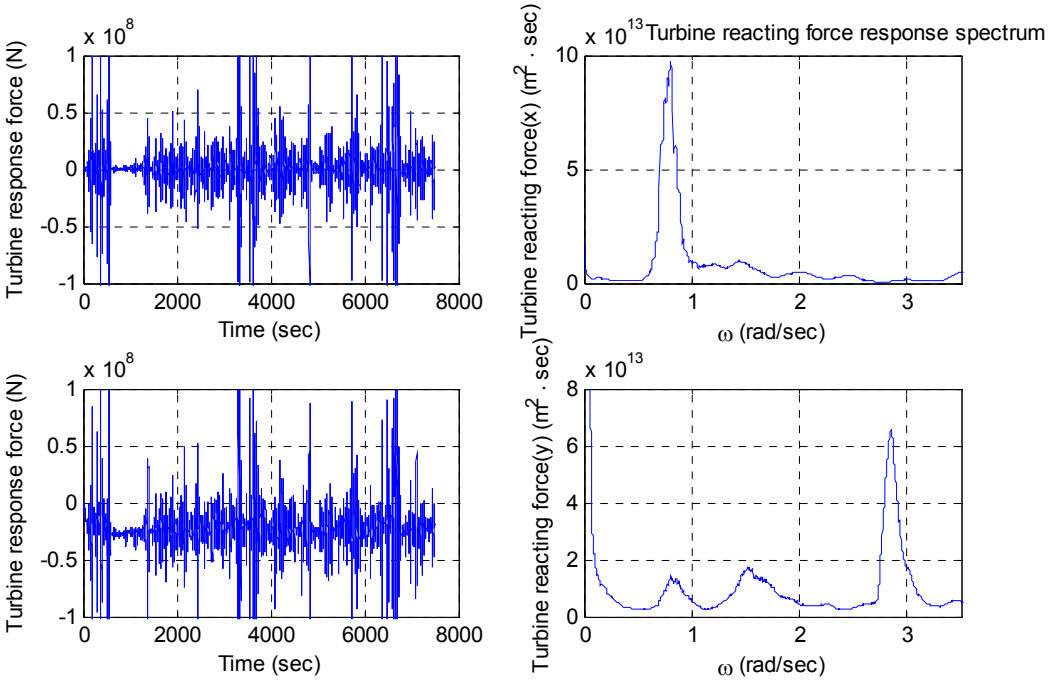

Figure 3-72 Turbine forces time series and spectra on the floating body of the modified coupled case in wind speed 11m/s with 0 degree wave and wind heading

3.3.1.2.2 Time series and spectra of the modified coupled case in wind speed 11 m/s with 0 degree wave and wind heading

Since we have bigger blades than that of previous simulations, there are big aerodynamic forces from the wind turbine. Figure 3-73 shows the modified coupled case's motion time history and spectrum of floating body in wind speed 11m/s. Figure 3-74 shows the time series and spectra of top tension of a tether.

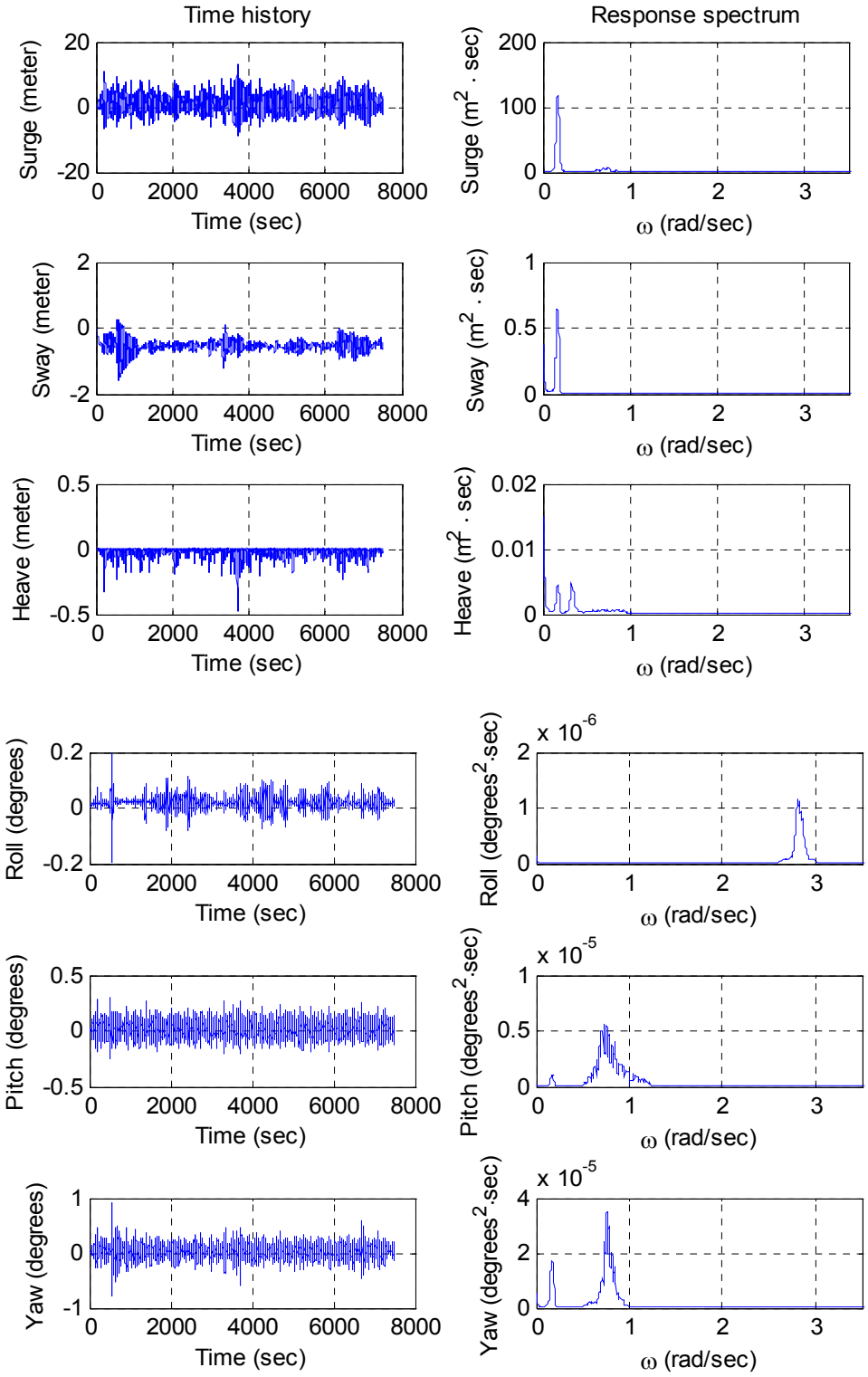

Figure 3-73 Motion time history and spectra of the modified coupled case in wind speed 11 m/s with 0 degree wave and wind heading

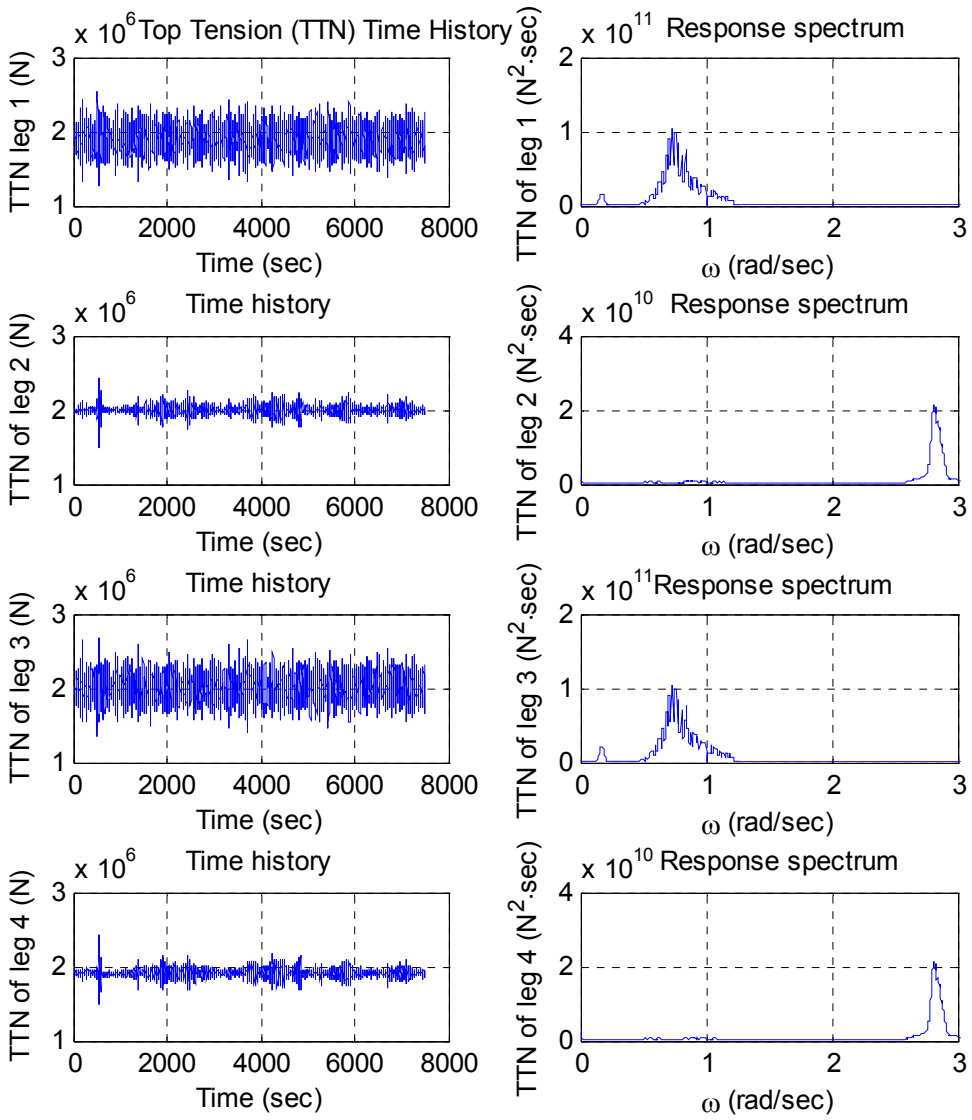

Figure 3-74 Top tension time series and spectra of the modified coupled case in wind speed 11 m/s with 0 degree wave and wind heading

3.3.1.3 Coupled VS Uncoupled in wind speed 11 m/s with 0 degree wave and wind heading

The motion time series and the spectra of all six degrees of freedom are shown in figures 3-75 to 3-77. It is also clearly shown that the modified coupled motion analysis gives bigger values in sway, roll, and yaw than that of the modified uncoupled analysis. In the spectra comparison, a big peak is observed in high frequency in roll motion. The top tension time series and spectra of tethers at 4 legs are shown in figures 3-78 and 3-79.

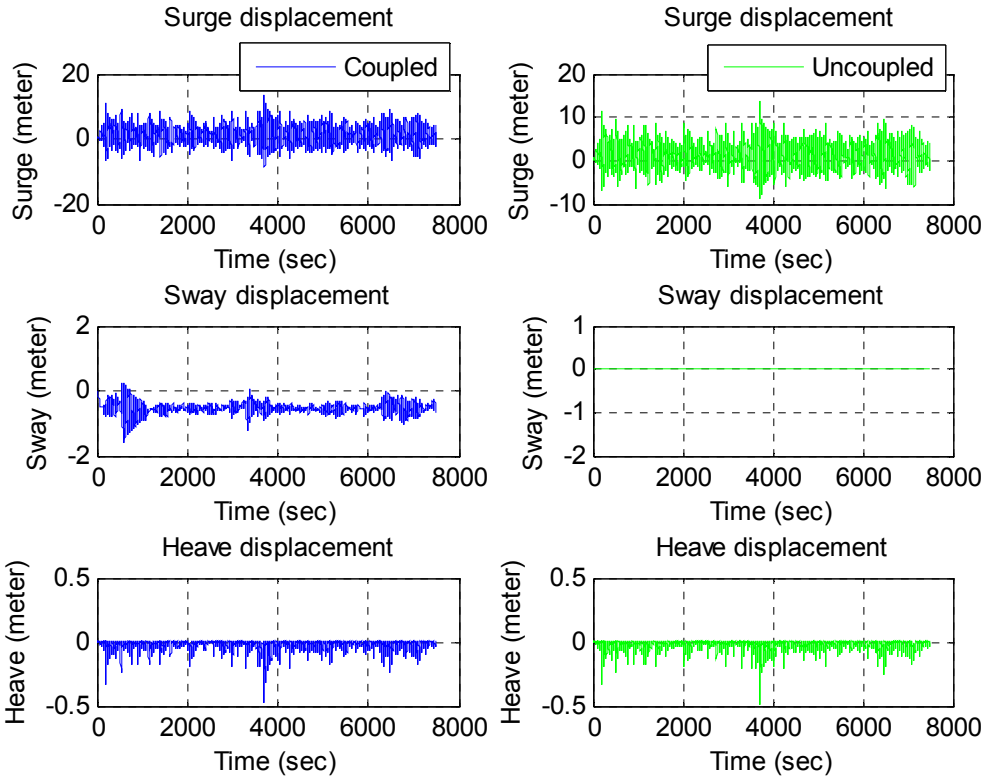

Figure 3-75 Axial motion time series comparison between modified coupled and uncoupled case in wind speed 11 m/s with 0 degree wave and wind heading

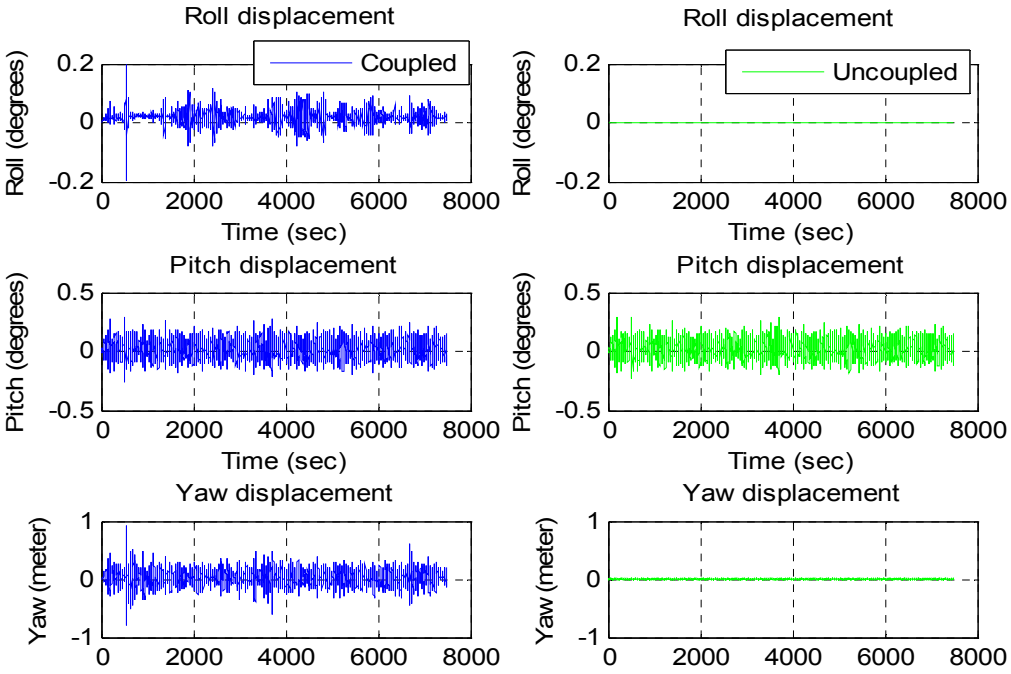

Figure 3-76 Rotational motion time series comparison between modified coupled and uncoupled case in wind speed 11 m/s with 0 degree wave and wind heading

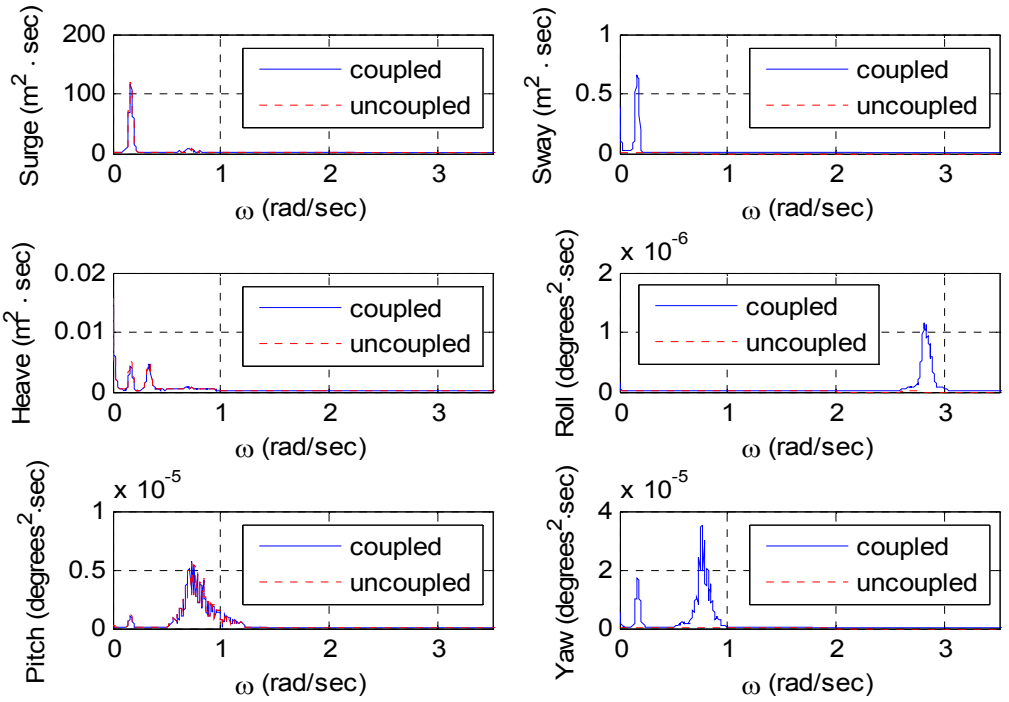

Figure 3-77 Motion spectra comparison between modified coupled and uncoupled case in wind speed 11 m/s with 0 degree wave and wind heading

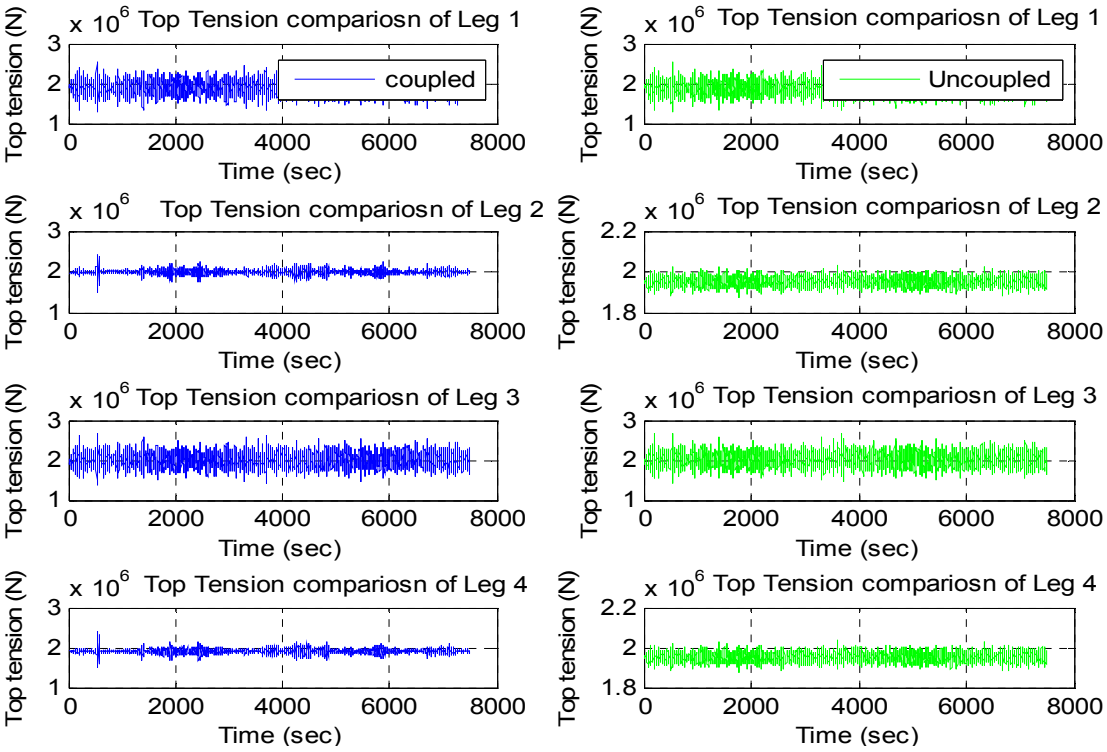

Figure 3-78 Top tension time history comparison between modified coupled and uncoupled case in wind speed 11 m/s with 0 degree wave and wind heading

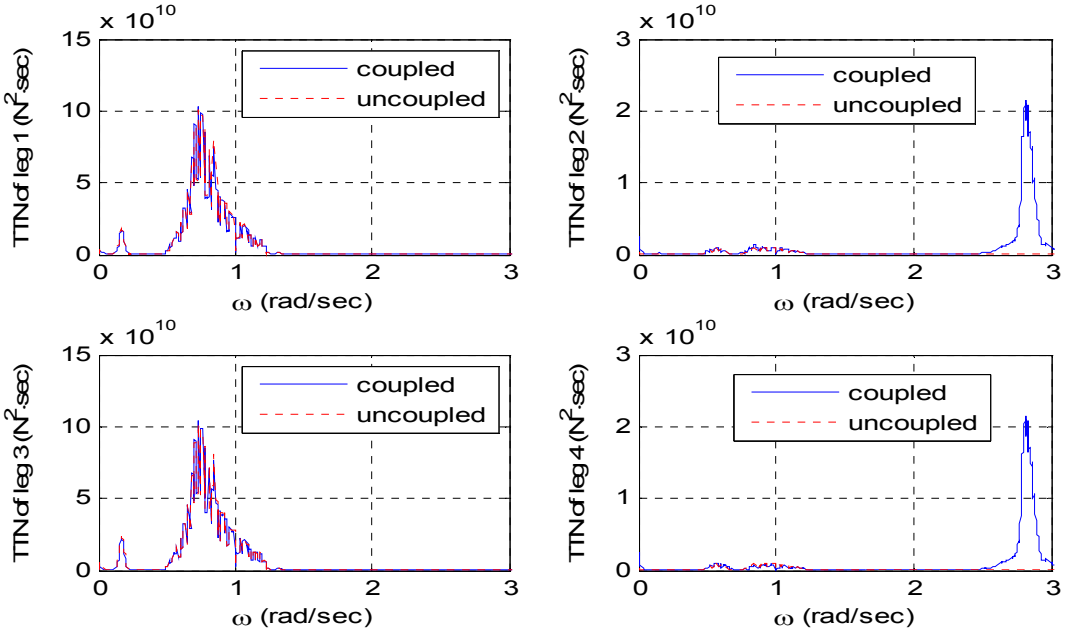

Figure 3-79 Top tension spectra comparison between modified coupled and uncoupled case in wind speed 11 m/s with 0 degree wave and wind heading

Based on these results we can observe the same trends as previous simulations. However more coupled effect is detected because bigger sizes of blades are used. Table 3-5 shows the statistics of top tensions of legs. In top tensions of tethers at leg 2 and leg 4, there is large standard deviation difference between the coupled and the uncoupled case. This might be helpful in designing the mooring line because big standard deviation and high frequency cycle can cause less fatigue life.

Table 3-6 Top tension comparison between modified coupled and uncoupled in wind speed 11 m/s

		Max.	Min.	Mean	STDEV
Top Tension of Tether at **Leg 1 (N)**	Uncoupled	2.536e6	1.283e6	1.888e6	1.550e5
	Coupled	2.554e6	1.275e6	1.896e6	1.540e5
Top Tension of Tether at **Leg 2 (N)**	Uncoupled	2.036e6	1.870e6	1.953e6	**2.024e4**
	Coupled	2.433e6	1.497e6	1.995e6	**5.489e4**
Top Tension of Tether at **Leg 3 (N)**	Uncoupled	2.672e6	1.394e6	2.018e6	1.568e5
	Coupled	2.682e6	1.356e6	2.010e6	1.563e5
Top Tension of Tether at **Leg 4 (N)**	Uncoupled	2.036e6	1.870e6	1.953e6	**2.024e4**
	Coupled	2.419e6	1.485e6	1.911e6	**5.400e4**

3.3.2 Wind speed 11 m/s with 45 degree wave and 0 degree wind heading

3.3.2.1 Modified uncoupled case in wind speed 11 m/s with 45 degree wave and 0 degree wind heading

3.3.2.1.1 External forces of the modified uncoupled case in wind speed 11 m/s with 45 degree wave and 0 degree wind heading

In uncoupled time domain analysis the time histories and spectra of two decomposed external forces are shown in figure 3-80. In uncoupled time domain simulation we have wind force and wave force as external forces on the floating body. In this case, since we have a bigger size of blades, we observe bigger wind force on the floating wind turbine.

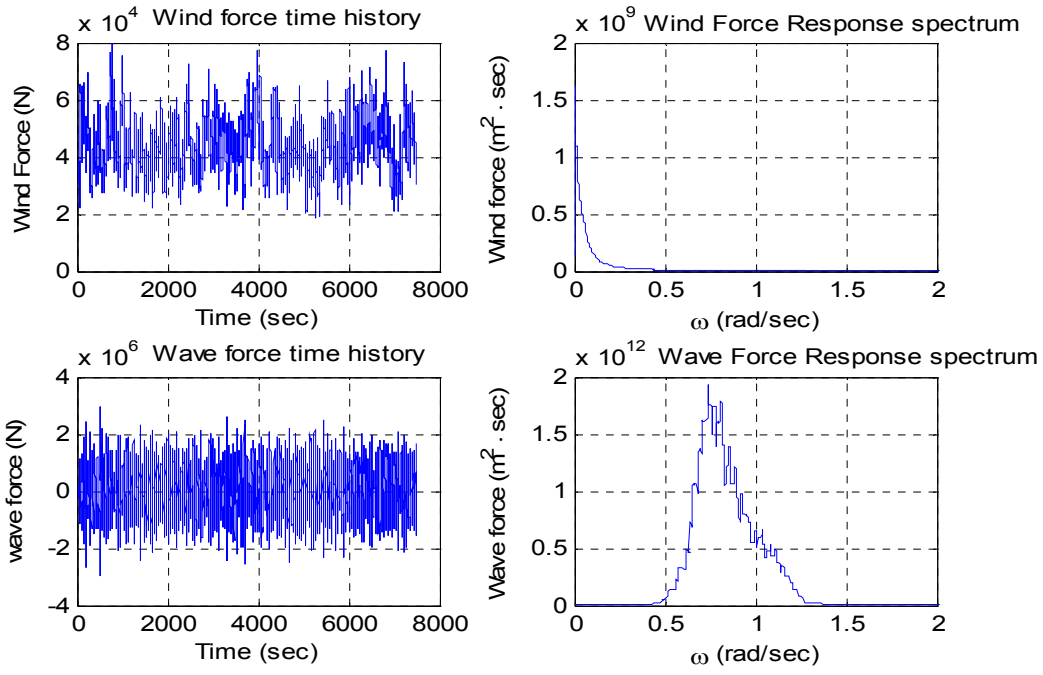

Figure 3-80 External force time series and spectra on the floating body of the uncoupled case in wind speed 11 m/s with 45 degree wave and 0 degree wave heading

3.3.2.1.2 Time series and spectra of the modified uncoupled case in wind speed 11 m/s with 45 degree wave and 0 degree wind heading

Figure 3-81 shows time series and spectrum of top tension of a tether. Figure 3-82 shows the uncoupled case's motion time history and spectra of the floating body in wind speed 11m/s with 45 degree wave and 0 degree wind heading. Since we have bigger wind forces on blades, we can observe large motions and spectra than that of previous simulations.

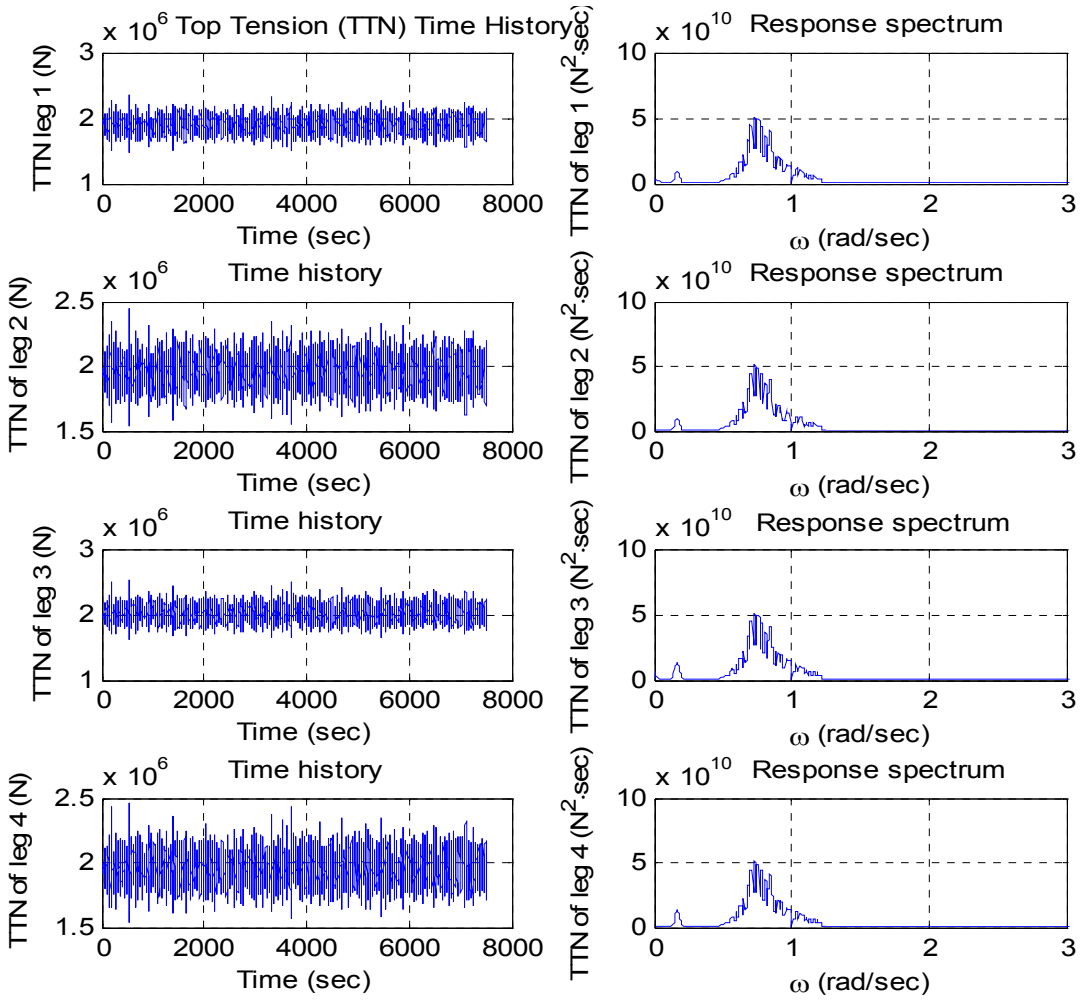

Figure 3-81 Top tension time series and spectra of the uncoupled case in wind speed 11 m/s with 45 degree wave and 0 degree wind heading

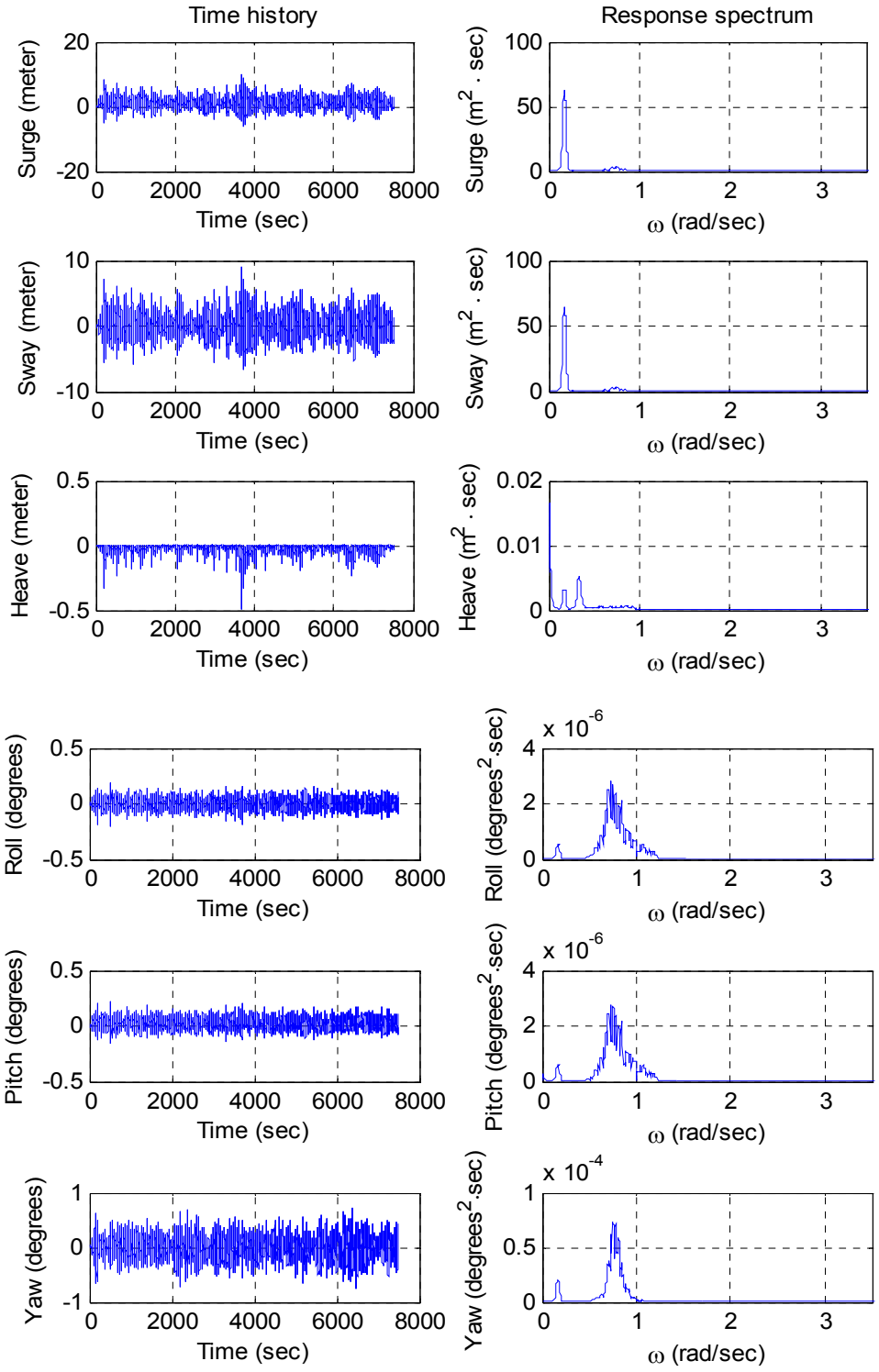

Figure 3-82 Motion time history and spectra of the uncoupled case in wind speed 11 m/s with 45 degree wave and 0 degree wave heading

3.3.2.2 Modified coupled case in wind speed 11 m/s with 45 degree wave and 0 degree wind heading

3.3.2.2.1 External forces of the modified coupled case in wind speed 11 m/s with 45 degree wave and 0 degree wind heading

In the modified coupled time domain analysis, the time histories of four decomposed external forces and spectra are show in figures 3-83 and 3-84. In the modified coupled time domain simulation, we have wind force, wave force, and reaction forces from dynamics of wind turbine as external forces on the floating body.

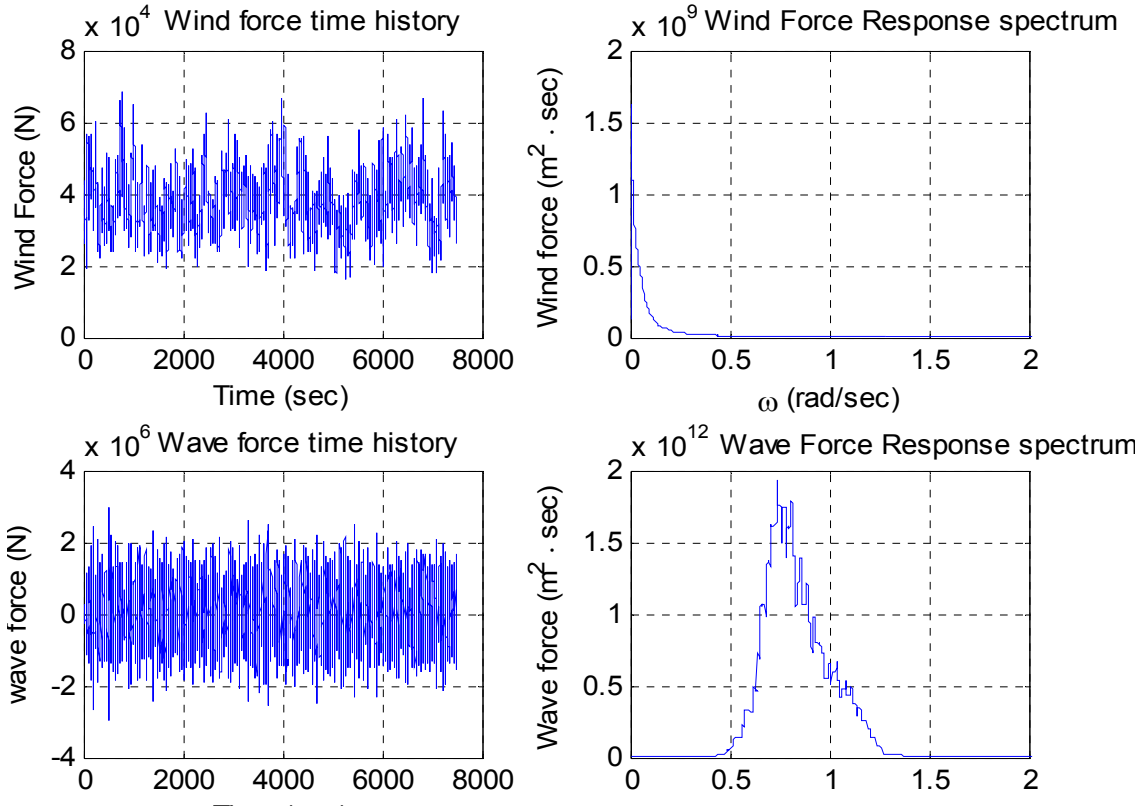

Figure 3-83 Environmental force time series and spectra on the floating body in wind speed 11 m/s with 45 degree wave and 0 degree wind heading

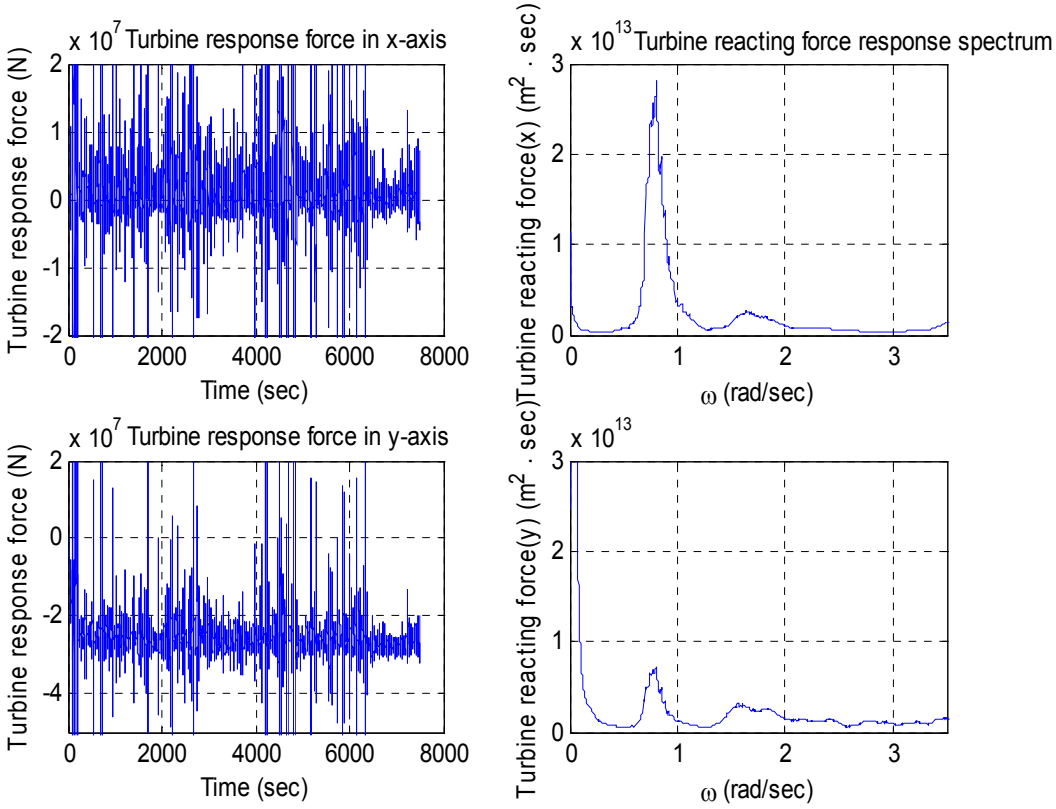

Figure 3-84 Turbine force time series and spectra on the floating body in wind speed 11 m/s with 45 degree wave and 0 degree wind heading

3.3.2.2.2 Time series and spectra of the modified coupled case in wind speed 11 m/s with 0 degree wave and wind heading

Figure 3-85 shows the modified coupled case's motion time history and spectrum of floating body in wind speed 11m/s. Figure 3-86 shows time series and spectrum of top tension of a tether.

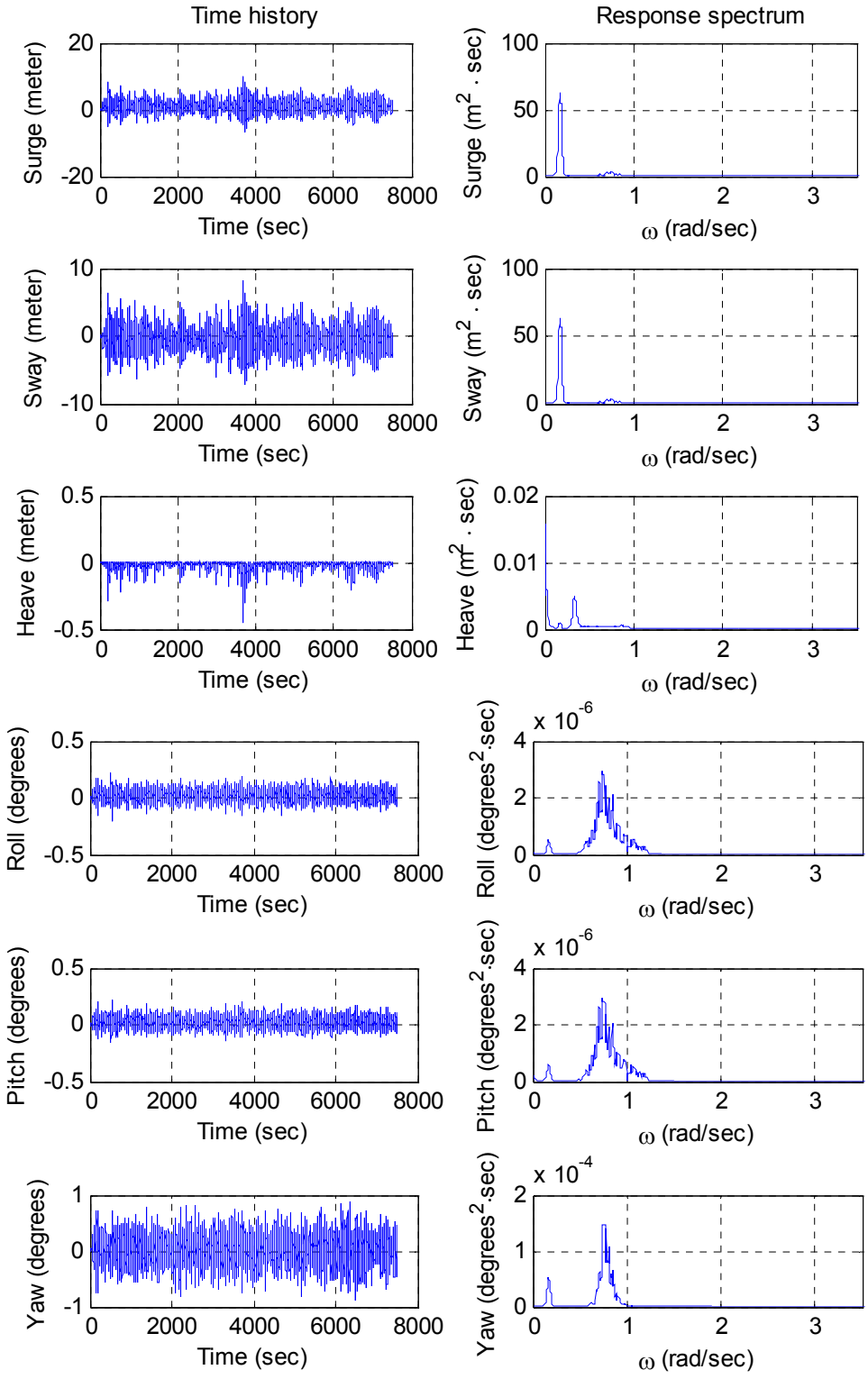

Figure 3-85 Motion time history and spectra of the coupled case in wind speed 11 m/s with 45 degree wave and 0 degree wind heading

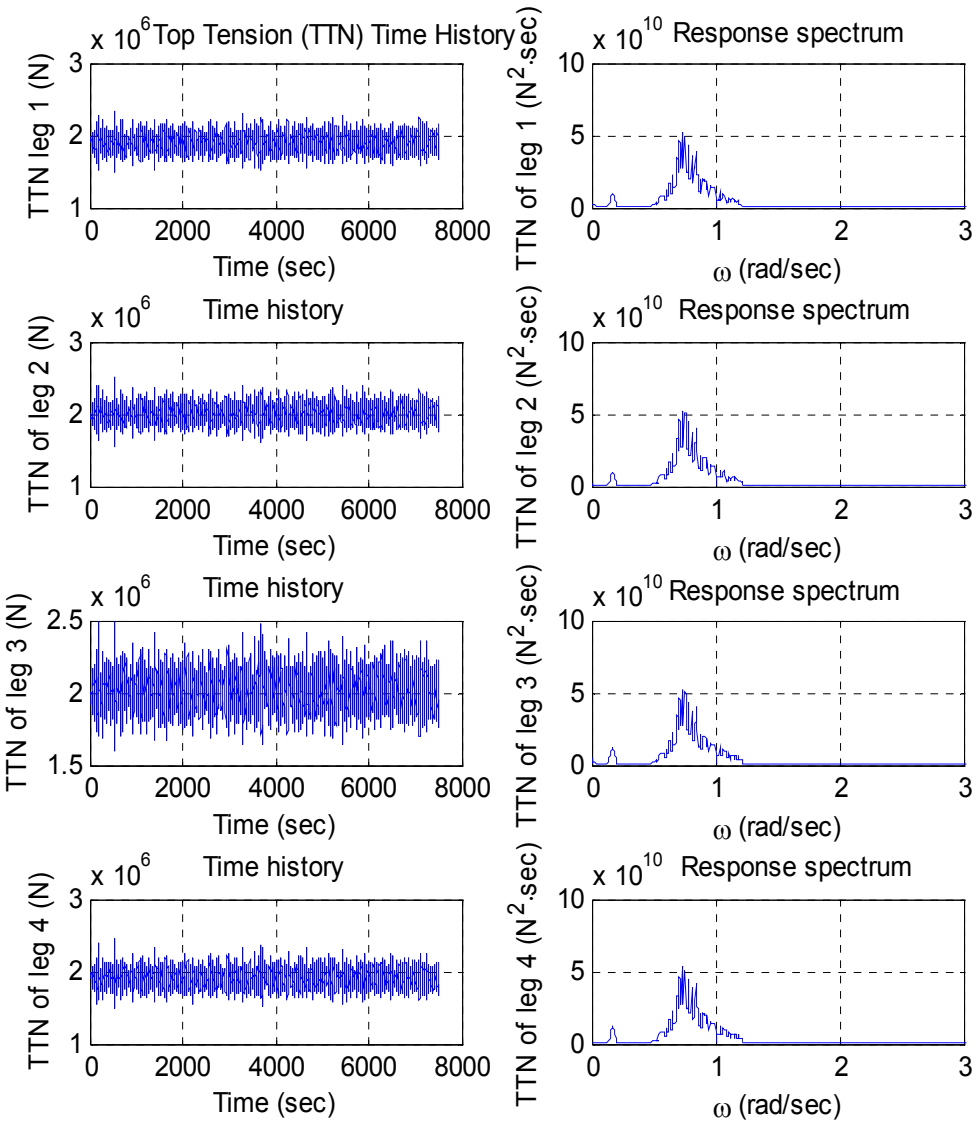

Figure 3-86 Top tension time series and spectra of the coupled case in wind speed 11 m/s with 45 degree wave and 0 degree wind heading

3.3.2.3 Coupled VS Uncoupled in wind speed 11 m/s with 45 degree wave and 0 degree wind heading

The motion time series and the spectra of all six degrees of freedom are shown in figures 3-87 to 3-89. It is not clearly shown that the modified coupled motion analysis gives bigger values than the modified uncoupled analysis in 11 m/s wind speed with 45 wave and 0 degree wind heading. In the motion spectra comparison, we cab observed a peak in high frequency in yaw motion. The top tension time series and spectra of tethers at 4 legs are shown in figures 3-90 and 3-91. In the top tension spectra, a very small peak is found in high frequency in coupled cases.

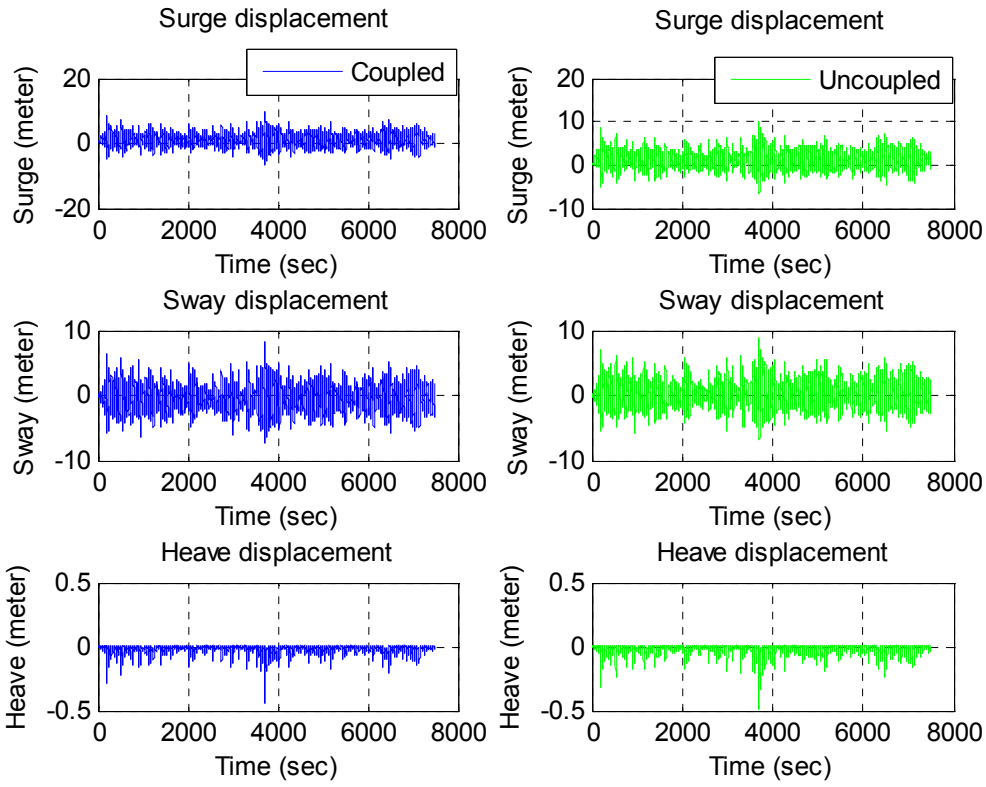

Figure 3-87 Axial Rotational motion time series comparison between modified coupled and uncoupled case in wind speed 11 m/s with 45 degree wave and 0 degree wind heading

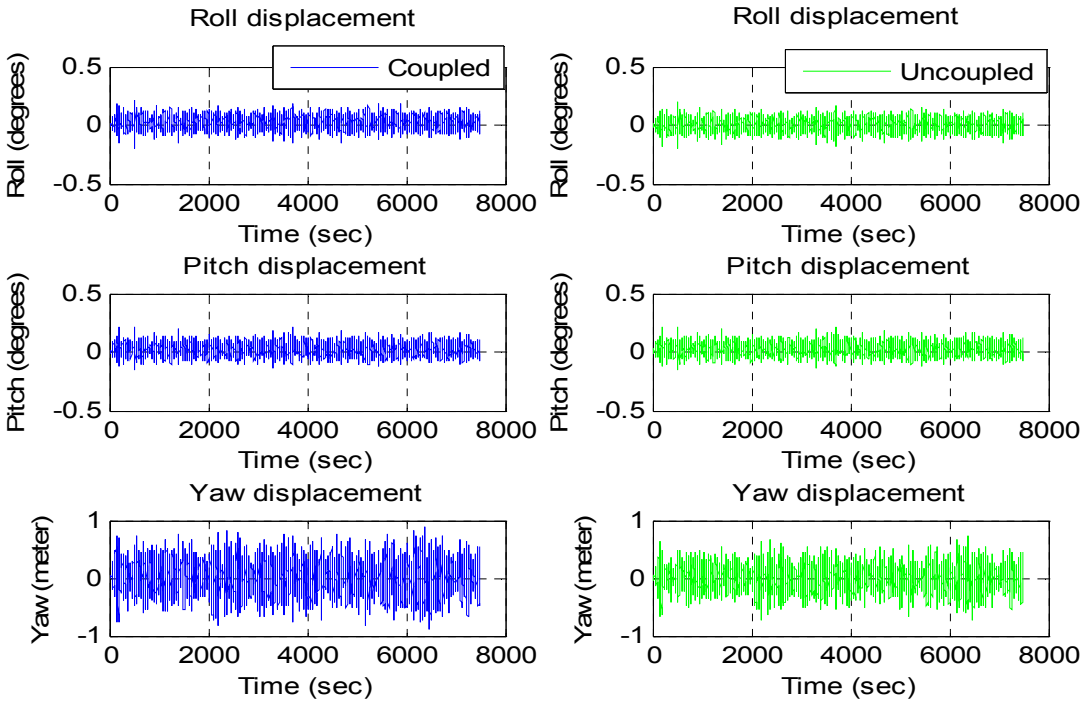

Figure 3-88 Rotational motion time series comparison between modified coupled and uncoupled case in wind speed 11 m/s with 45 degree wave and 0 degree wind heading

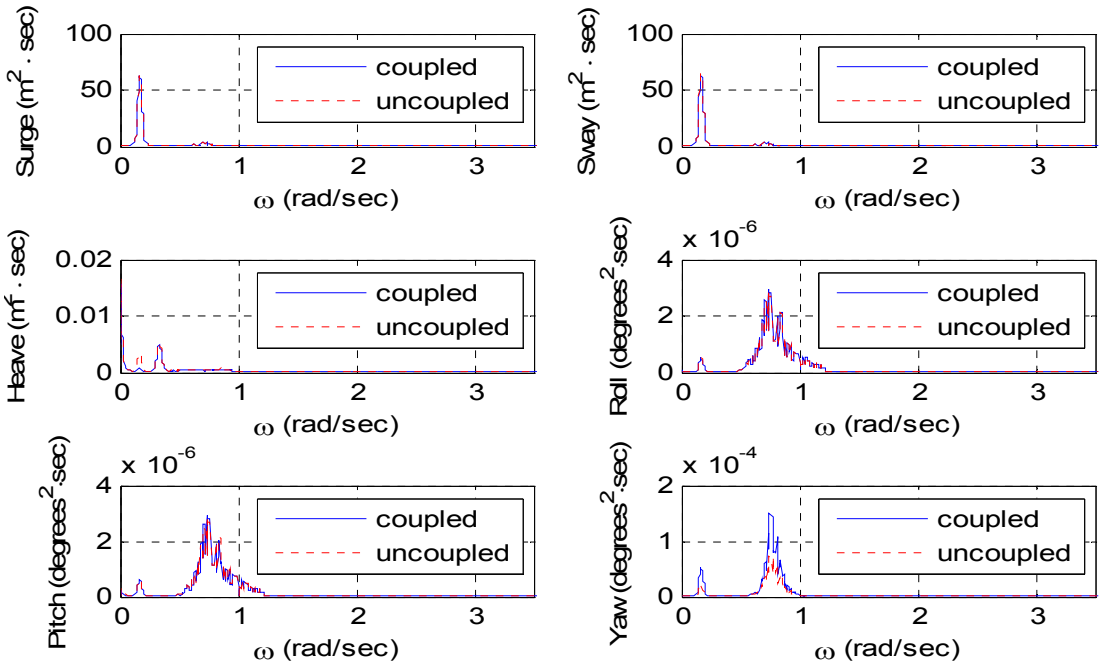

Figure 3-89 Motion spectra comparison between coupled and uncoupled case in wind speed 11 m/s with 45 degree wave and 0 degree wind heading

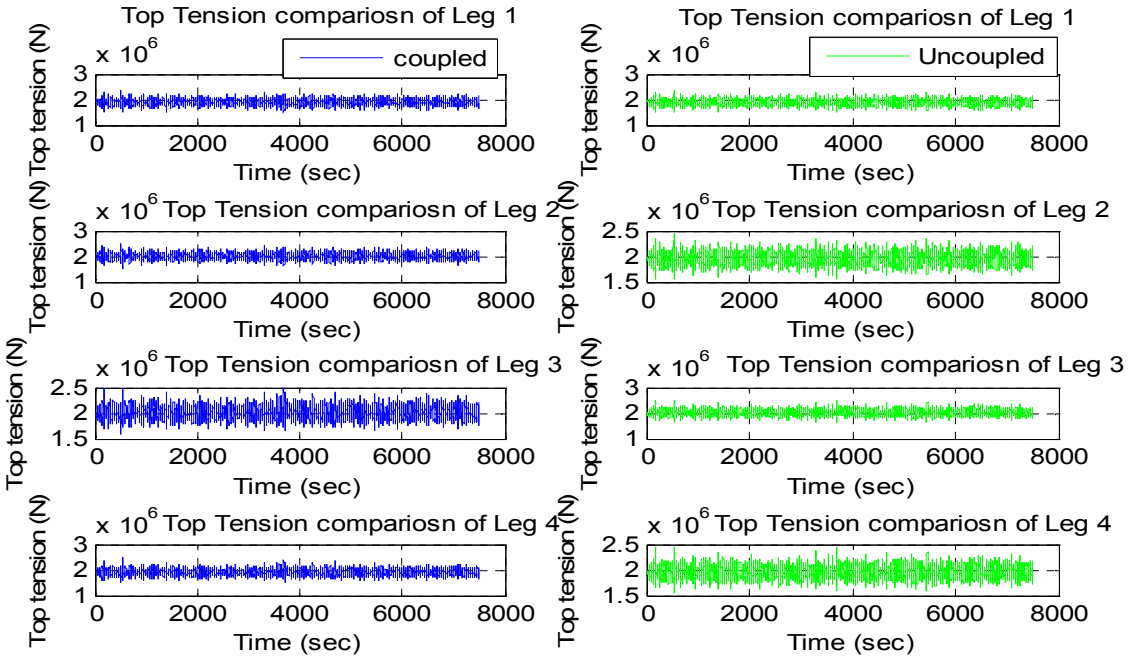

Figure 3-90 Top tension time history comparison between modified coupled and uncoupled case in wind speed 11 m/s with 45 degree wave and 0 degree wind heading

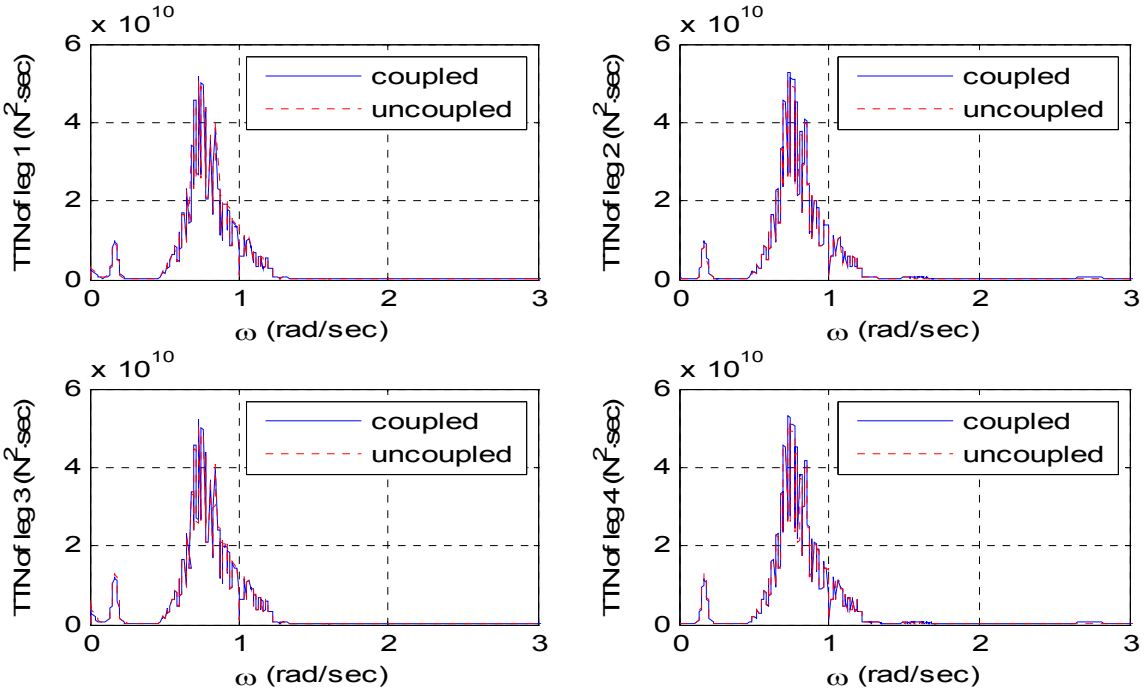

Figure 3-91 Top tension spectra comparison between modified coupled and uncoupled case in wind speed 11 m/s with 45 degree wave and 0 degree wind heading

Table 3-7 shows the statistics of the top tensions of each leg. Since wave heading is 45 degrees, bigger top tension standard deviation values are observed in leg 2 and 4 than that of 0 degree wave heading case.

Table 3-7 Top tension comparison between coupled and uncoupled in wind speed 11 m/s with 45 degree wave and 0 degree wind heading

		Max.	Min.	Mean	STDEV
Top Tension of Tether at **Leg 1 (N)**	Uncoupled	2.370e6	1.480e6	1.890e6	1.107e5
	Coupled	2.352e6	1.481e6	1.898e6	1.102e5
Top Tension of Tether at **Leg 2 (N)**	Uncoupled	2.450e6	1.537e6	1.954e6	1.100e5
	Coupled	2.508e6	1.532e6	2.002e6	1.119e5
Top Tension of Tether at **Leg 3 (N)**	Uncoupled	2.520e6	1.612e6	2.021e6	1.128e5
	Coupled	2.498e6	1.593e6	2.014e6	1.122e5
Top Tension of Tether at **Leg 4 (N)**	Uncoupled	2.462e6	1.536e6	1.957e6	1.117e5
	Coupled	2.470e6	1.489e6	1.910e6	1.134e5

3.4 Fatigue analysis

Since big standard deviation and high frequency cycle of top tension are observed from coupled cases, comparison study of expected fatigue life is performed. In this study, the wind speed 11 m/s with 0 degree wave and wind heading case study is selected for fatigue analysis because this case shows biggest significant coupling effect. The fatigue damage is computed by Narrow Band theory (API RM 2SK, 2001). The annual fatigue damage is initially computed. The annual fatigue damage is following:

$$D = N\left(\sqrt{2}\cdot R_{rms}\right)^{M}\Gamma\left(1+M/2\right)/K$$

Where:

D = annual fatigue damage

K = the intercept parameter of the T/N curve

M = the slope of the T/N curve

R_{rms} = the ratios of rms tension range to a reference breaking strength (the rms tension range should be taken as twice the rms tension)

N = the numbers of tension cycles per year.

Fatigue analysis should be covered all mooring system components (mooring line, chain, connecting link, shackle, and etc.) because the meaning of the breaking one component is the failure of whole mooring system. In this section, two main components (tether and chain) are selected for fatigue analysis. For two components (tether and chain), material properties are required for fatigue analysis and we get these values from API RM 2SK (2005), HMPE property report (Gilmore J., Miller J., 2006) and API RM 2SM (2001).

For fatigue analysis for tethers, High Modulus PolyEthylene (HMPE) is used as a tether material and HMPE tether properties (K , M , and R_{rms}) are calculated from API codes. In the tether fatigue analysis, API recommended safety factor 10 for HMPE is applied. By Narrow Band theory, fatigue lives of tethers at leg 2 are shown in table 3-8.

.

Table 3-8 Fatigue analysis of tethers at leg 2 for uncoupled and coupled case

	Uncoupled	Coupled
K	7.5	7.5
M	9	9
Breaking strength (tons)	701.73	701.73
rms (N)	2.02E4	5.49E4
R_{rms}	5.88E-3	1.59E-2
N	3.01E6	1.41E7
D	4.0E-12	1.48E-7
L (years)	2.50E11	6.76E6

Based on Narrow Band Theory, fatigue life of tethers for coupled case is almost two times less than uncoupled case. Since HMPE is used for tether materials, fatigue life is very large.

The studless chain is selected for fatigue analysis. The studless chain was developed in the 1990s and it has been used by the offshore industry for permanent

mooring system. In this fatigue analysis, 142 mm diameter of studless chain is selected because this size of chain has enough breaking load. The chain material properties (K, M, and R_{rms}) are calculated from API codes. In the studless chain fatigue analysis, API recommended safety factor 3 for the steel chain is applied. By Narrow Band theory, fatigue lives of the studless chain at leg 2 are shown in table 3-9

Table 3-9 Fatigue analysis of the studless chain at leg 2 for uncoupled and coupled case

	Uncoupled	Coupled
K	316	316
M	3	3
Breaking load (KN)	13887	13887
rms (N)	2.02E4	5.49E4
R_{rms}	2.91E-3	7.91E-2
N	3.01E6	1.41E7
D	8.87E-4	8.26E-2
L (years)	3.76E2	4.04

For uncoupled case and coupled case, fatigue lives of tethers are 376 years and 4 years respectively. This result shows us significant difference of fatigue life between uncoupled case and coupled case. In addition, this is the main reason why coupled analysis of offshore floating wind turbines is required.

4. SUMMARY AND CONCLUSION

So far, most of wind farm research has been limited to fixed towers in shallow-water areas. In this research, a new concept-the performance of offshore floating wind turbine system is investigated. A numerical model has been developed to analyze the fully coupled dynamics of an offshore floating wind turbine system including rotor dynamics, mooring dynamics, and floater motions. The mini-TLP-type-floater developed by the National Renewable Energy Laboratory (NREL) has been selected for the coupled analysis. The coupling effects between the floating system with tethers and the wind turbine with blades have been numerically simulated in time domain for three different wind speeds and two blade sizes. The motion and tension time series and spectra are produced to demonstrate the general functionality and dynamic coupling effects in both time and frequency domain.

It is seen that the rotor-floater coupling effects increase with wind velocity and blade size. The rotor dynamics additionally cause high-frequency vibrations on the floater in the direction perpendicular to the wind. The coupling effects also increase the rms dynamic tension of tethers, which may be a concern for tendon fatigue failure. The present study is applicable to any types of new offshore floating wind farms in the future.

REFERENCES

API RP 2SK, 2005., Desing and Analysis of Stationkeeping Systems for Floating Structus, American Petroleum Institute, Washington, DC.

API RP 2SM, 2001., Recommended Practice for Design, Manufacture, Installation, and Maintenance of Synthetic Fiber Ropes for Offshore Mooring, American Petroleum Institute, Washington, DC.

Cozijn J.L, and Bunnik. T.H.J, 2004., Coupled Mooring Analysis for Deep Water Calm Buoy, OMAE conference, pp.1-11.

Gilmore J., Miller J., 2006., Mooring with High Modulus PolyEthylene (HMPE) Fiber lines, Samson Rope Technologies, Ferndale, WA.

Henderson, A.R, Leutz R, and Fujii T., 2002., Potential for Floating Offshore Wind Energy in Japanese Waters, ISOPE conference, pp. 505-512.

Henderson A.R.; Bulder B.; Huijsmans R.; Peeringa J.; Pierik J.; Snijders E.; van Hees M.; Wijnants G.H.; Wolf M.J., 2004., Floating Windframs for Shallow Offshore Sites, ISOPE conference, pp. 405-418.

Jonkman J.M, 2003., Modeling of the UAE Wind Turbine for Refinement of FAST_AD,NREL/TP-500-34755, National Renewable Energy Laboratory, Golden, CO.

Jonkman J.M and Buhl, Marshall L.B., 2004., FAST User's Guide NREL/EL-500-29798, National Renewable Energy Laboratory, Golden, CO.

Jonkman J M, and Sclvounos, P, D., 2006., Development of Fully Coupled Aerodlastic and Hydrodynamic Models for Offshore Wind Turbines, NREL/CP-500-39066,

National Renewable Energy Laboratory, Golden,CO.

Kim, M. H., 1997., WINTCOL/WINPOST User's Manual. Ocean Engineering Program, Civil Engineering Department, Texas A&M University, College Station, TX.

Kosugi A, Ogata R, Kagemoto H, Akutsu Y, and Kinoshita T., 2002., A Feasibility Study on a Floating Wind Farm off Japan Coast, ISOPE conference, pp499-505. .

Musial W, Butterfield S, and Boone A., 2003., Feasibility of Floating Platform Systems for Wind Turbines", NREL/CP-500-34874, National Renewable Energy Laboratory, Golden, CO.

Wayman E.N, Sclavounos P.D, Butterfield S, Jonkman J, Musial W., 2006., Coupled Dynamic Modeling of Floating Wind Turbine Systems, OTC, Houston, TX.

Withee J.E., 2004., Fully Coupled Dynamic Analysis of a Floating Wind Turbine System, Ph.D. Dissertation, Department of Ocean Engineering, Massachusetts Institute of Technology, Cambridge, MA.

World Renewable Energy Congress., 2003., Renewable Energy Past, Present, and Future, National Renewable Energy Laboratory, Golden, CO.

APPENDIX

Blade input files for the 1.5 MW Baseline wind turbine (70 m diameter blades)

s818_2702.dat Re=4,000,000 (windward modified the flat Cl section near stall)
FROM Dayton Griffin, sept28 '00, post stall blended with flat plate. Foilchcked by Windward on 10-Oct-2000 at 10:23.

1 Number of airfoil tables in this file
0.00 Table ID parameter
12.50 Stall angle (deg)
0.00 No longer used, enter zero
0.00 No longer used, enter zero
0.00 No longer used, enter zero
-5.31 Zero lift angle of attack (deg)
6.1084 Cn slope for zero lift (dimensionless)
1.9560 Cn at stall value for positive angle of attack
-0.8000 Cn at stall value for negative angle of attack
-4.5000 Angle of attack for minimum CD (deg)
0.0082 Minimum CD value

-180.00	-0.170	0.0200
-170.00	0.640	0.0500
-160.00	0.840	0.3100
-150.00	1.080	0.6200
-140.00	1.150	0.9600
-130.00	1.090	1.3000
-120.00	0.880	1.5200
-110.00	0.600	1.6600
-100.00	0.310	1.7600
-90.00	0.000	1.8000
-80.00	-0.310	1.7600
-70.00	-0.600	1.6600
-60.00	-0.880	1.5200
-50.00	-1.090	1.3000
-40.00	-1.150	0.9600
-30.00	-1.080	0.6200
-20.00	-0.840	0.3100
-10.00	-0.640	0.0144
-8.00	-0.480	0.0124
-6.00	-0.090	0.0082
-5.00	0.020	0.0082
-4.00	0.130	0.0082
-3.00	0.240	0.0082
-2.00	0.350	0.0086
-1.00	0.460	0.0086
0.00	0.570	0.0087
1.00	0.670	0.0088
2.00	0.780	0.0090
3.00	0.890	0.0093
4.00	0.990	0.0096
5.00	1.100	0.0099
6.00	1.200	0.0103
7.00	1.310	0.0108
8.00	1.410	0.0113
9.00	1.510	0.0118
10.00	1.560	0.0194
11.00	1.610	0.0221
12.00	1.650	0.0245
13.00	1.650	0.0269
14.00	1.630	0.0296
15.00	1.620	0.0520
30.00	1.080	0.6200
40.00	1.150	0.9600
50.00	1.090	1.3000
60.00	0.880	1.5200
70.00	0.600	1.6600
80.00	0.310	1.7600

90.00	0.000	1.8000
100.00	-0.310	1.7600
110.00	-0.600	1.6600
120.00	-0.880	1.5200
130.00	-1.090	1.3000
140.00	-1.150	0.9600
150.00	-1.080	0.6200
160.00	-0.840	0.3100
170.00	-0.640	0.0500
180.00	-0.170	0.0200

s818_2702.dat Re=4,000,000 (windward modified the flat Cl section near stall)
FROM Dayton Griffin, sept28 '00, post stall blended with flat plate. Foilchcked by Windward on 10-Oct-2000 at 10:23.
1 Number of airfoil tables in this file
0.00 Table ID parameter
12.50 Stall angle (deg)
0.00 No longer used, enter zero
0.00 No longer used, enter zero
0.00 No longer used, enter zero
-5.31 Zero lift angle of attack (deg)
6.10840 Cn slope for zero lift (dimensionless)
1.9560 Cn at stall value for positive angle of attack
-0.8000 Cn at stall value for negative angle of attack
-4.5000 Angle of attack for minimum CD (deg)
0.0082 Minimum CD value

-180.00	-0.170	0.0200
-170.00	0.640	0.0500
-160.00	0.840	0.3100
-150.00	1.080	0.6200
-140.00	1.150	0.9600
-130.00	1.090	1.3000
-120.00	0.880	1.5200
-110.00	0.600	1.6600
-100.00	0.310	1.7600
-90.00	0.000	1.8000
-80.00	-0.310	1.7600
-70.00	-0.600	1.6600
-60.00	-0.880	1.5200
-50.00	-1.090	1.3000
-40.00	-1.150	0.9600
-30.00	-1.080	0.6200
-20.00	-0.840	0.3100
-10.00	-0.640	0.0144
-8.00	-0.480	0.0124
-6.00	-0.090	0.0082
-5.00	0.020	0.0082
-4.00	0.130	0.0082
-3.00	0.240	0.0082
-2.00	0.350	0.0086
-1.00	0.460	0.0086
0.00	0.570	0.0087
1.00	0.670	0.0088
2.00	0.780	0.0090
3.00	0.890	0.0093
4.00	0.990	0.0096
5.00	1.100	0.0099
6.00	1.200	0.0103
7.00	1.310	0.0108
8.00	1.410	0.0113
9.00	1.510	0.0118
10.00	1.560	0.0194
11.00	1.610	0.0221
12.00	1.650	0.0245
13.00	1.650	0.0269
14.00	1.630	0.0296
15.00	1.620	0.0520
30.00	1.080	0.6200
40.00	1.150	0.9600
50.00	1.090	1.3000
60.00	0.880	1.5200
70.00	0.600	1.6600
80.00	0.310	1.7600
90.00	0.000	1.8000
100.00	-0.310	1.7600
110.00	-0.600	1.6600
120.00	-0.880	1.5200
130.00	-1.090	1.3000
140.00	-1.150	0.9600
150.00	-1.080	0.6200

160.00	-0.840	0.3100
170.00	-0.640	0.0500
180.00	-0.170	0.0200

s826_1601.dat Re=3,000,000 (windward modified the flat Cl section near stall)
FROM Dayton Griffin, Sept 28'00, post stall combined with flat plate. Foilchcked by Windward on 10-Oct-2000 at 10:37.
1 Number of airfoil tables in this file
0.00 Table ID parameter
12.00 Stall angle (deg)
0.00 No longer used, enter zero
0.00 No longer used, enter zero
0.00 No longer used, enter zero
-6.61 Zero lift angle of attack (deg)
6.16567 Cn slope for zero lift (dimensionless)
2.0013 Cn at stall value for positive angle of attack
-0.8000 Cn at stall value for negative angle of attack
-4.0000 Angle of attack for minimum CD (deg)
0.0067 Minimum CD value

-180.00	-0.170	0.0200
-170.00	0.640	0.0500
-160.00	0.840	0.3100
-150.00	1.080	0.6200
-140.00	1.150	0.9600
-130.00	1.090	1.3000
-120.00	0.880	1.5200
-110.00	0.600	1.6600
-100.00	0.310	1.7600
-90.00	0.000	1.8000
-80.00	-0.310	1.7600
-70.00	-0.600	1.6600
-60.00	-0.880	1.5200
-50.00	-1.090	1.3000
-40.00	-1.150	0.9600
-30.00	-1.080	0.6200
-20.00	-0.840	0.3100
-10.00	-0.640	0.0144
-8.00	-0.480	0.0124
-6.00	0.060	0.0092
-5.00	0.170	0.0082
-4.00	0.280	0.0067
-3.00	0.390	0.0068
-2.00	0.500	0.0069
-1.00	0.600	0.0070
0.00	0.710	0.0072
1.00	0.820	0.0074
2.00	0.930	0.0076
3.00	1.040	0.0078
4.00	1.140	0.0082
5.00	1.250	0.0087
6.00	1.350	0.0104
7.00	1.440	0.0146
8.00	1.530	0.0184
9.00	1.630	0.0200
10.00	1.650	0.0219
11.00	1.670	0.0239
12.00	1.680	0.0262
13.00	1.670	0.0288
14.00	1.650	0.0316
15.00	1.630	0.0520
30.00	1.080	0.6200
40.00	1.150	0.9600
50.00	1.090	1.3000
60.00	0.880	1.5200
70.00	0.600	1.6600
80.00	0.310	1.7600
90.00	0.000	1.8000
100.00	-0.310	1.7600
110.00	-0.600	1.6600
120.00	-0.880	1.5200
130.00	-1.090	1.3000
140.00	-1.150	0.9600
150.00	-1.080	0.6200
160.00	-0.840	0.3100
170.00	-0.640	0.0500
180.00	-0.170	0.0200

Blade input files for the modified Baseline wind turbine (126 m diameter blades)

DU21 airfoil with an aspect ratio of 17. Original -180 to 180deg Cl, Cd, and Cm versus AOA data taken from Appendix A of DOWEC document 10046_009.pdf (numerical values obtained from Koert Lindenburg of ECN).
Cl and Cd values corrected for rotational stall delay and Cd values corrected using the Viterna method for 0 to 90deg AOA by Jason Jonkman using AirfoilPrep_v2p0.xls.
1 Number of airfoil tables in this file
0.0 Table ID parameter
8.00 Stall angle (deg)
0.0 No longer used, enter zero
0.0 No longer used, enter zero
0.0 No longer used, enter zero
-5.0609 Zero Cn angle of attack (deg)
6.2047 Cn slope for zero lift (dimensionless)
1.4144 Cn extrapolated to value at positive stall angle of attack
-0.5324 Cn at stall value for negative angle of attack
-1.50 Angle of attack for minimum CD (deg)
0.0057 Minimum CD value

-180.00	0.000	0.0185	0.0000
-175.00	0.394	0.0332	0.1978
-170.00	0.788	0.0945	0.3963
-160.00	0.670	0.2809	0.2738
-155.00	0.749	0.3932	0.3118
-150.00	0.797	0.5112	0.3413
-145.00	0.818	0.6309	0.3636
-140.00	0.813	0.7485	0.3799
-135.00	0.786	0.8612	0.3911
-130.00	0.739	0.9665	0.3980
-125.00	0.675	1.0625	0.4012
-120.00	0.596	1.1476	0.4014
-115.00	0.505	1.2206	0.3990
-110.00	0.403	1.2805	0.3943
-105.00	0.294	1.3265	0.3878
-100.00	0.179	1.3582	0.3796
-95.00	0.060	1.3752	0.3700
-90.00	-0.060	1.3774	0.3591
-85.00	-0.179	1.3648	0.3471
-80.00	-0.295	1.3376	0.3340
-75.00	-0.407	1.2962	0.3199
-70.00	-0.512	1.2409	0.3049
-65.00	-0.608	1.1725	0.2890
-60.00	-0.693	1.0919	0.2722
-55.00	-0.764	1.0002	0.2545
-50.00	-0.820	0.8990	0.2359
-45.00	-0.857	0.7900	0.2163
-40.00	-0.875	0.6754	0.1958
-35.00	-0.869	0.5579	0.1744
-30.00	-0.838	0.4405	0.1520
-25.00	-0.791	0.3256	0.1262
-24.00	-0.794	0.3013	0.1170
-23.00	-0.805	0.2762	0.1059
-22.00	-0.821	0.2506	0.0931
-21.00	-0.843	0.2246	0.0788
-20.00	-0.869	0.1983	0.0631
-19.00	-0.899	0.1720	0.0464
-18.00	-0.931	0.1457	0.0286
-17.00	-0.964	0.1197	0.0102
-16.00	-0.999	0.0940	-0.0088
-15.00	-1.033	0.0689	-0.0281
-14.50	-1.050	0.0567	-0.0378
-12.01	-0.953	0.0271	-0.0349
-11.00	-0.900	0.0303	-0.0361
-9.98	-0.827	0.0287	-0.0464
-8.12	-0.536	0.0124	-0.0821
-7.62	-0.467	0.0109	-0.0924
-7.11	-0.393	0.0092	-0.1015
-6.60	-0.323	0.0083	-0.1073
-6.50	-0.311	0.0089	-0.1083
-6.00	-0.245	0.0082	-0.1112
-5.50	-0.178	0.0074	-0.1146
-5.00	-0.113	0.0069	-0.1172
-4.50	-0.048	0.0065	-0.1194
-4.00	0.016	0.0063	-0.1213
-3.50	0.080	0.0061	-0.1232
-3.00	0.145	0.0058	-0.1252

-2.50	0.208	0.0057	-0.1268
-2.00	0.270	0.0057	-0.1282
-1.50	0.333	0.0057	-0.1297
-1.00	0.396	0.0057	-0.1310
-0.50	0.458	0.0057	-0.1324
0.00	0.521	0.0057	-0.1337
0.50	0.583	0.0057	-0.1350
1.00	0.645	0.0058	-0.1363
1.50	0.706	0.0058	-0.1374
2.00	0.768	0.0059	-0.1385
2.50	0.828	0.0061	-0.1395
3.00	0.888	0.0063	-0.1403
3.50	0.948	0.0066	-0.1406
4.00	0.996	0.0071	-0.1398
4.50	1.046	0.0079	-0.1390
5.00	1.095	0.0090	-0.1378
5.50	1.145	0.0103	-0.1369
6.00	1.192	0.0113	-0.1353
6.50	1.239	0.0122	-0.1338
7.00	1.283	0.0131	-0.1317
7.50	1.324	0.0139	-0.1291
8.00	1.358	0.0147	-0.1249
8.50	1.385	0.0158	-0.1213
9.00	1.403	0.0181	-0.1177
9.50	1.401	0.0211	-0.1142
10.00	1.358	0.0255	-0.1103
10.50	1.313	0.0301	-0.1066
11.00	1.287	0.0347	-0.1032
11.50	1.274	0.0401	-0.1002
12.00	1.272	0.0468	-0.0971
12.50	1.273	0.0545	-0.0940
13.00	1.273	0.0633	-0.0909
13.50	1.273	0.0722	-0.0883
14.00	1.272	0.0806	-0.0865
14.50	1.273	0.0900	-0.0854
15.00	1.275	0.0987	-0.0849
15.50	1.281	0.1075	-0.0847
16.00	1.284	0.1170	-0.0850
16.50	1.296	0.1270	-0.0858
17.00	1.306	0.1368	-0.0869
17.50	1.308	0.1464	-0.0883
18.00	1.308	0.1562	-0.0901
18.50	1.308	0.1664	-0.0922
19.00	1.308	0.1770	-0.0949
19.50	1.307	0.1878	-0.0980
20.00	1.311	0.1987	-0.1017
20.50	1.325	0.2100	-0.1059
21.00	1.324	0.2214	-0.1105
22.00	1.277	0.2499	-0.1172
23.00	1.229	0.2786	-0.1239
24.00	1.182	0.3077	-0.1305
25.00	1.136	0.3371	-0.1370
26.00	1.093	0.3664	-0.1433
28.00	1.017	0.4246	-0.1556
30.00	0.962	0.4813	-0.1671
32.00	0.937	0.5356	-0.1778
35.00	0.947	0.6127	-0.1923
40.00	0.950	0.7396	-0.2154
45.00	0.928	0.8623	-0.2374
50.00	0.884	0.9781	-0.2583
55.00	0.821	1.0846	-0.2782
60.00	0.740	1.1796	-0.2971
65.00	0.646	1.2617	-0.3149
70.00	0.540	1.3297	-0.3318
75.00	0.425	1.3827	-0.3476
80.00	0.304	1.4202	-0.3625
85.00	0.179	1.4423	-0.3763
90.00	0.053	1.4512	-0.3890
95.00	-0.073	1.4480	-0.4004
100.00	-0.198	1.4294	-0.4105
105.00	-0.319	1.3954	-0.4191
110.00	-0.434	1.3464	-0.4260
115.00	-0.541	1.2829	-0.4308
120.00	-0.637	1.2057	-0.4333
125.00	-0.720	1.1157	-0.4330
130.00	-0.787	1.0144	-0.4294
135.00	-0.836	0.9033	-0.4219
140.00	-0.864	0.7845	-0.4098
145.00	-0.869	0.6605	-0.3922
150.00	-0.847	0.5346	-0.3682
155.00	-0.795	0.4103	-0.3364
160.00	-0.711	0.2922	-0.2954
170.00	-0.788	0.0969	-0.3966
175.00	-0.394	0.0334	-0.1978
180.00	0.000	0.0185	0.0000

DU25 airfoil with an aspect ratio of 17. Original -180 to 180deg Cl, Cd, and Cm

versus AOA data taken from Appendix A of DOWEC document 10046_009.pdf (numerical values obtained from Koert Lindenburg of ECN).
Cl and Cd values corrected for rotational stall delay and Cd values corrected using the Viterna method for 0 to 90deg AOA by Jason Jonkman using AirfoilPrep_v2p0.xls.
1 Number of airfoil tables in this file
0.0 Table ID parameter
8.50 Stall angle (deg)
0.0 No longer used, enter zero
0.0 No longer used, enter zero
0.0 No longer used, enter zero
-4.2422 Zero Cn angle of attack (deg)
6.4462 Cn slope for zero lift (dimensionless)
1.4336 Cn extrapolated to value at positive stall angle of attack
-0.6873 Cn at stall value for negative angle of attack
0.00 Angle of attack for minimum CD (deg)
0.0065 Minimum CD value

-180.00	0.000	0.0202	0.0000
-175.00	0.368	0.0324	0.1845
-170.00	0.735	0.0943	0.3701
-160.00	0.695	0.2848	0.2679
-155.00	0.777	0.4001	0.3046
-150.00	0.828	0.5215	0.3329
-145.00	0.850	0.6447	0.3540
-140.00	0.846	0.7660	0.3693
-135.00	0.818	0.8823	0.3794
-130.00	0.771	0.9911	0.3854
-125.00	0.705	1.0905	0.3878
-120.00	0.624	1.1787	0.3872
-115.00	0.530	1.2545	0.3841
-110.00	0.426	1.3168	0.3788
-105.00	0.314	1.3650	0.3716
-100.00	0.195	1.3984	0.3629
-95.00	0.073	1.4169	0.3529
-90.00	-0.050	1.4201	0.3416
-85.00	-0.173	1.4081	0.3292
-80.00	-0.294	1.3811	0.3159
-75.00	-0.409	1.3394	0.3017
-70.00	-0.518	1.2833	0.2866
-65.00	-0.617	1.2138	0.2707
-60.00	-0.706	1.1315	0.2539
-55.00	-0.780	1.0378	0.2364
-50.00	-0.839	0.9341	0.2181
-45.00	-0.879	0.8221	0.1991
-40.00	-0.898	0.7042	0.1792
-35.00	-0.893	0.5829	0.1587
-30.00	-0.862	0.4616	0.1374
-25.00	-0.803	0.3441	0.1154
-24.00	-0.792	0.3209	0.1101
-23.00	-0.789	0.2972	0.1031
-22.00	-0.792	0.2730	0.0947
-21.00	-0.801	0.2485	0.0849
-20.00	-0.815	0.2237	0.0739
-19.00	-0.833	0.1990	0.0618
-18.00	-0.854	0.1743	0.0488
-17.00	-0.879	0.1498	0.0351
-16.00	-0.905	0.1256	0.0208
-15.00	-0.932	0.1020	0.0060
-14.00	-0.959	0.0789	-0.0091
-13.00	-0.985	0.0567	-0.0243
-13.00	-0.985	0.0567	-0.0243
-12.01	-0.953	0.0271	-0.0349
-11.00	-0.900	0.0303	-0.0361
-9.98	-0.827	0.0287	-0.0464
-8.98	-0.753	0.0271	-0.0534
-8.47	-0.691	0.0264	-0.0650
-7.45	-0.555	0.0114	-0.0782
-6.42	-0.413	0.0094	-0.0904
-5.40	-0.271	0.0086	-0.1006
-5.00	-0.220	0.0073	-0.1107
-4.50	-0.152	0.0071	-0.1135
-4.00	-0.084	0.0070	-0.1162
-3.50	-0.018	0.0069	-0.1186
-3.00	0.049	0.0068	-0.1209

-2.50	0.115	0.0068	-0.1231
-2.00	0.181	0.0068	-0.1252
-1.50	0.247	0.0067	-0.1272
-1.00	0.312	0.0067	-0.1293
-0.50	0.377	0.0067	-0.1311
0.00	0.444	0.0065	-0.1330
0.50	0.508	0.0065	-0.1347
1.00	0.573	0.0066	-0.1364
1.50	0.636	0.0067	-0.1380
2.00	0.701	0.0068	-0.1396
2.50	0.765	0.0069	-0.1411
3.00	0.827	0.0070	-0.1424
3.50	0.890	0.0071	-0.1437
4.00	0.952	0.0073	-0.1448
4.50	1.013	0.0076	-0.1456
5.00	1.062	0.0079	-0.1445
6.00	1.161	0.0099	-0.1419
6.50	1.208	0.0117	-0.1403
7.00	1.254	0.0132	-0.1382
7.50	1.301	0.0143	-0.1362
8.00	1.336	0.0153	-0.1320
8.50	1.369	0.0165	-0.1276
9.00	1.400	0.0181	-0.1234
9.50	1.428	0.0211	-0.1193
10.00	1.442	0.0262	-0.1152
10.50	1.427	0.0336	-0.1115
11.00	1.374	0.0420	-0.1081
11.50	1.316	0.0515	-0.1052
12.00	1.277	0.0601	-0.1026
12.50	1.250	0.0693	-0.1000
13.00	1.246	0.0785	-0.0980
13.50	1.247	0.0888	-0.0969
14.00	1.256	0.1000	-0.0968
14.50	1.260	0.1108	-0.0973
15.00	1.271	0.1219	-0.0981
15.50	1.281	0.1325	-0.0992
16.00	1.289	0.1433	-0.1006
16.50	1.294	0.1541	-0.1023
17.00	1.304	0.1649	-0.1042
17.50	1.309	0.1754	-0.1064
18.00	1.315	0.1845	-0.1082
18.50	1.320	0.1953	-0.1110
19.00	1.330	0.2061	-0.1143
19.50	1.343	0.2170	-0.1179
20.00	1.354	0.2280	-0.1219
20.50	1.359	0.2390	-0.1261
21.00	1.360	0.2536	-0.1303
22.00	1.325	0.2814	-0.1375
23.00	1.288	0.3098	-0.1446
24.00	1.251	0.3386	-0.1515
25.00	1.215	0.3678	-0.1584
26.00	1.181	0.3972	-0.1651
28.00	1.120	0.4563	-0.1781
30.00	1.076	0.5149	-0.1904
32.00	1.056	0.5720	-0.2017
35.00	1.066	0.6548	-0.2173
40.00	1.064	0.7901	-0.2418
45.00	1.035	0.9190	-0.2650
50.00	0.980	1.0378	-0.2867
55.00	0.904	1.1434	-0.3072
60.00	0.810	1.2333	-0.3265
65.00	0.702	1.3055	-0.3446
70.00	0.582	1.3587	-0.3616
75.00	0.456	1.3922	-0.3775
80.00	0.326	1.4063	-0.3921
85.00	0.197	1.4042	-0.4057
90.00	0.072	1.3985	-0.4180
95.00	-0.050	1.3973	-0.4289
100.00	-0.170	1.3810	-0.4385
105.00	-0.287	1.3498	-0.4464
110.00	-0.399	1.3041	-0.4524
115.00	-0.502	1.2442	-0.4563
120.00	-0.596	1.1709	-0.4577
125.00	-0.677	1.0852	-0.4563
130.00	-0.743	0.9883	-0.4514
135.00	-0.792	0.8818	-0.4425
140.00	-0.821	0.7676	-0.4288
145.00	-0.826	0.6481	-0.4095
150.00	-0.806	0.5264	-0.3836
155.00	-0.758	0.4060	-0.3497
160.00	-0.679	0.2912	-0.3065
170.00	-0.735	0.0995	-0.3706
175.00	-0.368	0.0356	-0.1846
180.00	0.000	0.0202	0.0000

DU30 airfoil with an aspect ratio of 17. Original -180 to 180deg Cl, Cd, and Cm versus AOA data taken from Appendix A

of DOWEC document 10046_009.pdf (numerical values obtained from Koert Lindenburg of ECN).
Cl and Cd values corrected for rotational stall delay and Cd values corrected using the Viterna method for 0 to 90deg AOA by Jason Jonkman using AirfoilPrep_v2p0.xls.
1 Number of airfoil tables in this file
0.0 Table ID parameter
9.00 Stall angle (deg)
0.0 No longer used, enter zero
0.0 No longer used, enter zero
0.0 No longer used, enter zero
-2.3220 Zero Cn angle of attack (deg)
7.3326 Cn slope for zero lift (dimensionless)
1.4490 Cn extrapolated to value at positive stall angle of attack
-0.6138 Cn at stall value for negative angle of attack
0.00 Angle of attack for minimum CD (deg)
0.0087 Minimum CD value

-180.00	0.000	0.0267	0.0000
-175.00	0.274	0.0370	0.1379
-170.00	0.547	0.0968	0.2778
-160.00	0.685	0.2876	0.2740
-155.00	0.766	0.4025	0.3118
-150.00	0.816	0.5232	0.3411
-145.00	0.836	0.6454	0.3631
-140.00	0.832	0.7656	0.3791
-135.00	0.804	0.8807	0.3899
-130.00	0.756	0.9882	0.3965
-125.00	0.690	1.0861	0.3994
-120.00	0.609	1.1730	0.3992
-115.00	0.515	1.2474	0.3964
-110.00	0.411	1.3084	0.3915
-105.00	0.300	1.3552	0.3846
-100.00	0.182	1.3875	0.3761
-95.00	0.061	1.4048	0.3663
-90.00	-0.061	1.4070	0.3551
-85.00	-0.183	1.3941	0.3428
-80.00	-0.302	1.3664	0.3295
-75.00	-0.416	1.3240	0.3153
-70.00	-0.523	1.2676	0.3001
-65.00	-0.622	1.1978	0.2841
-60.00	-0.708	1.1156	0.2672
-55.00	-0.781	1.0220	0.2494
-50.00	-0.838	0.9187	0.2308
-45.00	-0.877	0.8074	0.2113
-40.00	-0.895	0.6904	0.1909
-35.00	-0.889	0.5703	0.1696
-30.00	-0.858	0.4503	0.1475
-25.00	-0.832	0.3357	0.1224
-24.00	-0.852	0.3147	0.1156
-23.00	-0.882	0.2946	0.1081
-22.00	-0.919	0.2752	0.1000
-21.00	-0.963	0.2566	0.0914
-20.00	-1.013	0.2388	0.0823
-19.00	-1.067	0.2218	0.0728
-18.00	-1.125	0.2056	0.0631
-17.00	-1.185	0.1901	0.0531
-16.00	-1.245	0.1754	0.0430
-15.25	-1.290	0.1649	0.0353
-14.24	-1.229	0.1461	0.0240
-13.24	-1.148	0.1263	0.0100
-12.22	-1.052	0.1051	-0.0090
-11.22	-0.965	0.0886	-0.0230
-10.19	-0.867	0.0740	-0.0336
-9.70	-0.822	0.0684	-0.0375
-9.18	-0.769	0.0605	-0.0440
-8.18	-0.756	0.0270	-0.0578
-7.19	-0.690	0.0180	-0.0590
-6.65	-0.616	0.0166	-0.0633
-6.13	-0.542	0.0152	-0.0674
-6.00	-0.525	0.0117	-0.0732
-5.50	-0.451	0.0105	-0.0766
-5.00	-0.382	0.0097	-0.0797
-4.50	-0.314	0.0092	-0.0825
-4.00	-0.251	0.0091	-0.0853
-3.50	-0.189	0.0089	-0.0884
-3.00	-0.120	0.0089	-0.0914

-2.50	-0.051	0.0088	-0.0942
-2.00	0.017	0.0088	-0.0969
-1.50	0.085	0.0088	-0.0994
-1.00	0.152	0.0088	-0.1018
-0.50	0.219	0.0088	-0.1041
0.00	0.288	0.0087	-0.1062
0.50	0.354	0.0087	-0.1086
1.00	0.421	0.0088	-0.1107
1.50	0.487	0.0089	-0.1129
2.00	0.554	0.0090	-0.1149
2.50	0.619	0.0091	-0.1168
3.00	0.685	0.0092	-0.1185
3.50	0.749	0.0093	-0.1201
4.00	0.815	0.0095	-0.1218
4.50	0.879	0.0096	-0.1233
5.00	0.944	0.0097	-0.1248
5.50	1.008	0.0099	-0.1260
6.00	1.072	0.0101	-0.1270
6.50	1.135	0.0103	-0.1280
7.00	1.197	0.0107	-0.1287
7.50	1.256	0.0112	-0.1289
8.00	1.305	0.0125	-0.1270
9.00	1.390	0.0155	-0.1207
9.50	1.424	0.0171	-0.1158
10.00	1.458	0.0192	-0.1116
10.50	1.488	0.0219	-0.1073
11.00	1.512	0.0255	-0.1029
11.50	1.533	0.0307	-0.0983
12.00	1.549	0.0370	-0.0949
12.50	1.558	0.0452	-0.0921
13.00	1.470	0.0630	-0.0899
13.50	1.398	0.0784	-0.0885
14.00	1.354	0.0931	-0.0885
14.50	1.336	0.1081	-0.0902
15.00	1.333	0.1239	-0.0928
15.50	1.326	0.1415	-0.0963
16.00	1.329	0.1592	-0.1006
16.50	1.326	0.1743	-0.1042
17.00	1.321	0.1903	-0.1084
17.50	1.331	0.2044	-0.1125
18.00	1.333	0.2186	-0.1169
18.50	1.340	0.2324	-0.1215
19.00	1.362	0.2455	-0.1263
19.50	1.382	0.2584	-0.1313
20.00	1.398	0.2689	-0.1352
20.50	1.426	0.2814	-0.1406
21.00	1.437	0.2943	-0.1462
22.00	1.418	0.3246	-0.1516
23.00	1.397	0.3557	-0.1570
24.00	1.376	0.3875	-0.1623
25.00	1.354	0.4198	-0.1676
26.00	1.332	0.4524	-0.1728
28.00	1.293	0.5183	-0.1832
30.00	1.265	0.5843	-0.1935
32.00	1.253	0.6492	-0.2039
35.00	1.264	0.7438	-0.2193
40.00	1.258	0.8970	-0.2440
45.00	1.217	1.0402	-0.2672
50.00	1.146	1.1686	-0.2891
55.00	1.049	1.2779	-0.3097
60.00	0.932	1.3647	-0.3290
65.00	0.799	1.4267	-0.3471
70.00	0.657	1.4621	-0.3641
75.00	0.509	1.4708	-0.3799
80.00	0.362	1.4544	-0.3946
85.00	0.221	1.4196	-0.4081
90.00	0.092	1.3938	-0.4204
95.00	-0.030	1.3943	-0.4313
100.00	-0.150	1.3798	-0.4408
105.00	-0.267	1.3504	-0.4486
110.00	-0.379	1.3063	-0.4546
115.00	-0.483	1.2481	-0.4584
120.00	-0.578	1.1763	-0.4597
125.00	-0.660	1.0919	-0.4582
130.00	-0.727	0.9962	-0.4532
135.00	-0.777	0.8906	-0.4441
140.00	-0.807	0.7771	-0.4303
145.00	-0.815	0.6581	-0.4109
150.00	-0.797	0.5364	-0.3848
155.00	-0.750	0.4157	-0.3508
160.00	-0.673	0.3000	-0.3074
170.00	-0.547	0.1051	-0.2786
175.00	-0.274	0.0388	-0.1380
180.00	0.000	0.0267	0.0000

DU35 airfoil with an aspect ratio of 17. Original -180 to 180deg Cl, Cd, and Cm versus AOA data taken from Appendix A

of DOWEC document 10046_009.pdf (numerical values obtained from Koert Lindenburg of ECN).
Cl and Cd values corrected for rotational stall delay and Cd values corrected using the Viterna method for 0 to 90deg AOA by Jason Jonkman using AirfoilPrep_v2p0.xls.
1 Number of airfoil tables in this file
0.0 Table ID parameter
11.50 Stall angle (deg)
0.0 No longer used, enter zero
0.0 No longer used, enter zero
0.0 No longer used, enter zero
-1.8330 Zero Cn angle of attack (deg)
7.1838 Cn slope for zero lift (dimensionless)
1.6717 Cn extrapolated to value at positive stall angle of attack
-0.3075 Cn at stall value for negative angle of attack
0.00 Angle of attack for minimum CD (deg)
0.0094 Minimum CD value

-180.00	0.000	0.0407	0.0000
-175.00	0.223	0.0507	0.0937
-170.00	0.405	0.1055	0.1702
-160.00	0.658	0.2982	0.2819
-155.00	0.733	0.4121	0.3213
-150.00	0.778	0.5308	0.3520
-145.00	0.795	0.6503	0.3754
-140.00	0.787	0.7672	0.3926
-135.00	0.757	0.8785	0.4046
-130.00	0.708	0.9819	0.4121
-125.00	0.641	1.0756	0.4160
-120.00	0.560	1.1580	0.4167
-115.00	0.467	1.2280	0.4146
-110.00	0.365	1.2847	0.4104
-105.00	0.255	1.3274	0.4041
-100.00	0.139	1.3557	0.3961
-95.00	0.021	1.3692	0.3867
-90.00	-0.098	1.3680	0.3759
-85.00	-0.216	1.3521	0.3639
-80.00	-0.331	1.3218	0.3508
-75.00	-0.441	1.2773	0.3367
-70.00	-0.544	1.2193	0.3216
-65.00	-0.638	1.1486	0.3054
-60.00	-0.720	1.0660	0.2884
-55.00	-0.788	0.9728	0.2703
-50.00	-0.840	0.8705	0.2512
-45.00	-0.875	0.7611	0.2311
-40.00	-0.889	0.6466	0.2099
-35.00	-0.880	0.5299	0.1876
-30.00	-0.846	0.4141	0.1641
-25.00	-0.784	0.3030	0.1396
-24.00	-0.768	0.2817	0.1345
-23.00	-0.751	0.2608	0.1294
-22.00	-0.733	0.2404	0.1243
-21.00	-0.714	0.2205	0.1191
-20.00	-0.693	0.2011	0.1139
-19.00	-0.671	0.1822	0.1086
-18.00	-0.648	0.1640	0.1032
-17.00	-0.624	0.1465	0.0975
-16.00	-0.601	0.1300	0.0898
-15.00	-0.579	0.1145	0.0799
-14.00	-0.559	0.1000	0.0682
-13.00	-0.539	0.0867	0.0547
-12.00	-0.519	0.0744	0.0397
-11.00	-0.499	0.0633	0.0234
-10.00	-0.480	0.0534	0.0060
-5.54	-0.385	0.0245	-0.0800
-5.04	-0.359	0.0225	-0.0800
-4.54	-0.360	0.0196	-0.0800
-4.04	-0.355	0.0174	-0.0800
-3.54	-0.307	0.0162	-0.0800
-3.04	-0.246	0.0144	-0.0800
-3.00	-0.240	0.0240	-0.0623
-2.50	-0.163	0.0188	-0.0674
-2.00	-0.091	0.0160	-0.0712
-1.50	-0.019	0.0137	-0.0746
-1.00	0.052	0.0118	-0.0778
-0.50	0.121	0.0104	-0.0806
0.00	0.196	0.0094	-0.0831
0.50	0.265	0.0096	-0.0863
1.00	0.335	0.0098	-0.0895
1.50	0.404	0.0099	-0.0924
2.00	0.472	0.0100	-0.0949

2.50	0.540	0.0102	-0.0973
3.00	0.608	0.0103	-0.0996
3.50	0.674	0.0104	-0.1016
4.00	0.742	0.0105	-0.1037
4.50	0.809	0.0107	-0.1057
5.00	0.875	0.0108	-0.1076
5.50	0.941	0.0109	-0.1094
6.00	1.007	0.0110	-0.1109
6.50	1.071	0.0113	-0.1118
7.00	1.134	0.0115	-0.1127
7.50	1.198	0.0117	-0.1138
8.00	1.260	0.0120	-0.1144
8.50	1.318	0.0126	-0.1137
9.00	1.368	0.0133	-0.1112
9.50	1.422	0.0143	-0.1100
10.00	1.475	0.0156	-0.1086
10.50	1.523	0.0174	-0.1064
11.00	1.570	0.0194	-0.1044
11.50	1.609	0.0227	-0.1013
12.00	1.642	0.0269	-0.0980
12.50	1.675	0.0319	-0.0953
13.00	1.700	0.0398	-0.0925
13.50	1.717	0.0488	-0.0896
14.00	1.712	0.0614	-0.0864
14.50	1.703	0.0786	-0.0840
15.50	1.671	0.1173	-0.0830
16.00	1.649	0.1377	-0.0848
16.50	1.621	0.1600	-0.0880
17.00	1.598	0.1814	-0.0926
17.50	1.571	0.2042	-0.0984
18.00	1.549	0.2316	-0.1052
19.00	1.544	0.2719	-0.1158
19.50	1.549	0.2906	-0.1213
20.00	1.565	0.3085	-0.1248
21.00	1.565	0.3447	-0.1317
22.00	1.563	0.3820	-0.1385
23.00	1.558	0.4203	-0.1452
24.00	1.552	0.4593	-0.1518
25.00	1.546	0.4988	-0.1583
26.00	1.539	0.5387	-0.1647
28.00	1.527	0.6187	-0.1770
30.00	1.522	0.6978	-0.1886
32.00	1.529	0.7747	-0.1994
35.00	1.544	0.8869	-0.2148
40.00	1.529	1.0671	-0.2392
45.00	1.471	1.2319	-0.2622
50.00	1.376	1.3747	-0.2839
55.00	1.249	1.4899	-0.3043
60.00	1.097	1.5728	-0.3236
65.00	0.928	1.6202	-0.3417
70.00	0.750	1.6302	-0.3586
75.00	0.570	1.6031	-0.3745
80.00	0.396	1.5423	-0.3892
85.00	0.237	1.4598	-0.4028
90.00	0.101	1.4041	-0.4151
95.00	-0.022	1.4053	-0.4261
100.00	-0.143	1.3914	-0.4357
105.00	-0.261	1.3625	-0.4437
110.00	-0.374	1.3188	-0.4498
115.00	-0.480	1.2608	-0.4538
120.00	-0.575	1.1891	-0.4553
125.00	-0.659	1.1046	-0.4540
130.00	-0.727	1.0086	-0.4492
135.00	-0.778	0.9025	-0.4405
140.00	-0.809	0.7883	-0.4270
145.00	-0.818	0.6684	-0.4078
150.00	-0.800	0.5457	-0.3821
155.00	-0.754	0.4236	-0.3484
160.00	-0.677	0.3066	-0.3054
170.00	-0.417	0.1085	-0.1842
175.00	-0.229	0.0510	-0.1013
180.00	0.000	0.0407	0.0000

DU40 airfoil with an aspect ratio of 17. Original -180 to 180deg Cl, Cd, and Cm versus AOA data taken from Appendix A of DOWEC document 10046_009.pdf (numerical values obtained from Koert Lindenburg of ECN).

Cl and Cd values corrected for rotational stall delay and Cd values corrected using the Viterna method for 0 to 90deg AOA by Jason Jonkman using AirfoilPrep_v2p0.xls.

1	Number of airfoil tables in this file
0.0	Table ID parameter
9.00	Stall angle (deg)
0.0	No longer used, enter zero

0.0 No longer used, enter zero
0.0 No longer used, enter zero
-1.3430 Zero Cn angle of attack (deg)
7.4888 Cn slope for zero lift (dimensionless)
1.3519 Cn extrapolated to value at positive stall angle of attack
-0.3226 Cn at stall value for negative angle of attack
0.00 Angle of attack for minimum CD (deg)
0.0113 Minimum CD value

-180.00	0.000	0.0602	0.0000
-175.00	0.218	0.0699	0.0934
-170.00	0.397	0.1107	0.1697
-160.00	0.642	0.3045	0.2813
-155.00	0.715	0.4179	0.3208
-150.00	0.757	0.5355	0.3516
-145.00	0.772	0.6535	0.3752
-140.00	0.762	0.7685	0.3926
-135.00	0.731	0.8777	0.4048
-130.00	0.680	0.9788	0.4126
-125.00	0.613	1.0700	0.4166
-120.00	0.532	1.1499	0.4176
-115.00	0.439	1.2174	0.4158
-110.00	0.337	1.2716	0.4117
-105.00	0.228	1.3118	0.4057
-100.00	0.114	1.3378	0.3979
-95.00	-0.002	1.3492	0.3887
-90.00	-0.120	1.3460	0.3781
-85.00	-0.236	1.3283	0.3663
-80.00	-0.349	1.2964	0.3534
-75.00	-0.456	1.2507	0.3394
-70.00	-0.557	1.1918	0.3244
-65.00	-0.647	1.1204	0.3084
-60.00	-0.727	1.0376	0.2914
-55.00	-0.792	0.9446	0.2733
-50.00	-0.842	0.8429	0.2543
-45.00	-0.874	0.7345	0.2342
-40.00	-0.886	0.6215	0.2129
-35.00	-0.875	0.5067	0.1906
-30.00	-0.839	0.3932	0.1670
-25.00	-0.777	0.2849	0.1422
-24.00	-0.761	0.2642	0.1371
-23.00	-0.744	0.2440	0.1320
-22.00	-0.725	0.2242	0.1268
-21.00	-0.706	0.2049	0.1215
-20.00	-0.685	0.1861	0.1162
-19.00	-0.662	0.1687	0.1097
-18.00	-0.635	0.1533	0.1012
-17.00	-0.605	0.1398	0.0907
-16.00	-0.571	0.1281	0.0784
-15.00	-0.534	0.1183	0.0646
-14.00	-0.494	0.1101	0.0494
-13.00	-0.452	0.1036	0.0330
-12.00	-0.407	0.0986	0.0156
-11.00	-0.360	0.0951	-0.0026
-10.00	-0.311	0.0931	-0.0213
-8.00	-0.208	0.0930	-0.0600
-6.00	-0.111	0.0689	-0.0500
-5.50	-0.090	0.0614	-0.0516
-5.00	-0.072	0.0547	-0.0532
-4.50	-0.065	0.0480	-0.0538
-4.00	-0.054	0.0411	-0.0544
-3.50	-0.017	0.0349	-0.0554
-3.00	0.003	0.0299	-0.0558
-2.50	0.014	0.0255	-0.0555
-2.00	0.009	0.0198	-0.0534
-1.50	0.004	0.0164	-0.0442
-1.00	0.036	0.0147	-0.0469
-0.50	0.073	0.0137	-0.0522
0.00	0.137	0.0113	-0.0573
0.50	0.213	0.0114	-0.0644
1.00	0.292	0.0118	-0.0718
1.50	0.369	0.0122	-0.0783
2.00	0.444	0.0124	-0.0835
2.50	0.514	0.0124	-0.0866
3.00	0.580	0.0123	-0.0887
3.50	0.645	0.0120	-0.0900
4.00	0.710	0.0119	-0.0914
4.50	0.776	0.0122	-0.0933
5.00	0.841	0.0125	-0.0947
5.50	0.904	0.0129	-0.0957
6.00	0.967	0.0135	-0.0967
6.50	1.027	0.0144	-0.0973
7.00	1.084	0.0158	-0.0972
7.50	1.140	0.0174	-0.0972

8.00	1.193	0.0198	-0.0968	95.00	0.002	1.3912	-0.4343
8.50	1.242	0.0231	-0.0958	100.00	-0.118	1.3795	-0.4437
9.00	1.287	0.0275	-0.0948	105.00	-0.235	1.3528	-0.4514
9.50	1.333	0.0323	-0.0942	110.00	-0.348	1.3114	-0.4573
10.00	1.368	0.0393	-0.0926	115.00	-0.453	1.2557	-0.4610
10.50	1.400	0.0475	-0.0908	120.00	-0.549	1.1864	-0.4623
11.00	1.425	0.0580	-0.0890	125.00	-0.633	1.1041	-0.4606
11.50	1.449	0.0691	-0.0877	130.00	-0.702	1.0102	-0.4554
12.00	1.473	0.0816	-0.0870	135.00	-0.754	0.9060	-0.4462
12.50	1.494	0.0973	-0.0870	140.00	-0.787	0.7935	-0.4323
13.00	1.513	0.1129	-0.0876	145.00	-0.797	0.6750	-0.4127
13.50	1.538	0.1288	-0.0886	150.00	-0.782	0.5532	-0.3863
14.50	1.587	0.1650	-0.0917	155.00	-0.739	0.4318	-0.3521
15.00	1.614	0.1845	-0.0939	160.00	-0.664	0.3147	-0.3085
15.50	1.631	0.2052	-0.0966	170.00	-0.410	0.1144	-0.1858
16.00	1.649	0.2250	-0.0996	175.00	-0.226	0.0702	-0.1022
16.50	1.666	0.2467	-0.1031	180.00	0.000	0.0602	0.0000
17.00	1.681	0.2684	-0.1069				
17.50	1.699	0.2900	-0.1110				
18.00	1.719	0.3121	-0.1157				
19.00	1.751	0.3554	-0.1242				
19.50	1.767	0.3783	-0.1291				
20.50	1.798	0.4212	-0.1384				
21.00	1.810	0.4415	-0.1416				
22.00	1.830	0.4830	-0.1479				
23.00	1.847	0.5257	-0.1542				
24.00	1.861	0.5694	-0.1603				
25.00	1.872	0.6141	-0.1664				
26.00	1.881	0.6593	-0.1724				
28.00	1.894	0.7513	-0.1841				
30.00	1.904	0.8441	-0.1954				
32.00	1.915	0.9364	-0.2063				
35.00	1.929	1.0722	-0.2220				
40.00	1.903	1.2873	-0.2468				
45.00	1.820	1.4796	-0.2701				
50.00	1.690	1.6401	-0.2921				
55.00	1.522	1.7609	-0.3127				
60.00	1.323	1.8360	-0.3321				
65.00	1.106	1.8614	-0.3502				
70.00	0.880	1.8347	-0.3672				
75.00	0.658	1.7567	-0.3830				
80.00	0.449	1.6334	-0.3977				
85.00	0.267	1.4847	-0.4112				
90.00	0.124	1.3879	-0.4234				

NACA64 airfoil with an aspect ratio of 17.
Original -180 to 180deg Cl, Cd, and Cm versus AOA data taken from Appendix A of DOWEC document 10046_009.pdf (numerical values obtained from Koert Lindenburg of ECN).
Cl and Cd values corrected for rotational stall delay and Cd values corrected using the Viterna method for 0 to 90deg AOA by Jason Jonkman using AirfoilPrep_v2p0.xls.

1	Number of airfoil tables in this file
0.0	Table ID parameter
9.00	Stall angle (deg)
0.0	No longer used, enter zero
0.0	No longer used, enter zero
0.0	No longer used, enter zero
-4.4320	Zero Cn angle of attack (deg)
6.0031	Cn slope for zero lift (dimensionless)
1.4073	Cn extrapolated to value at positive stall angle of attack
-0.7945	Cn at stall value for negative angle of attack
-1.00	Angle of attack for minimum

CD (deg)				-13.50	-1.053	0.0158	-0.0521
0.0052	Minimum CD value			-13.00	-1.015	0.0151	-0.0610
-180.00	0.000	0.0198	0.0000	-12.00	-0.904	0.0134	-0.0707
-175.00	0.374	0.0341	0.1880	-11.00	-0.807	0.0121	-0.0722
-170.00	0.749	0.0955	0.3770	-10.00	-0.711	0.0111	-0.0734
-160.00	0.659	0.2807	0.2747	-9.00	-0.595	0.0099	-0.0772
-155.00	0.736	0.3919	0.3130	-8.00	-0.478	0.0091	-0.0807
-150.00	0.783	0.5086	0.3428	-7.00	-0.375	0.0086	-0.0825
-145.00	0.803	0.6267	0.3654	-6.00	-0.264	0.0082	-0.0832
-140.00	0.798	0.7427	0.3820	-5.00	-0.151	0.0079	-0.0841
-135.00	0.771	0.8537	0.3935	-4.00	-0.017	0.0072	-0.0869
-130.00	0.724	0.9574	0.4007	-3.00	0.088	0.0064	-0.0912
-125.00	0.660	1.0519	0.4042	-2.00	0.213	0.0054	-0.0946
-120.00	0.581	1.1355	0.4047	-1.00	0.328	0.0052	-0.0971
-115.00	0.491	1.2070	0.4025	0.00	0.442	0.0052	-0.1014
-110.00	0.390	1.2656	0.3981	1.00	0.556	0.0052	-0.1076
-105.00	0.282	1.3104	0.3918	2.00	0.670	0.0053	-0.1126
-100.00	0.169	1.3410	0.3838	3.00	0.784	0.0053	-0.1157
-95.00	0.052	1.3572	0.3743	4.00	0.898	0.0054	-0.1199
-90.00	-0.067	1.3587	0.3636	5.00	1.011	0.0058	-0.1240
-85.00	-0.184	1.3456	0.3517	6.00	1.103	0.0091	-0.1234
-80.00	-0.299	1.3181	0.3388	7.00	1.181	0.0113	-0.1184
-75.00	-0.409	1.2765	0.3248	8.00	1.257	0.0124	-0.1163
-70.00	-0.512	1.2212	0.3099	8.50	1.293	0.0130	-0.1163
-65.00	-0.606	1.1532	0.2940	9.00	1.326	0.0136	-0.1160
-60.00	-0.689	1.0731	0.2772	9.50	1.356	0.0143	-0.1154
-55.00	-0.759	0.9822	0.2595	10.00	1.382	0.0150	-0.1149
-50.00	-0.814	0.8820	0.2409	10.50	1.400	0.0267	-0.1145
-45.00	-0.850	0.7742	0.2212	11.00	1.415	0.0383	-0.1143
-40.00	-0.866	0.6610	0.2006	11.50	1.425	0.0498	-0.1147
-35.00	-0.860	0.5451	0.1789	12.00	1.434	0.0613	-0.1158
-30.00	-0.829	0.4295	0.1563	12.50	1.443	0.0727	-0.1165
-25.00	-0.853	0.3071	0.1156	13.00	1.451	0.0841	-0.1153
-24.00	-0.870	0.2814	0.1040	13.50	1.453	0.0954	-0.1131
-23.00	-0.890	0.2556	0.0916	14.00	1.448	0.1065	-0.1112
-22.00	-0.911	0.2297	0.0785	14.50	1.444	0.1176	-0.1101
-21.00	-0.934	0.2040	0.0649	15.00	1.445	0.1287	-0.1103
-20.00	-0.958	0.1785	0.0508	15.50	1.447	0.1398	-0.1109
-19.00	-0.982	0.1534	0.0364	16.00	1.448	0.1509	-0.1114
-18.00	-1.005	0.1288	0.0218	16.50	1.444	0.1619	-0.1111
-17.00	-1.082	0.1037	0.0129	17.00	1.438	0.1728	-0.1097
-16.00	-1.113	0.0786	-0.0028	17.50	1.439	0.1837	-0.1079
-15.00	-1.105	0.0535	-0.0251	18.00	1.448	0.1947	-0.1080
-14.00	-1.078	0.0283	-0.0419	18.50	1.452	0.2057	-0.1090

19.00	1.448	0.2165	-0.1086
19.50	1.438	0.2272	-0.1077
20.00	1.428	0.2379	-0.1099
21.00	1.401	0.2590	-0.1169
22.00	1.359	0.2799	-0.1190
23.00	1.300	0.3004	-0.1235
24.00	1.220	0.3204	-0.1393
25.00	1.168	0.3377	-0.1440
26.00	1.116	0.3554	-0.1486
28.00	1.015	0.3916	-0.1577
30.00	0.926	0.4294	-0.1668
32.00	0.855	0.4690	-0.1759
35.00	0.800	0.5324	-0.1897
40.00	0.804	0.6452	-0.2126
45.00	0.793	0.7573	-0.2344
50.00	0.763	0.8664	-0.2553
55.00	0.717	0.9708	-0.2751
60.00	0.656	1.0693	-0.2939
65.00	0.582	1.1606	-0.3117
70.00	0.495	1.2438	-0.3285
75.00	0.398	1.3178	-0.3444
80.00	0.291	1.3809	-0.3593
85.00	0.176	1.4304	-0.3731
90.00	0.053	1.4565	-0.3858
95.00	-0.074	1.4533	-0.3973
100.00	-0.199	1.4345	-0.4075
105.00	-0.321	1.4004	-0.4162
110.00	-0.436	1.3512	-0.4231
115.00	-0.543	1.2874	-0.4280
120.00	-0.640	1.2099	-0.4306
125.00	-0.723	1.1196	-0.4304
130.00	-0.790	1.0179	-0.4270
135.00	-0.840	0.9064	-0.4196
140.00	-0.868	0.7871	-0.4077
145.00	-0.872	0.6627	-0.3903
150.00	-0.850	0.5363	-0.3665
155.00	-0.798	0.4116	-0.3349
160.00	-0.714	0.2931	-0.2942
170.00	-0.749	0.0971	-0.3771
175.00	-0.374	0.0334	-0.1879
180.00	0.000	0.0198	0.0000

VITA

Sangyun Shim
Coastal and Ocean Engineering Division,
Zachry Department of Civil Engineering,
3136 TAMU, College Station, TX, 77843
Phone: (979) 845-4515
Email: shimsangyun@gmail.com

EDUCATION

• Master of Science: December 2007
Major: Ocean Engineering
Texas A&M University
GPA: 3.78/4.0

• Bachelor of Science: August 2004
Major: Naval Architecture and Ocean Engineering, *Minor: Business
Inha University, Incheon, Korea
GPA: 3.88/4.5

EXPERIENCE

• SOFEC, Inc., Houston, Texas (August 2007 – Present)
Research Engineer

• ABS – American Bureau of Shipping, Houston, Texas (June 2006 – August 2006)
Internship at Technology group